

Parameter extraction of single, double, and three diodes photovoltaic model based on guaranteed convergence arithmetic optimization algorithm and modified third order Newton Raphson methods



Hussein Mohammed Ridha^{a,b,c,*}, Hashim Hizam^{a,b,**}, Seyedali Mirjalili^{d,e}, Mohammad Lutfi Othman^{a,b}, Mohammad Effendy Ya'acob^{b,f}, Masoud Ahmadipour^g

^a Department of Electrical and Electronics Engineering, Faculty of Engineering, Universiti Putra Malaysia, 43400, Serdang, Malaysia

^b Advanced Lightning, Power and Energy Research (ALPER), Faculty of Engineering, Universiti Putra Malaysia, 43400, Serdang, Malaysia

^c Department of Computer Engineering, University of Al-Mustansiriyah, 10001, Baghdad, Iraq

^d Centre for Artificial Intelligence Research and Optimization, Torrens University Australia, Fortitude Valley, Brisbane, 4006, QLD, Australia

^e Yonsei Frontier Lab, Yonsei University, Seoul, South Korea

^f Department of Process and Food Engineering, Faculty of Engineering, Universiti Putra Malaysia, Serdang, 43400, Selangor, Malaysia

^g School of Electrical Engineering, College of Engineering, Universiti Teknologi MARA, 40450, Shah Alam, Selangor, Malaysia

ARTICLE INFO

Keywords:

Photovoltaic cell
I-V curve
Arithmetic optimization algorithm
Newton raphson method
Optimization

ABSTRACT

Extraction of the photovoltaic (PV) model parameters is critical for forecasting these systems' energy output. Numerous research have reviewed and presented approaches for figuring out the PV models parameter optimization problem in the literature. However, few studies have been undertaken to construct the objective function, or no review papers have been published on the applied methodologies for solving the equations of nonlinear, multi-variable, and complicated PV models based on the datasheet information or actual experimental data. Therefore, this study seeks to first explore the acquired approaches to solve the equations of PV models. Then, utilizing actual measured laboratory data collected under a variety of environmental circumstances, a hybrid approach for efficiently determining unknown the parameters of the single, double, and three diodes PV model has been developed. The proposed guaranteed convergence arithmetic optimization algorithm based on efficient modified third order Newton Raphson (GCAOA_{EmNR}) method highlights important contributions to the literature in terms of methodology (explorer-exploiter phases) and objective function design. The experimental findings exhibit that the GCAOA_{EmNR} minimizes the error to zero under diverse statistical criteria and environmental conditions. Moreover, the GCAOA_{EmNR} beats all well-published approaches in the literature in terms of accuracy, stability, and convergence rate while requiring a reasonable amount of processing time.

1. Introduction

In the last decades, solar energy utilization has increased tremendously. This rapid rise is a consequence of critical issues such as conventional energy's depletion, global warming, and recession triggered by the COVID-19 pandemic [1]. Additionally, solar energy is freely accessible around the world and has been considerable efficiency gains, particularly when it comes to confronting the bifacial PV technology [2]. However, this technology has a number of drawbacks, such as a high total cost and a low conversion efficiency [3].

The solar cells' performance under outside weather conditions are strongly dependent on their physical characteristics. Therefore, it is very necessary to address these parameters precisely while taking the range of environmental circumstances into consideration utilizing real experimental data [4]. PV mathematical models are grouped into three broad categories: single diode (SD) model, double diode (DD) model, and three diode (TD) model. To plot the I-V and P-V curves, the parameters of these models must be optimally estimated. As an outcome, such parameter may be determined either by minimizing the error between the simulated model and real experimental data, or by obtaining the three main reference points under ideal conditions: open-circuit (OC),

^{**} Corresponding author. Department of Electrical and Electronics Engineering, Faculty of Engineering, Universiti Putra Malaysia, 43400, Serdang, Malaysia.

* Corresponding author. Department of Electrical and Electronics Engineering, Faculty of Engineering, Universiti Putra Malaysia, 43400, Serdang, Malaysia.

E-mail addresses: hussain_mhammad@yahoo.com (H.M. Ridha), hhizam@upm.edu.my (H. Hizam), ali.mirjalili@gmail.com (S. Mirjalili), lutfi@upm.edu.my (M.L. Othman), m_effendy@upm.edu.my (M.E. Ya'acob), maseod.ahmadipour@gmail.com (M. Ahmadipour).

Nomenclature			
I_{Ph}	photocurrent (A)	GRG	generalized reduced gradient
I_{01-3}	saturation current (A)	GNDO	generalized normal distribution optimization
d_{1-3}	diode ideality factor	HHO	harris hawk optimization
R_s	series resistor (Ω)	ICA	imperialist competitive algorithm
R_p	shunt resistor (Ω)	IEM	improved electromagnetic-like algorithm
KB	boltzmann's constant	IPM	interior point method
e	random Gaussian distribution	LSM	least square method
RL	levy flight strategy	LM	levenberg Marquardt
Abbreviations		LPSR	Linear population size reduction
ABSO	artificial bee swarm optimization	MRFO	manta ray foraging optimization
ACT	approximation and correction technique	MPP	maximum power point
AWDO	adaptive wind driven optimization	MPA	marine predictor algorithm
AEO	ecosystem optimizer	MVA	multi-verse algorithm
BFA	bacterial foraging algorithm	NOCT	nominal operating cell temperature
BMA	barnacles mating algorithm	NM	nelder mead simplex algorithm
COA	coyote optimization algorithm	OC	open circuit
CMAES	covariance matrix adaption evolution strategy	OBL	opposition based learning
CL	comprehensive learning	OL	orthogonal learning
DE	differential evolution	PS	pattern search
DSO	drone squadron optimization	SA	simulated annealing
DEIM	differential evolution and integrated mutation	SC	short circuit
EPO	emperor penguin optimization	SFS	stochastic fractal search
FA	firefly algorithm	SMA	slim mould algorithm
FF	fill factor	SSO	shark smell optimization
FFO	farmland fertility optimizer	STC	standard test condition
FPA	flower pollination algorithm	STF	special trans function
GA	genetic algorithm	TLBO	teaching learning based optimization
GOL	generalized opposition learning	TRR	trust region reflective
		WDA	wind driven algorithm
		WOA	whale optimization algorithm

short-circuit (SC), and maximum power point (MPP) [5].

Extracting the unknown parameters of the PV models utilizing actual experimental data gathered at a variety of weather circumstances is regarded to be more suitable and accurately represents the actual behavior of the PV cells. However, a significant hurdle to using these methods is a lack of broad and varied experimental data across a range of weather conditions [6]. The literature describes a number of approaches to parameter extraction optimization, involving analytical, numerical, stochastic, hybrid, and software tools [7,8].

Analytical approaches are derived to obtain the characteristics of PV cells from their manufacturer's datasheets under Standard Test Conditions (STCs) [9]. These methods have the benefits of being simple, and their equations are quickly computed. Contrarily, any miscalculation in one of these equations might result in a substantial error value. Additionally, Furthermore, the manufacturer's specification is based on unrealistic conditions that may not properly reflect the PV cells' real performance [10]. Iterative procedures are employed to overcome the constraints of the analytical methods, since they are more accurate and competent of efficiently solving nonlinearity and multivariable problems such as NR [11,12], Levenberg Marquardt [13], Lambert W function [14], Bezier Curve [15], f-solve [16], Taylor series (TS) [17], and curve fitting method (least square error) [18] as illustrated in Fig. 1 [19]. The biggest obstacles of these techniques is that the initial root solutions of the PV model must be carefully set. These approaches can certainly beat the analytical approaches, they struggle to replicate real currents at zigzag and hard edges [20].

To overcome the limitations of the classical approaches outlined above, stochastic methods have been addressed to handle the parameter estimation optimization problem for the PV model [21,22]. These methods' accuracy, precision, and CPU computing time are dependent on the complexity of the problem, control parameters, number of

evaluation, the exploratory and exploitative tactics, population size, and objective function design (OFD) [23]. As a corollary, the methods' performance varies according to the concept of No Free Lunch (NFL). This theorem asserts that almost no specific optimization algorithm is optimum for all possible optimization problems [24]. The above permits researchers to develop new hybrid methods that use a variety of strategies in order to optimize the performance of the proposed PV model and decrease the error to the maximum level of perfection. These approaches overcome the constraints of the preceding methods by acquiring their advantages and mitigating their shortcomings. In this respect, the majority of scholars focus on optimizing the methodology itself, whether through the use of a control parameter to efficiently manage the explorative and exploitative mechanisms, or through implementation of novel strategies capable of rapidly discovering new areas (diversifying) and obtaining a high-quality solutions (intensification). Numerous review articles have extensively covered the improvements in the algorithms applied for optimizing the PV models [7,10, 25–27]. However, there is no review paper has explored or analyzed the formulation of the objective function, revealing a theoretical gap in this topic. Hence, the PV model's equation is multi-dimensional, nonlinearity, and multi-variable, necessitating the use of sophisticated proficient methods to solve this equation [28].

On the other hand, little studies focused on the OFD; instead, the majority of research papers improve on the methodology which they solve the PV model's equation linearly by replacing the parameters directly into the equation. The other authors, on the other hand, utilize the NR and Lambert W function (LW) methods to solve the PV model's equation [29]. These methods are more accurate in terms of precisely picking initial solutions and enhancing the convergence rate by decreasing the root mean square error (RMSE) to a specific domain, resulting in a significant theoretical gap [30]. As a reason, we will

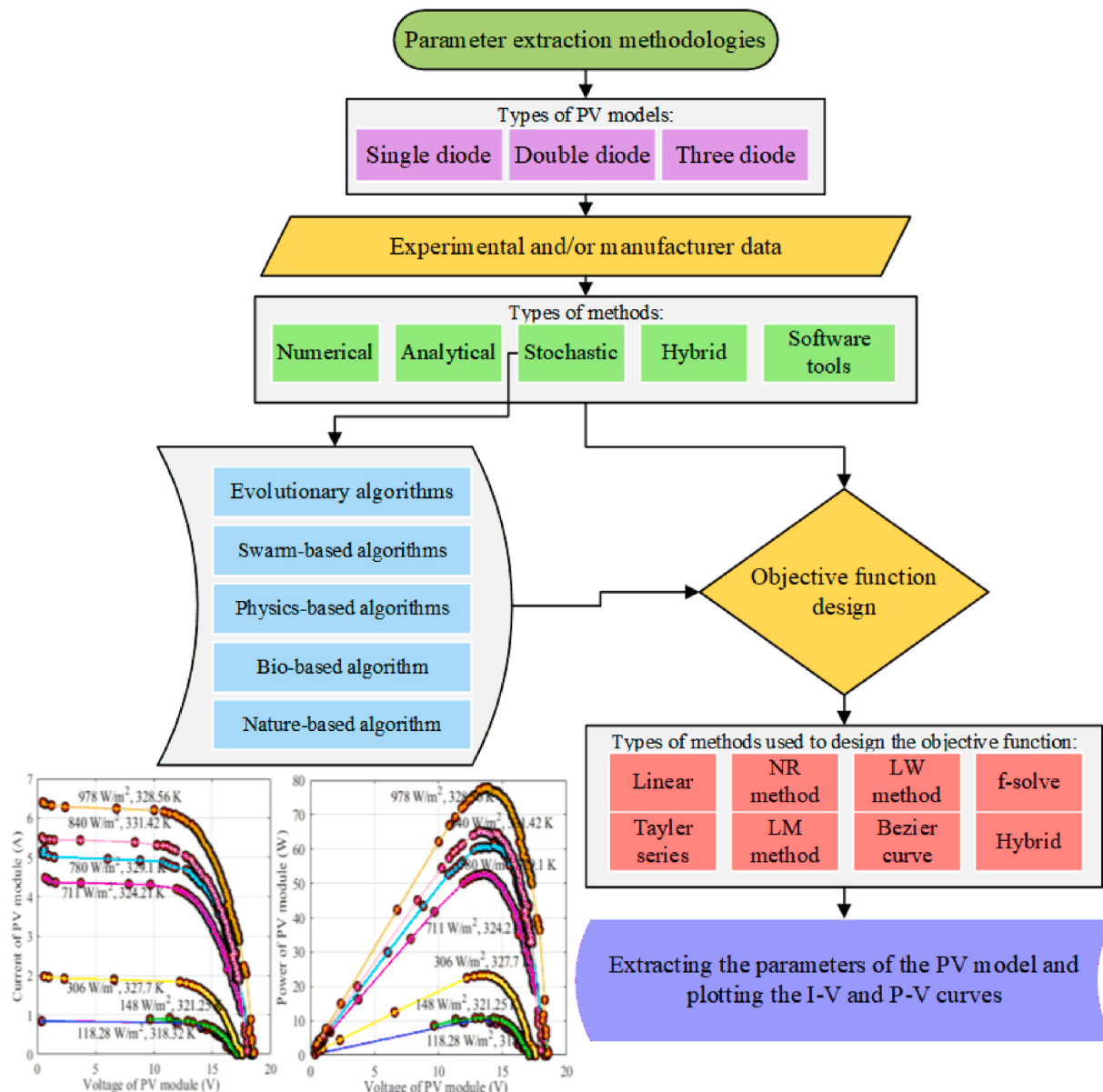


Fig. 1. Diagram of parameter extraction methodologies [19].

discuss the methodology and OFD concurrently in this research study.

The existing work and their contributions as presented in Table 1.

As per the above table, the majority of scholars employ conventional NR and LW methods, and only a few research works advance them, such as separating the I-V and P-V curves into two areas and use the NR method [46,47], substituting STF with LW in the Ref. [107], and integrating a constant LM parameter with NR method in the Ref. [20]. In Ref. [19], an integration of second order convergence NR method with adaptive LM's parameter method is addressed to estimate the SD and DD PV models named as HAOA_{ENR}. The experimental findings reveal that the proposed HAOA_{ENR} has a high-level of accuracy and agreement with experimental data for the both models. However, slow convergence and perturbation solutions are slightly appeared in extracting the TD PV model. Moreover, guaranteed convergence AOA algorithm with adaptive damping LM's parameter GCAOA_{AdLM} is proposed to only determine the parameters of the TD PV model [115]. The GCAOA_{AdLM} exhibits great experimental results in terms of methodology and OFD, which allows to minimize the RMSE to zero values for all environmental conditions. Despite considerable attempts to increase the accuracy of the PV

models, but the improvements are still not premature enough to be applied for real-world applications in the PV systems. It is worth mentioning that the OFD of the most of the analytical approaches are built at STC for the main three reference points. As a consequence, ideal climatic conditions such as 1000 W/m^2 solar irradiance and temperature of 25°C do not actually exist in real-world applications. Furthermore, these approaches are incapable of simulating the change in the parameters caused by natural oscillations during the day. To address this, it is imperative to extract the PV model's parameters from actual experimental tests made of the I-V data curves. Replicating all of the experimental data points with minimum or no error values under various weather circumstances continues to be a big challenge.

The goals of this research study are to discuss the methodologies that have obtained for objective function design. Then, presents a method to address new contributions in terms of the methodology and objective function design as given by the following:

In terms of designing objective function:

Table 1

The utilized methods in designing the objective function of the PV models.

Reference	Model	OFD	Method	Contribution
[31]	SD	NR with adaptive LM parameter	Numerical	The initial parameters are calculated iteratively. Then, using NR with an adjustable LM parameter, the PV current is forecasted.
[14]	SD, DD	LM	Analytical	The analytical expressions serve as initial values for the parameters of PV models.
[32]	SD	NR	Analytical	These parameters are extracted analytically by employing three critical points.
[33]	SD, DD	NR	Stochastic	COA is obtained to forecast the current for both PV models.
[34]	TD	NR	Hybrid	Two methods are presented: RWOA updates the population using ranking method. While HWOA incorporates cyclical exploration and exploitation stages with RWOA, HWOA outperforms other algorithms.
[35]	DD	LW	Hybrid	rbcNM algorithm is demonstrated to be more accurate while being more time intensive.
[36]	DD	Derivative of power at MPP	Hybrid	I_{ph} , I_{o1} , and R_p are analytically computed, while d_1 , d_2 , I_{o2} , and R_s are computed using DE algorithm.
[37]	TD	NR	Hybrid	HMPA is a hybrid algorithm that combines the MPA and SMA algorithms. HMPA provides a minimum RMSE and consistency.
[38]	SD, DD	NR	Stochastic	DSO is offered as a method for extracting parameter from PV models. OFD is evaluated using both Linear and NR methods.
[39]	SD, DD	NR	Hybrid	ISA is integrated with DE to enhance local and global search capabilities. The parameters extending the limits of the PV cells displays more accuracy.
[40]	SD	Derivative of power at MPP	Hybrid	The R_s , G_{sh} , and d parameters are determined using PS algorithm, while the I_{ph} and I_o parameters are analytically derived. The performance is verified by monitoring the current and power faults at MPP regions.
[41]	SD, DD, TD	LW	Hybrid	The SMA is improved by the LF mechanism, resulting more diversity of population.
[42]	SD, DD,	NR	Stochastic	FFO is employed to find the parameters of the PV models.
[43]	SD	LW	Analytical	The data-driven method is considered for solving PV model problem analytically.
[44]	SD	LW	Analytical	The PV model's parameters are analytically derived from three key points.
[45]	SD	LW	Analytical	The reduced form method is obtained to extract the five parameters.
[46,47]	SD and DD	Splitting I-V curve	Stochastic	FA is presented, and the OFD is solved by separating the I-V curve into two regions: one for computation current and another for the voltage computation.
[48]	SD and DD	NR	Stochastic	DSO is used to tackle the challenge of optimizing PV model. The authors investigate the accuracy of the Linear and NR methods.
[49]	SD	MOOP	Hybrid	The GA combined with IPM methods to extract the following parameters: d , R_s , and R_p , whereas I_{ph} and I_o are analytically derived. The STC and NOCT is consult as input information. The two objectives are treated as single objective function to be optimized.
[50,51]	SD, TD	NR	Hybrid	AWDO and IWDO are employed in this study. The Chenlo's model is used to shift from one meteorological state to another. The IWDO is enhanced by mutation and CMAES techniques.
[52]	DD	LW	Hybrid	ITLBO is improved by the use of elite learning with hybrid learning strategies.
[53,54]	SD	Derivative of power at MPP	Hybrid	DE is used to extract d , R_s , and R_p , on the other hand, I_{ph} and I_o are analytically computed. By BFA.
[55]	TD	NR	Stochastic	AEFA is presented to predict the nine parameters of the PV model.
[56]	SD, DD	NR	Hybrid	GA is employed to extract d_1 , d_2 , R_s , and R_p , whereas, I_{ph} , I_{o1} , and I_{o2} are analytically computed. The OFD is treated by NR using datasheet information and its operations are simulated by MATLAB software.
[57]	SD, DD	NR	Hybrid	WDAWOAPSO is proposed based on combination of several meta-heuristic algorithms.
[58]	SD, DD	NR	Hybrid	NLBIMA incorporates with Laplacian-based crossover search and neighborhood wandering search to better exploration and exploitation tactics.
[59]	SD	NR	Hybrid	Improved EM takes the benefit of the nonlinear formula to adjust the particle's length and total force formula is omitted.
[60]	SD, DD	NR	Hybrid	Chaotic based on Rao-1 algorithm is presented in this study for more solution diversity.
[61]	SD	LW and NR	Numerical	LSM based on NR method shows a better accuracy compared with other methods.
[28]	SD, DD, TD	NR	hybrid	Fractional chaos maps are addressed for FC-EPSO algorithm to prevent premature convergence and improve the exploration phase.
[62]	TD	Sum of SC, OC, and MPP absolute differences	Hybrid	I_{ph} and R_p are mathematically determined first, then the SFO is applied to extract seven parameters.
[18]	SD	LSM	Stochastic	PSO is used to reduce the sum of absolute errors of the PV model's current by using LSM and FF. LSM is a function built in MATLAB.
[63]	DD	Derivative of power at MPP	Hybrid	Social learning is utilized to improve DE algorithm (SL-DE), which is used to extract the $d_{1,2}$ and R_s , whilst the I_{ph} , $I_{o1,2}$, and R_p are derived analytically. OFD is based on NR which obtains I_{sc} as starting point.
[13]	SD	LM	Analytical	The SA is employed to find best value of λ of the LM algorithm.
[17]	SD	Modified TS	Analytical	The parameters are analytically computed using main three key points from datasheet which is much faster than LW method.
[9]	SD	LM	Analytical	The parameters are analytically computed based on three key points. Then, the OFS is based on LM method using 'fsolve' function.
[64]	SD, DD	LM	Analytical	The parameters two models are analytically calculated then 'fsolve' command is used as ready function in MATLAB based on LM method.
[65]	SD, DD	NR	Hybrid	Enhanced leader PSO (ELPSO) is proposed as a result of five successive mutations based on best fitness function obtained so far.
[66]	DD	NR	Hybrid	R_s and R_p are numerically computed, whilst the others five parameters are estimated using datasheet information obtained by MATLAB simulator.
[67]	SD	LW	Analytical	The PV model's parameters are extracted based on Laplace transfer function and integral based linear square system using datasheet information.
[68]	DD	LW	Analytical	This model is separated into two parts: linear, which is solved by Thevenin's theorem, and nonlinear, which is solved by piecewise linear model.
[69]	SD	GRG	Analytical	The five parameters are analytically estimated.
[70]	SD	LW	Analytical	The parameters are analytically computed from datasheet information.
[71]	SD	NR	Hybrid	I_{ph} and I_o are analytically analyzed, whereas R_p , R_s , and d are computed by EPO.
[72]	SD	Piecewise method	Numerical	The parameters are mathematically computed from template data.
[73]	DD	NR	Analytical	The seven parameters are extracted analytically from datasheet information.

(continued on next page)

Table 1 (continued)

Reference	Model	OFD	Method	Contribution
[74,75]	SD, DD	NR	Hybrid	I_{ph} and $I_{o1,2}$ are analytically analyzed, while R_p , R_s , and $d_{1,2}$ are calculated by BPFPA.
[11,76]	SD, DD	NR	Hybrid	DEIM and DEAM are improved using mutation scaling factor and crossover rate is updated by new formula.
[77]	SD, DD	NR	Hybrid	Guaranteed convergence PSO is improved by using adjusting the movements of the particles. The hyperbolic strategy is used to prevent the particles from traveling outside the search space.
[78]	SD, DD	NR	Stochastic	FPA is employed to extract the parameters of PV models.
[79]	SD, DD	NR and LM	Analytical	A comparative study of NR, LW, and GA is given. The parameters of these models are reduced to three. LW is used to analyze the R_p , R_s , and $d_{1,2}$ parameters.
[80]	SD	NR	Stochastic	MVO is employed to extract the five parameters under uniform and ununiform weather conditions.
[81,82]	SD, DD	NR	Stochastic	AEO is proposed to estimate the parameters of the PV models.
[83]	SD	Sum of SC, OC, and MPP absolute differences	Stochastic	BFO is obtained to extract the five parameters of PV model using the summation error of the key points between the expected and datasheet information.
[84]	SD	NR	Software	TRR least square algorithm implemented in MATLAB using "Fmincon" command is proposed to extract the parameters at MPP under STC.
[85]	SD	Derivative of power at MPP	Software	At STC, Powell's method is obtained to extract the parameters by PSIM software tools. R_p , R_s , and d are taken from datasheet information, and then I_{ph} and I_o are analytically derived.
[86]	SD	LW	Hybrid	The d is iteratively computed, while others derived from template data.
[87]	SD	LW	Stochastic	ALO is used to extract the five parameter of PV model.
[88]	SD, DD	NR	Hybrid	Multiswarm spiral leader PSO is multi-search mechanisms is proposed, which each swarm has a leader who provides directions to optimal solutions.
[89]	SD	LW	Analytical	The parameters are determined via three key points. The variation of d is employed to extract the other parameters.
[90]	SD, DD	Error at MPP	Stochastic	ICA is applied to determine the parameters of both models at STC.
[16]	SD, DD	Sum of SC, OC, and MPP absolute differences	Hybrid	LSHADE is employed to extract R_p , R_s , and d parameters, meanwhile I_{ph} and I_o are determined analytically. The 'fsolve' command is employed to plot I-V curve for set of optimal solutions.
[91]	SD, DD	LW	Stochastic	Several approaches are utilized to verify performance of the PV models using different types of objective function. The results indicate that the R^2 has minimal error and LW is best OFD but takes prolong time.
[92]	DD	Derivative of power at MPP	Hybrid	FWA is utilized to calculate R_p , R_s , and d parameters, while the I_{ph} and I_o are computed manually under STC.
[93]	TD	Sum of SC, OC, and MPP absolute differences	Hybrid	HHO is used to optimize R_p , R_s , and $d_{1,2,3}$, while I_{ph} and $I_{o1,2,3}$ are derived analytically at STC and NOCT.
[94]	SD, DD	NR	Hybrid	An improved mutated PSO algorithm is proposed to determine the parameters of PV models. MPSO shows better performance in terms of accuracy and stagnation avoidance.
[95]	SD, DD	NR	Hybrid	HPSOSA algorithm is proposed, the SA is connected for preventing PSO from converging prematurely. The complexity and processing time have been increased.
[96]	SD	Fit-curve method	Hybrid	Improved SSO is proposed based on three critical points obtained by manufacturer. ISSO divides the population into two parts: global and local searches. ISSO verified by using R.T.C France experimental data.
[97]	SD, DD	LW	Stochastic	The basic DE is applied to experimentally extract the parameters of PV models.
[98]	SD	LW	Hybrid	R_s and d are firstly analyzed, while R_p , I_{ph} , and I_o are calculated by using LSM under STC and experimental data.
[99]	SD, DD	NR	Hybrid	MFPA obtains a dynamic switch probability as well as dynamic step size function to improve overall performance of the proposed algorithm.
[23]	SD, DD, TD	NR and LW	Stochastic	Several meta-heuristic algorithms are employed to estimate the parameters of PV models. MPA outperformed others models. The authors prove that NR and LW can significantly enhance the performance of PV models.
[100]	SD	NR	Analytical	ACT is used to extract the parameters of PV models. The parameters are analytically derived, then five-loop iterations are used for adjustments.
[101]	SD	LW	Analytical	The five parameters of PV models analytically extracted from datasheet information.
[102]	SD	Reduced form	Analytical	Based on the main three points equations, the five equation is reduced to two R_s and d , then graphical optimization method is employed to solve the PV equation. The other parameters are derived mathematically.
[103]	SD, DD	NR	Hybrid	Chaotic heterogeneous comprehensive learning PSO is proposed to extract the parameters of static and dynamic PV models. The population is divided into two parts. A comprehensive learning and learning probability procedures are obtained to improve its performance. While chaotic tactics is used to avoid premature convergence.
[104]	SD, DD	NR	Hybrid	Hybrid Rao is proposed to extract the parameters of the static and dynamic PV models. The chaotic map and performance learning strategies are employed to improve the exploration and exploitation phases.
[105]	SD	LW	Analytical	R_p , R_s , I_{ph} , and I_o parameters are firstly derived by LW. Then, these equations are obtained to be solved by NR method. The d parameter is analytically determined. This method is complicated due to procedure obtained to extract the parameters of PV model.
[106]	SD, DD	NR	Hybrid	TVACPSO is presented to extract the parameters of PV models. An acceleration coefficient is linearly increased to improve its performance using large number of population size.
[107]	SD	STF	Numerical	Ranking based branch selection and modified NM algorithm is proposed in this study. When the STF objective function was replaced with LW, the accuracy improved. However, the distinction is trivial between them.
[29]	SD, DD	LW and NR	Stochastic	MPA is employed with seven levels of experimental. The results show that the LW has better convergence at high voltage ranges.
[108]	SD	NR	Hybrid	Boosted HHO method is improved using Levy flight and mutation trajectories. The exploration and exploitation phases are significantly improved.
[20]	TD	Improved NR	Hybrid	Enhanced LSHADE method is proposed by using guided-chaotic strategy to enrich the population diversity during the second half of iterations.
[109]	TD	NR	Hybrid	Improved AVO is enhanced by obtaining OBL and OL. IAVO boosts the convergence rate.
[110]	SD, DD	NR	Stochastic	The traditional SFS algorithm is introduced to experimentally optimize the PV models.
[111]	SD, DD, TD	NR	Stochastic	MRFO is proposed to experimentally estimate the parameters of PV models.

(continued on next page)

Table 1 (continued)

Reference	Model	OFD	Method	Contribution
[112]	TD	NR	Hybrid	Premature convergence and ranking based updating methods are integrated to enhance the GNGO algorithm.
[113]	DD	NR	Hybrid	Hybridized WDO's exploitation and Fruit Fly's exploration are presented in this study.
[114]	SD	ImLM	Analytical	A new reduced form based on Brent's algorithm is implemented to calculate the initial values.
[19]	SD, DD	LM's adaptive parameter and NR	Hybrid	Hybridized of AOA is proposed by LF and Brownian tactics. The population is divided into two phases. Then, chaotic map and mutation technique are included.

- The third order of the modified NR method is proposed to prioritize the estimation of the initial roots solution of the PV models.
- An adaptive LM parameter is applied to mimic the nonlinearity of the PV models' equation and reduce the oscillations.
- New quadratic and fourth convergences are addressed in order to broaden the problem's search space.

In terms of methodologically and algorithmically:

- The population is separated into two subpopulations to appropriately maintain an optimal between exploration and exploitation.
- For better global search and local optima avoidance, we use nonlinear equation, levy flight mechanism, and randomized Gaussian function.
- To direct the local search strongly, dynamic probability factors based on Cauchy distribution are provided, including the current, best, and worst solutions.
- To modify solutions that have exceeded their lower and upper bounds, a transition from localized to global tactic is proposed.
- A rigorous exploration and exploitation mechanism based on a pre-defined number of iterations is provided to ensure that the AOA converges throughout problem optimization.
- The proposed novel GCAOA_{EmNR} is intended to experimentally determine the parameters of the SD, DD, and TD PV models at different environmental circumstances and compared to numerous well-published methodologies utilizing a range of statistical criteria.

This paper is structured as follows: Section 2 discusses the PV model and OFD. The proposed AOA method and its advancements are discussed in Section 3. The findings, discussion, and performance comparison with various well-known algorithms are presented in Section 4. Section 5 concludes the study findings and recommendations for future research.

2. Photovoltaic model and objective function design

In this work, real experimental data is obtained from various climates conditions to validate and analyze the performance of the SD, DD, and TD PV models. Tables 2 and 3 detail the characteristics of the PV module under STCs and the number of the I-V data points at different of environmental conditions [11].

2.1. Single diode PV model

This is the most often applied PV model in the literature owing to its simplicity, needing only five physical parameter to be optimality extracted. The five physical parameters are as follows: an ideality factor d linked in opposite direction to represent the PV cell's output voltage, a parallel-connected photovoltaic current source I_{ph} in (A) parallelly connected, a diode saturation current I_o , a small series resistance R_s in (Ω), and a large shunt resistance R_p in (Ω) linked in parallel to describe the saturation current of the diode. Fig. 2, illustrates The physical parameters of the SD PV model. Therefore, utilizing Kirchhoff's rule, the output current of the cell I in (A) can be calculated as follows:

$$I = I_{ph} - I_d - I_p \quad (1)$$

where I_d represents the current flowing through diode in (A) and I_p refers to the current flowing through the shunt resistor in (A). The I_d may be computed by deriving Shockley diode law in the following manner:

$$I = I_o \left[\exp \left(\frac{V + IR_s}{V_t} \right) - 1 \right] \quad (2)$$

where V is the output voltage (V) and V_t refers to the thermal diode voltage (V). The V_t can be computed as follows:

$$V_t = \frac{dKBT_c}{q} \quad (3)$$

Where KB is the Boltzmann's constant ($1.38 \times 10^{-23} J/K$), T_c refers to the cell temperature (K), and q is to the electron charge ($1.60 \times 10^{-19} C$). The I_p is expressed by the following:

$$I_p = \frac{V + IR_s}{R_p} \quad (4)$$

As a result of solving Eqs. (1)–(4), the I is described using the following equation:

$$I = I_{ph} - I_o \left[\exp \left(\frac{V + IR_s}{V_t} \right) - 1 \right] - \frac{V + IR_s}{R_p} \quad (5)$$

Therefore, the five parameters (d , I_{ph} , I_o , R_s , and R_p) must be determined in order to plot the I-V and P-V characteristics curves [116].

2.2. Double diode PV model

The DD PV model is then employed to compensate the preceding PV model's poor accuracy. This model has a superior accuracy, especially at high solar irradiance conditions [19]. A second diode d_2 is inserted to reflect the recombination losses that occur in the depletion zone. Fig. 3 depicts the physical electrical components of the DD PV model, whereas the output current is represented as follows:

$$I = I_{ph} - I_{o1} \left[\exp \left(\frac{V + IR_s}{V_{t1}} \right) - 1 \right] - I_{o2} \left[\exp \left(\frac{V + IR_s}{V_{t2}} \right) - 1 \right] - \frac{V + IR_s}{R_p} \quad (6)$$

where I_{o1} and I_{o2} are reverse diode saturation currents, and V_{t1} and V_{t2} are diode thermal voltages written as follows:

$$V_{t1} = \frac{d_1 KBT_c}{q}, \quad V_{t2} = \frac{d_2 KBT_c}{q} \quad (7)$$

where d_1 and d_2 denote to the first and second ideality factors of the diodes, respectively. It is worth noting that extracting the seven parameters from the DD PV model involves additional computing time.

2.3. Three diode PV model

The TD PV model has garnered more attention from scholars and academics due to its great accuracy in compared to prior PV models, which included another diode ideality factor d_3 and saturation dark current I_{o3} . Fig. 4 exhibits the electrical equivalent circuit of the TD PV model, while the output current may be described as follows [115]:

$$I = I_{Ph} - I_{o1} \left[\exp\left(\frac{V + IR_s}{V_{t1}}\right) - 1 \right] - I_{o2} \left[\exp\left(\frac{V + IR_s}{V_{t2}}\right) - 1 \right] - I_{o3} \left[\exp\left(\frac{V + IR_s}{V_{t3}}\right) - 1 \right] \frac{V + IR_s}{R_p} \quad (8)$$

where V_{t1} , V_{t2} , and V_{t3} are the diode's thermal voltage and expressed by the following:

$$V_{t1} = \frac{d_1 KBT_c}{q}, \quad V_{t2} = \frac{d_2 KBT_c}{q}, \quad \text{and} \quad V_{t3} = \frac{d_3 KBT_c}{q} \quad (9)$$

This model is complicated, and needs more computing time to extract its nine parameters.

2.4. State-of-the Art

2.4.1. Objective function design

The primary objective of the PV model's design and parameter extraction is to minimize the disparity between the predicted and experimental currents at a range of meteorological conditions. Thus, the estimate of the five, seven, and nine parameters may be described by considering RMSE as a fitness function that must to be reduced.

The equations (5), (6) and (8) are nonlinearity explicit transcendent equations with five, seven, and nine unknown parameters, respectively. As per the literature [7,23], the Lambert W function and NR methods are frequently obtained to determine the parameters of the PV models. Nevertheless, these methods' decision-maker on how to spread solutions in the feature space are limited by the LW function's approximation mechanism and the NR method derivative order. As a result, we presented a new medications for further guessing initial points in the search space of the problem. The NR, Lambert W function, and the new modified third-order NR methods are given as follows:

2.4.2. Newton Raphson method

The NR methods is able to solve nonlinear and multi-variable equation to specific range of error. Therefore, the parameters of the SD, DD, and TD PV models can be determined and then plotting the I-V and P-V characteristics curves at a variety of climatic conditions, which is written by Ref. [11]:

For the SD PV model:

$$I = I - \frac{I_{Ph} - I - I_{o1} \left(\exp\left(\frac{V+R_s I}{d_1 V_t}\right) - 1 \right) - \frac{V+R_s I}{R_p}}{-1 - I_{o1} \left(\frac{R_s}{d_1 V_t} \right) \exp\left(\frac{V+R_s I}{d_1 V_t}\right) - \frac{R_s}{R_p}} \quad (10)$$

For the DD PV model:

$$I = I - \frac{I_{Ph} - I - I_{o1} \left(\exp\left(\frac{V+R_s I}{d_1 V_t}\right) - 1 \right) - I_{o2} \left(\exp\left(\frac{V+R_s I}{d_2 V_t}\right) - 1 \right) - \frac{V+R_s I}{R_p}}{-1 - I_{o1} \left(\frac{R_s}{d_1 V_t} \right) \exp\left(\frac{V+R_s I}{d_1 V_t}\right) - I_{o2} \left(\frac{R_s}{d_2 V_t} \right) \exp\left(\frac{V+R_s I}{d_2 V_t}\right) - \frac{R_s}{R_p}} \quad (11)$$

For the TD PV model:

$$I = I - \frac{I_{Ph} - I - I_{o1} \left(\exp\left(\frac{V+R_s I}{d_1 V_t}\right) - 1 \right) - I_{o2} \left(\exp\left(\frac{V+R_s I}{d_2 V_t}\right) - 1 \right) - I_{o3} \left(\exp\left(\frac{V+R_s I}{d_3 V_t}\right) - 1 \right) - \frac{V+R_s I}{R_p}}{-1 - I_{o1} \left(\frac{R_s}{d_1 V_t} \right) \exp\left(\frac{V+R_s I}{d_1 V_t}\right) - I_{o2} \left(\frac{R_s}{d_2 V_t} \right) \exp\left(\frac{V+R_s I}{d_2 V_t}\right) - I_{o3} \left(\frac{R_s}{d_3 V_t} \right) \exp\left(\frac{V+R_s I}{d_3 V_t}\right) - \frac{R_s}{R_p}} \quad (12)$$

Table 2

Technical datasheet for the Kyocera (KC120-1) PV module.

Characteristics	Value
Maximum power at STC (P_{mp})	120 Wp
Open-circuit voltage (V_{oc})	16.9 V
Short-circuit current (I_{sc})	7.45 A
MPP's current (I_{mp})	7.1 A
MPP's voltage (V_{mp})	16.9 V
Number of connected cells in series	36
Nominal Operation Cell Temperature (NOCT)	43.6 °C
Temperature coefficient of I_{sc} (α)	1.325 mA/k
Temperature coefficient of V_{sc} (β)	-77 mV/k

2.4.3. Lambert W function method

The lambert W function is produced to account the voltage-current implicit coupling due to its considerable degree of accuracy, particularly at heterogeneous operating temperatures [52,117,118]. Thus, the output currents of the SD, DD, and TD PV models that use the Lambert W function are as follows:

For the SD PV model:

$$I = \frac{R_p(I_{Ph} + I_{o1}) - V}{R_p + R_s} - \frac{V_t}{R_s} [d_1 W(\beta_1)] \quad (13)$$

For the DD PV model:

$$I = \frac{R_p(I_{Ph} + I_{o1} + I_{o2}) - V}{R_p + R_s} - \frac{V_t}{R_s} [d_1 W(\beta_1) + d_2 W(\beta_2)] \quad (14)$$

For the TD PV model:

$$I = \frac{R_p(I_{Ph} + I_{o1} + I_{o2} + I_{o3}) - V}{R_p + R_s} - \frac{V_t}{R_s} [d_1 W(\beta_1) + d_2 W(\beta_2) + d_3 W(\beta_3)] \quad (15)$$

where

$$\begin{aligned} \beta_1 &= \frac{I_{o1} R_s R_p}{d_1 V_{t1} (R_s + R_p)} \exp\left\{\frac{R_p(R_s I_{Ph} + R_s I_{o1} + V)}{d_1 V_{t1} (R_s + R_p)}\right\}, \\ \beta_2 &= \frac{I_{o2} R_s R_p}{d_2 V_{t2} (R_s + R_p)} \exp\left\{\frac{R_p(R_s I_{Ph} + R_s I_{o2} + V)}{d_2 V_{t2} (R_s + R_p)}\right\}, \text{ and} \\ \beta_3 &= \frac{I_{o3} R_s R_p}{d_3 V_{t3} (R_s + R_p)} \exp\left\{\frac{R_p(R_s I_{Ph} + R_s I_{o3} + V)}{d_3 V_{t3} (R_s + R_p)}\right\} \end{aligned} \quad (16)$$

2.4.4. The proposed efficient modified Newton-Raphson (EmNR) method

Considering quick coverage of the NR and Lambert W function's perceived accuracy at specified levels of meteorological conditions [29, 79], there are some immovable impediments, including the following:

Table 3

Experimental conducted in a variety of meteorological conditions [11].

Operating condition	S_1	S_2	S_3	S_4	S_5	S_6	S_7
Length of data points	22	24	50	91	92	101	102
Weather condition (W/m^2)	118.28	148	306	711	780	840	978
Cell temperature (K)	318.32	321.25	327.7	324.21	329.1	331.42	328.56

- The basic NR method may approach different initial roots at multi-variable optimization problem resulting in not enough approximation to the desired roots.
- Increasing the number of entire iterations does not increase the accuracy of the chosen initial roots as the successive approximations continue to alternate back and forth between the solutions.
- In all previous forms of the objective function, having a collection of vectors containing the best solution imposes restrictions on achieving globally.
- Effects of noise associated experimental measurements.
- Oscillatory action in PV cells and intermittent of solar irradiance in environment may result in an accurate evolution of the PV cell's performance.
- Their precision degrades when data points with rough and zigzag edges are found at I-V and P-V curves.

Generally, the minimum global guaranteed solutions may be derived by disregarding the oscillation, highly nonlinearity, and fluctuation characteristics of the PV model's equation. This may be performed by combining third order of NR method with an adjustable Levenberg parameter (λ), in addition to the newly modified second and fourth convergence as shown below [119]:

$$I = I - \lambda \frac{2 \times F(X)^4}{[F_3'(X+1) + F_1'(X)]^2} \quad (17)$$

where $F_1'(X+1)$ is the first order derivative of $F(X)$ with respect $(X+1)$ [120], $F_3'(X+1)$ is the third order derivative of $F(X)$, and λ is computed by Ref. [121],

$$e^{-\left(\frac{5C_{iter}}{M_{iter}}\right)^{2.5}} \quad (18)$$

It is important to explain how the new modified NR method is constructed. At first step, the first order derivative is utilized. Then, the second order derivative is obtained in the second step. Finally, the third order derivative the PV model's equation is employed in the third step. The number of the iteration is utilized for one time at first, second, and third derivative orders to provide the best stability, accuracy, and prediction for the initial root values. In the proposed method, the approximate to the roots value is involved by a trapezoid scheme as shown in Fig. 5. The MATLAB code of the proposed EmNR method is given in Appendix 1.

In this work, the adaptive Levenberg parameter (λ) with modified NR method is proposed to formulate the objective function [122,123]. Premature convergence is indeed prevented at all weather situations and

even at sharp I-V and P-V curves data points [121]. Accordingly, the objective function is expressed as follows:

$$RMSE = \sqrt{1/N \sum_{i=1}^N P(V_e, I_e, \theta)^2} \quad (19)$$

where N denotes to the size of the I-V data curve, V_e and I_e refer to the experimental voltage-current for PV model, and θ is the vector holding the parameters that must to be adequately extracted.

3. The arithmetic optimization algorithm (AOA)

The Arithmetic optimization algorithm (AOA) is comparable to previous population-based optimization approaches published in 2021 by Abualigah et al. [124]. Multiplication ($M \times$), Division ($D \div$), Subtraction ($S -$), and Addition ($A +$) are mathematical operators arithmetic operators that established the diversity and exploitative stages in AOA.

3.1. Inspiration

Arithmetic is necessary but sufficient conditions for number theory, analysis, algebra, modern mathematics, and geometry. As a result, these four straightforward operators may be employed to locate the optimal solutions while maintaining between the exploration and exploitation periods.

3.2. Initialization phase

The first phase is used to establish a list of possible solutions (X). The best solution from all iterations is preserved as the most optimal solutions found so far.

$$X = X_{LB} + rand(X_{UB} - X_{LB}) \quad (20)$$

where X is a collection of initialized solutions, $rand$ is a random variable between $[0,1]$, X_{UB} and X_{LB} determine the upper and lower limits of the problem. The Math Optimizer Accelerated (MOA) function is utilized to distinguish the exploration and exploitation stages, which is computed as follows:

$$MOA(C_{iter}) = Min + C_{iter} \times \left(\frac{Max - Min}{M_{iter}} \right) \quad (21)$$

where $MOA(C_{iter})$ defines the value at the t th iteration and C_{iter} indicates the current iteration and its range between 1 and the maximum number of iteration's (M_{iter}). The accelerated function's maximum and lowest

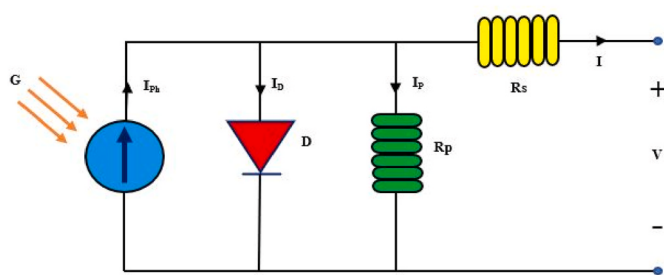


Fig. 2. The electrical circuit of the SD PV model.

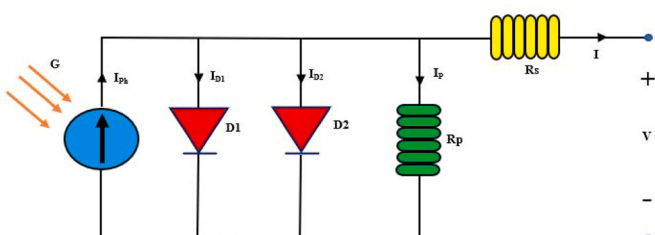


Fig. 3. The electrical circuit of the DD PV model.

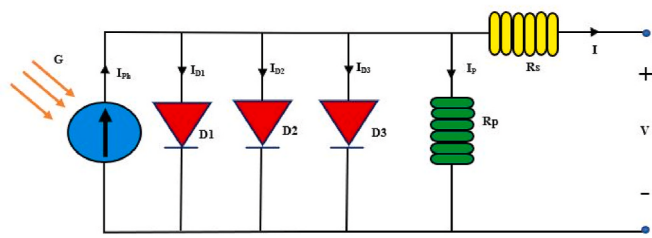


Fig. 4. The electrical circuit of the TD PV model.

values are denoted by *Max* and *Min*. The next sections will go into depth about the exploration and exploitation stages.

3.3. Exploration stage

Due to their widely distributed values in design space, the *D* or *M* operators are employed for the exploratory phase. The exploration phase is confined by the MOA function: if the $r_1 > \text{MOA}$ is identified, the *D* and *M* operators are utilized; otherwise, the *A* and *S* operators are maintained. The exploration part can be expressed by the following equations:

$$x_{i,j}(C_{iter}+1) = \begin{cases} \text{best}(x_j) \div (MOP + \epsilon) \times ((UB_j - LB_j) \times \mu + LB_j) & r2 > 0.5 \\ \text{best}(x_j) \times MOP \times ((UB_j - LB_j) \times \mu + LB_j) & \text{otherwise} \end{cases} \quad (22)$$

where r_2 is randomly generated number that is conditioned between the *D* and *M* operations. UB_j and LB_j represent the lower and upper limits, respectively; ϵ is a tiny integer value, and μ is a control variable set to 0.5 to alter the search procedure.

$$MOP(C_{iter}) = 1 - \frac{C_{iter}^{1/\alpha}}{M_{iter}^{1/\alpha}} \quad (23)$$

in this case Math Optimizer Probability is a coefficient denoted by the symbol (*MOP*) and α is a sensitive control parameter set to 5, which specifies accuracy of the exploitation across the iterations.

3.4. Exploitation stage

Although the *A* and *S* operators have a high degree of density, they are readily approachable owing to their modest dispersion. The *S* and *An* operators may be represented in the following manner:

$$x_{i,j}(C_{iter}+1) = \begin{cases} \text{best}(x_j) - MOP \times ((UB_j - LB_j) \times \mu + LB_j) & r3 > 0.5 \\ \text{best}(x_j) + MOP \times ((UB_j - LB_j) \times \mu + LB_j) & \text{otherwise} \end{cases} \quad (24)$$

where r_3 is a randomly generated number that serves as a denotation for the *A* and *S* operators.

3.5. The proposed guaranteed convergence AOA procedure

Numerous restrictions in the fundamental AOA diminish its performance, especially when dealing with high-dimensional, multi-nonlinearity, and challenging optimization problems. Thus, the proposed improvements make an effort to ensure convergence to optimal solutions at each execution. Once the optimization process starts, the poorest solution is abandoned in favor of the best one found so far. This procedure will be repeated indefinitely. Additional enhancements to the planned GCAOA_{EmNR} include the following:

3.5.1. Improved exploration stage

We divided the population into two groups by employing four arithmetic operators: the following section summarizes the exploration phase:

$$x_{i,j}(C_{iter}+1) = \begin{cases} \text{best}(x_j) \div (Mu + \epsilon) \times ((UB_j - LB_j) \times RL_{i,j} + e_j) & r2 > 0.5 \\ \text{best}(x_j) \times F_1 \times (Bst_j - x_{i,j}) - F_2 \times (Wrst_j - x_{i,j}) & \text{otherwise} \end{cases} \quad (25)$$

where *Mu* is expressed by,

$$Mu = 2e^{-\left(\frac{4C_{iter}}{M_{iter}}\right)^2} \quad (26)$$

where *Mu* is critical in enhancing the diversity of solutions during the early stages of optimization and assuring the intensification during the latter stages of optimization, e_j is randomly vector based on Gaussian or other probability [129], F_1 and F_2 represent two factors derived utilizing Cauchy distribution with ranges of [0, 1] [130], $RL_{i,j}$ is Levy flight mechanism with randomly selected step sizes depending on the probability function and expressed by,

$$RL_{i,j} \approx |L_j|^{1-\alpha} \quad (27)$$

where L_j defines to the flight's length and the power-exponent's law is between [1,2,131]. In integral form, the probability density of the Levy distribution is written as [132]:

$$f_L(x, \mu, \sigma) = \frac{1}{\pi} \int_0^{\infty} \exp(-\gamma q^{\alpha}) \cos(qx) dq \quad (28)$$

where α is the distribution index that may adjust the process's scale attributes, and γ is obtained to determine the scale unit. When the integral is equal 2, it represents Gaussian distribution; when α is equal 1, it represents a Cauchy distribution [133]. When x exceeds a certain value, a series expansion approach is necessary, as demonstrated by the following:

$$f_L(x, \mu, \sigma) = \frac{\gamma \Gamma(1+\alpha) \sin\left(\frac{\pi \alpha}{2}\right)}{\pi x^{(1+\alpha)}}, \quad x = \infty \quad (29)$$

where Γ refers the gamma function in which $\Gamma(1+\alpha)$ equals to $\alpha!$. According to Ref. [132], α was between 0.3 and 1.99. The Mantegna technique is utilized in this study to create a random number using Levy distribution, as shown by the following:

$$\text{Lvy}(\alpha) = 0.05 \times \frac{x}{|y|^{1/\alpha}} \quad (30)$$

where y and x are variables with normal distribution that may be presented as follows:

$x = \text{Normal}(0, \sigma_x^2)$, and $y = \text{Normal}(0, \sigma_y^2)$, where the σ_x can be calculated as follows:

$$\sigma_x = \left[\frac{\Gamma(1+\alpha) n \left(\frac{\pi \alpha}{2} \right)}{\Gamma\left(\frac{(1+\alpha)}{2} \right) \alpha 2^{\frac{\alpha-1}{2}}} \right]^{1/\alpha}, \quad \text{where, } \sigma_y = 1 \text{ and } \alpha = 1.5. \quad (31)$$

The Levy mechanism combines small steps sizes with large jumps. Bst_j and $Wrst_j$ are the current iteration's best and worst solutions.

3.5.2. Improved exploitation stage

The *S* operator is critical for traversing from local to global levels,

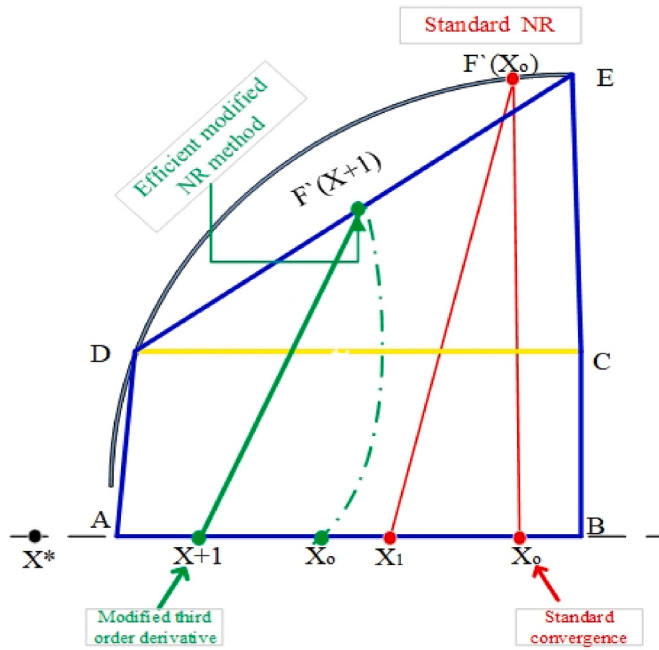


Fig. 5. Area approximation by the trapezoid ABED of the modified NR method [120].

particularly when addressing the Gaussian distributions and Levy flight mechanisms are involved. By utilizing the *Mu* mechanism's small step size, the *A* operator permits decision-making to discover the most optimal solution given neighborhood information

Generalized Opposition Learning (GOL) mechanism may be obtained to effectively locate the search space's furthest region [134]. The GOL is strengthen by incorporating with RL tactic, then this vector will be included to the population [135]. Remember that RL is very capable of transforming from its current location to new unexplored places. The improved (IGOL) is defined as,

$$x_{i,j}^{IGOL} = x_{new,i} + RL_i \times (\text{rand} \times (A_j + B_j) - x_{new,i}); \text{ where: } x_i^{IGOL} \in [A_j, B_j]; j = 1, 2, \dots, D \quad (34)$$

$$x_{i,j}(C_{iter} + 1) = \begin{cases} \text{best}(x_j) - Mu \times ((UB_j - LB_j) \times RL_{i,j} + e_j) & r2 > 0.5 \\ \text{best}(x_j) + F_1 \times (Bst_j - x_{i,j}) - F_2 \times (Wrst_j - x_{i,j}) & \text{otherwise} \end{cases} \quad (32)$$

3.5.3. Particle transition from the locality to optimum areas

Throughout the optimization process, and as a consequence of the usage of various random tactics, some of newly produced solutions crossed the optimization problem's upper and lower bounds. The majority of optimization methods provide simple lower and upper bounds, which might slow down the convergence rate to optimum solutions. To address this shortcoming, we presented the following mathematical model for transforming particles from predetermined upper and lower boundaries to near-optimum areas:

$$x_{i,j} = \text{best}(x_j) + \epsilon \times (\text{rand} \times (UB_j - LB_j)) \times \text{rand} \times LB_j \quad (33)$$

The aforesaid equations significantly increase the diversity of the previously discovered best optimum solutions. This means that not only are particles moved from their locality to their optimum new areas, but the quality of the solutions is also improved by gaining information from the best particle's neighborhood.

3.5.4. Mechanism for systematic exploration and exploitation

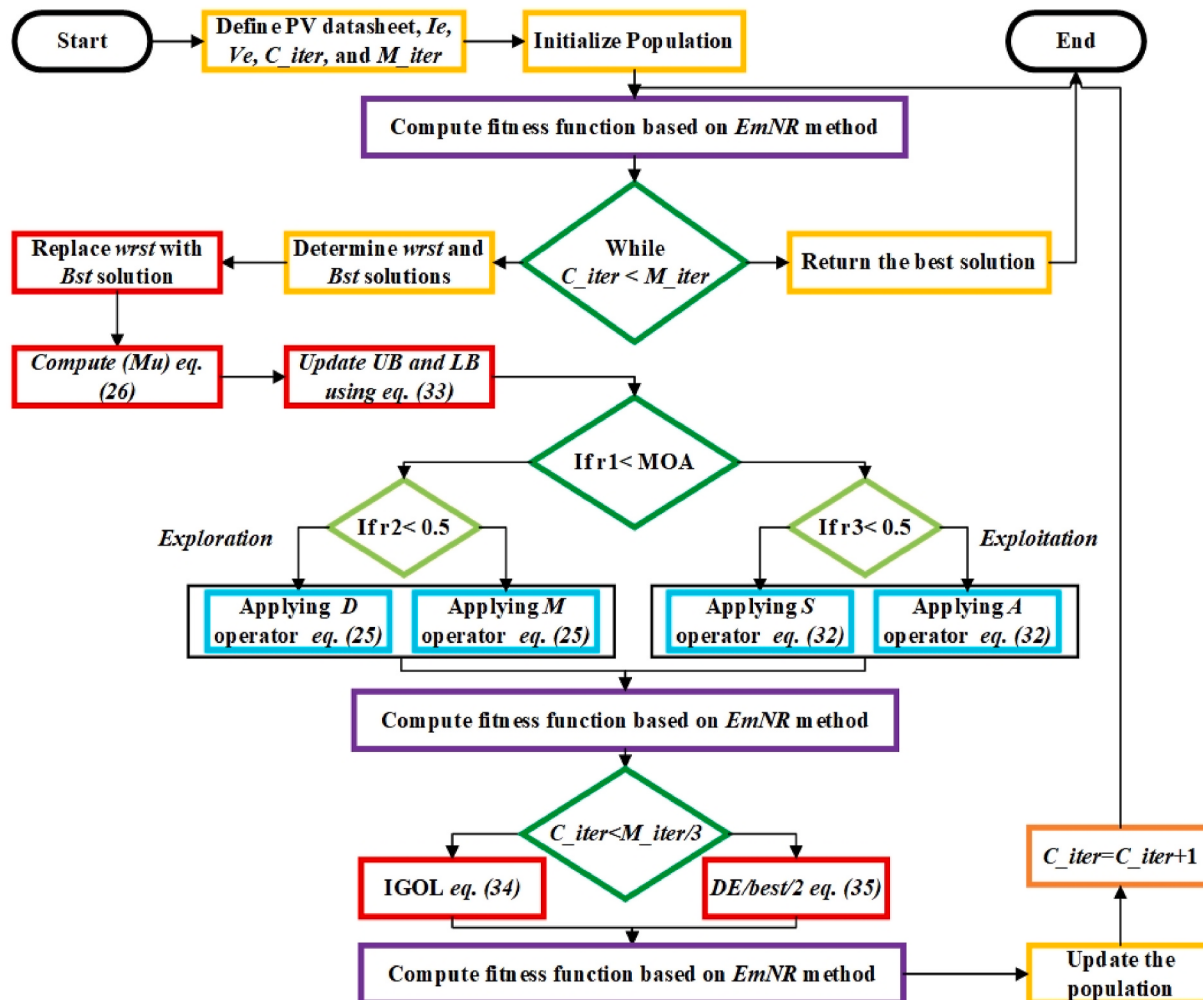
When the exploration and exploitation steps are complete, the

where A_j and B_j denotes the current iteration's lowest and maximum values. Therefore, IGOL guards the algorithm against premature convergence and locality [136]. After various possible improvements to the proposed algorithm's performance, we determined that the IGOL strategy becomes unsuccessful after tertiary sector of the population. As an outcome, we expanded the methodology by acquiring a well-established and promising (DE/best/2/bin) mutation strategy for the remaining generations. As such, this approach considers any little changes in the value of any variable that might remarkably lower the RMSE. Thus, is then obtained to ensure the completion of such a difficult work, as detailed in [137]:

$$x_i(C_{iter} + 1) = \text{best}(x_j) + F_1 \times (\text{best}(x_j) - x_{new,3}) + F_2 \times (x_{new,1} - x_{new,2}) \quad (35)$$

where *best* is the best obtained solution, and $x_{new,1-3}$ denote three distinct vectors randomly picked the population. This procedure will be repeated until the stopping requirement is fulfilled. Fig. 6 illustrates the operation and comprehensive process of the GCAOA_{EmNR}.

The proposed GCAOA leverages several integrations strategies to randomly explore the search space of the TD PV model during the exploration phase, employing nonlinear formulae, Levy flight and Gaussian distributions. Whereas the *Best*, *Bst*, two scaling factors, and *Wrst* vectors are quite useful for performing local searches. Furthermore, the worst solution is exchanged with best current solution at each gen-

Fig. 6. Flowchart of the proposed GCAOA_{EmNR}.

eration, taking the new updating boundary strategy into account. Please bear in mind that even minor variations in the values of any parameter in the SD, DD, and TD PV models have a major effect on the findings. Lastly, the systematic explorer-exploiter technique is constructed to ensure convergence and avoidance of localities throughout each execution. The first 166 iterations are performed using IGOL, while the remaining iterations are accomplished using the robust mutation DE/best/2/bin scheme. This is seen in the result sections' evaluations of the fitness function. However, the GCAOA is more advanced and needs much more processing time than conventional AOA. Bear in mind that the parameters estimation of the PV models are offline optimization problem, and computation time is irrelevant to the PV models' accuracy.

4. Experimental results and discussions

The proposed GCAOA_{EmNR} model is employed to forecast the parameters of the SD, DD, and TD PV models at diverse climatic circumstances based on numerous criteria analyses. Along with the experimental data from the Kyocera (KC120-1) PV module, comparisons are made utilizing four distinct objective function designs for the GCAOA, namely GCAOA_{mNR}, GCAOA_{INR}, GCAOA_{LW}, and GCAOA_{NR}, respectively. Meanwhile, the articles are chosen based on their parallel treatment of methodology and objective function design. These

approaches are: GCAOA_{AdLM} [115], HAOA_{ENR} [19], AEO_{NR} [81], ELPSONR [65], ELSHADE_{INR} [20], FFA_{NR} [43], MPA_{LW} [23,29], MPSO_{NR} [94], MRFO_{NR} [111], ALO_{LW} [87], ImSMA_{LW} [41], CHCLPSO_{NR} [103], and DEAM_{NR} [76]. The utilized statistical criteria to experimentally evaluate the performance of these algorithms are: Root Mean Square Error (RMSE), Mean Bias Error (MBE), DRMSE deviation of solar radiation's levels (d_i), Determination Coefficient (R^2), Test Statistical (TS), Absolute Error (AE), and CPU-execution time. For fair comparison, all environmental settings are assumed to be the same, including the search space of the nine variables [20,29], where the maximum number of iterations (M_{iter}) is 500, size of the population is 30 (N), dimension (Dim) of the problem is 9, and each algorithm is executed 30 times for each level of weather conditions (S_{1-7}). It is worth noting that the **Boldface** are remarked for having the best statistical values across all tables.

4.1. Results on single diode PV model

The extracted parameters of the SD PV model utilizing the proposed GCAOA_{EmNR} model and other peers at various experimental unlight and ambient temperature conditions is tabulated in Table 4. It is clear that the d is within feasible ranges of the of the problem dimension, which are (1.0309–1.5570). This is because the defect density has increased, reflecting the improvement in Donor-Acceptor pairings [138]. The I_{ph}

Table 4

Parameters extracted from the SD PV model using various approaches.

Parameter	Method	S_1	S_2	S_3	S_4	S_5	S_6	S_7
d	GCAOA _{EmNR}	1.5570	1.3748	1.0309	1.3573	1.3627	1.3621	1.2646
	GCAOA _{AdLM}	1.5488	1.3007	1.3293	1.4136	1.3656	1.3338	1.3778
	HAOA _{ENR}	1.4216	1.5127	1.4208	1.3347	1.1178	1.3416	1.0629
	GCAOA _{InNR}	1.0000	1.0000	1.0000	1.1759	1.2198	1.3490	1.3770
	GCAOA _{mNR}	1.5626	1.4980	1.4201	1.4184	1.3932	1.3589	1.2626
	GCAOA _{NR}	1.0000	1.0000	1.0000	1.1764	1.2428	1.3492	1.3771
	GCAOA _{LW}	1.0000	1.0004	1.0000	1.1764	1.2428	1.3492	1.3771
	AEO _{NR}	1.0055	1.1958	1.0337	1.2114	1.2427	1.3492	1.3771
	ELPSO _{NR}	1.0000	1.3140	1.1315	1.1979	1.2319	1.3492	1.3772
	ELSHADE _{INR}	1.0040	1.2282	1.0240	1.1827	1.2198	1.3490	1.3770
	FFA _{NR}	1.2061	1.3282	1.1491	1.2544	1.3633	1.3485	1.3771
	MPA _{LW}	1.0000	1.3246	1.1387	1.2492	1.2835	1.3492	1.3771
	MPSO _{NR}	1.2630	1.4714	1.2319	1.3775	1.3582	1.3475	1.3756
	MRFO _{NR}	1.0680	1.2741	1.1562	1.2375	1.2603	1.3492	1.3771
	ALO _{LW}	1.3448	1.4525	1.0934	1.0797	1.2878	1.3266	1.3647
	ImSMA _{LW}	1.0000	1.3743	1.0000	1.1921	1.2748	1.1998	1.3771
	CHCLPSO _{NR}	1.2978	1.3562	1.1959	1.2782	1.2901	1.3491	1.3771
	DEAM _{NR}	1.0000	1.1478	1.0004	1.1764	1.2458	1.3492	1.3771
I_{ph}	GCAOA _{EmNR}	0.8067	0.9602	1.9421	4.4545	5.4916	5.8938	6.7673
	GCAOA _{AdLM}	0.8792	0.9978	1.9596	4.4160	5.2462	5.5307	6.6678
	HAOA _{ENR}	0.6595	0.7915	1.9606	4.4995	5.7425	5.7804	7.0524
	GCAOA _{InNR}	0.8406	1.0545	1.9714	4.4472	5.1663	5.5482	6.4669
	GCAOA _{mNR}	0.9232	1.0253	2.0398	4.5312	5.4318	5.8750	6.7711
	GCAOA _{NR}	0.8403	1.0537	1.9713	4.4473	5.1631	5.5493	6.4691
	GCAOA _{LW}	0.8403	1.0597	1.9713	4.4473	5.1631	5.5493	6.4691
	AEO _{NR}	0.8359	0.9994	1.9602	4.4402	5.1631	5.5493	6.4691
	ELPSO _{NR}	0.8337	0.9699	1.9548	4.4466	5.1570	5.5427	6.4609
	ELSHADE _{INR}	0.8394	0.9865	1.9727	4.4463	5.1663	5.5482	6.4669
	FFA _{NR}	0.8464	0.9486	1.9348	4.4151	5.1399	5.5216	6.4691
	MPA _{LW}	0.8403	0.9782	1.9604	4.4325	5.1517	5.5493	6.4691
	MPSO _{NR}	0.8459	0.9228	1.9468	4.3924	5.1459	5.6110	6.5090
	MRFO _{NR}	0.8357	0.9789	1.9512	4.4331	5.1575	5.5493	6.4691
	ALO _{LW}	0.8475	0.9071	1.9618	4.4685	5.1588	5.5413	6.4165
	ImSMA _{LW}	0.8496	0.9223	1.9671	4.4213	5.1375	5.5165	6.4444
	CHCLPSO _{NR}	0.8489	0.9438	1.9549	4.4284	5.1549	5.5484	6.4693
	DEAM _{NR}	0.8403	1.0121	1.9702	4.4473	5.1619	5.5493	6.4691
I_o	GCAOA _{EmNR}	7.82E-06	3.91E-06	1.34E-06	5.50E-06	6.76E-06	9.27E-06	2.98E-06
	GCAOA _{AdLM}	9.38E-06	1.68E-06	4.28E-06	9.78E-06	7.72E-06	8.39E-06	1.00E-05
	HAOA _{ENR}	2.53E-06	1.00E-05	1.00E-05	4.61E-06	5.17E-07	1.00E-05	2.40E-07
	GCAOA _{InNR}	1.97E-08	2.96E-08	6.16E-08	6.76E-07	1.71E-06	1.00E-05	1.00E-05
	GCAOA _{mNR}	1.00E-05	9.21E-06	9.97E-06	1.00E-05	1.00E-05	1.00E-05	2.91E-06
	GCAOA _{NR}	1.95E-08	2.96E-08	6.15E-08	6.80E-07	2.26E-06	1.00E-05	1.00E-05
	GCAOA _{LW}	1.95E-08	2.97E-08	6.15E-08	6.80E-07	2.26E-06	1.00E-05	1.00E-05
	AEO _{NR}	2.15E-08	5.12E-07	1.09E-07	1.08E-06	2.26E-06	1.00E-05	1.00E-05
	ELPSO _{NR}	1.95E-08	1.90E-06	4.67E-07	9.03E-07	1.99E-06	1.00E-05	1.00E-05
	ELSHADE _{INR}	2.12E-08	7.53E-07	9.28E-08	7.40E-07	1.71E-06	1.00E-05	1.00E-05
	FFA _{NR}	4.03E-07	2.21E-06	5.96E-07	1.83E-06	8.32E-06	9.96E-06	1.00E-05
	MPA _{LW}	1.95E-08	2.11E-06	5.14E-07	1.72E-06	3.61E-06	1.00E-05	1.00E-05
	MPSO _{NR}	7.61E-07	8.01E-06	1.64E-06	6.95E-06	7.76E-06	9.90E-06	9.92E-06
	MRFO _{NR}	6.07E-08	1.26E-06	6.53E-07	1.49E-06	2.77E-06	1.00E-05	1.00E-05
	ALO _{LW}	1.83E-06	6.92E-06	2.73E-07	1.63E-07	3.78E-06	7.97E-06	8.84E-06
	ImSMA _{LW}	1.93E-08	3.48E-06	6.17E-08	8.39E-07	3.29E-06	1.90E-06	1.00E-05
	CHCLPSO _{NR}	1.14E-06	2.91E-06	1.07E-06	2.42E-06	3.88E-06	1.00E-05	1.00E-05
	DEAM _{NR}	1.95E-08	2.78E-07	6.19E-08	6.80E-07	2.34E-06	1.00E-05	1.00E-05
R_s	GCAOA _{EmNR}	1.0824	0.1514	0.6658	0.4977	0.2202	0.1467	0.1000
	GCAOA _{AdLM}	1.9997	0.3800	0.6551	0.5104	0.2256	0.1981	0.1000
	HAOA _{ENR}	1.9280	0.1000	1.6090	0.5433	0.8575	2.0000	0.4023
	GCAOA _{InNR}	1.9091	0.6962	0.7763	0.5642	0.2980	0.1832	0.1874
	GCAOA _{mNR}	0.9864	0.1000	0.5224	0.4780	0.1789	0.1168	0.1000
	GCAOA _{NR}	1.9324	0.6956	0.7779	0.5638	0.2911	0.1829	0.1863
	GCAOA _{LW}	1.9324	0.6889	0.7779	0.5638	0.2911	0.1829	0.1863
	AEO _{NR}	1.9389	0.4513	0.7479	0.5506	0.2911	0.1829	0.1863
	ELPSO _{NR}	1.9675	0.3169	0.6900	0.5582	0.2932	0.1836	0.1880
	ELSHADE _{INR}	1.9007	0.4074	0.7516	0.5621	0.2980	0.1832	0.1874
	FFA _{NR}	1.6153	0.3631	0.6951	0.5435	0.2569	0.1850	0.1863
	MPA _{LW}	1.9324	0.2916	0.6884	0.5393	0.2796	0.1829	0.1863
	MPSO _{NR}	1.5906	0.1821	0.6357	0.5047	0.2643	0.1757	0.1838
	MRFO _{NR}	1.8012	0.3603	0.6909	0.5459	0.2863	0.1829	0.1863
	ALO _{LW}	1.2956	0.2186	0.7122	0.5981	0.2759	0.1921	0.1965
	ImSMA _{LW}	1.9053	0.3009	0.7788	0.5660	0.2825	0.2406	0.1899
	CHCLPSO _{NR}	1.4327	0.3002	0.6524	0.5292	0.2774	0.1830	0.1865
	DEAM _{NR}	1.9324	0.5056	0.7787	0.5638	0.2905	0.1829	0.1863
R_p	GCAOA _{EmNR}	144.6563	5321.7500	78.3588	51.5203	12.6161	12.1412	12.6111
	GCAOA _{AdLM}	3079.1766	104.6595	863.5085	1206.0607	23.8380	63.7312	15.8294

(continued on next page)

Table 4 (continued)

Parameter	Method	S_1	S_2	S_3	S_4	S_5	S_6	S_7
HAOA _{ENR}	8000.0000	7999.9941	7999.9995	7999.9916	274.3559	7999.9986	63.3865	
GCAOA _{INR}	1034.7265	68.2723	141.5190	102.4428	37.6832	35.7043	30.7151	
GCAOA _{mNR}	99.1825	93.4519	88.7373	59.8153	15.0594	13.0945	12.6104	
GCAOA _{NR}	1115.5439	68.5547	141.9168	102.3205	38.6282	35.4627	30.3048	
GCAOA _{LW}	1115.5890	66.3251	141.9170	102.3208	38.6289	35.4626	30.3047	
AEO _{NR}	2753.4721	106.5292	165.4429	116.4521	38.6173	35.4626	30.3047	
ELPSO _{NR}	8000.0000	156.2157	249.6031	110.0246	38.6948	36.1666	31.1062	
ELSHADE _{INR}	1238.1926	121.1932	144.3291	105.0424	37.6812	35.7043	30.7151	
FFA _{NR}	7619.8576	232.2642	650.3396	205.1513	46.9430	38.6652	30.3079	
MPA _{LW}	1115.4853	142.4117	239.2829	142.8768	41.5760	35.4638	30.3058	
MPSO _{NR}	4458.0302	756.0616	619.2735	7953.5955	43.7802	29.4943	27.9039	
MRFO _{NR}	6204.1189	136.3551	389.5226	135.5446	39.9224	35.4625	30.3047	
ALO _{LW}	2945.8324	5075.7104	197.4474	74.3513	40.3039	36.0138	35.2169	
ImSMA _{LW}	532.7951	506.2372	150.4747	154.6411	43.5597	37.6367	32.7075	
CHCLPSO _{NR}	7409.3610	258.4475	340.9560	164.9366	41.2881	35.5683	30.3414	
DEAM _{NR}	1115.5887	93.7005	143.3269	102.3212	38.9140	35.4626	30.3047	

reflects the fact that the photocurrent is increasing according to sun irradiation and its dramatically increased from 0.8067 to 6.7673 (A). I_o is within ranges of (9.27E-6- 1.34E-06), indicating that the saturation currents are favorably linked with ambient temperature. Finally, both R_s and R_p start large then subsequently decline from (1.0824–0.1000) for series resistance and (144.65–12.61) for the shunt resistance. However, the HAOA_{ENR} model exhibits a perturbation distribution for the extract five parameters of the SD PV model. This is because of that the HAOA_{ENR} model has various random strategies in terms of methodology, and the provided initial solutions to the objective function are based on second order convergence of the NR method, which may have a little effect on the results.

The I-V and P-V characteristics curves between the experimental and simulated of the SD PV models based on seven environmental conditions is depicted in Fig. 7. From Fig. 7, the magnified figures reveal that the proposed GCAOA_{EmNR} model does indeed all experimental data points at all climatic conditions, including those seen at maximum power points. Additionally, there is notable change in the distance between actual and simulated data points for those models that employed traditional OFD based on LW and NR methods. Bear in mind that the PV crystalline PV module exhibits sharp data points at MPP owing to the low R_s and high R_p .

A detailed clarifications and statistical analysis on the findings of the SD PV models, including the RMSE, MBE, R^2 , d_i , TS, and CPU computing time statistical analysis for the GCAOA_{EmNR} and other methods are given in Table 5. The proposed GCAOA_{EmNR} produces unique results in which the RMSE, MBE, d_i , and TS are zero under all weather conditions and the R^2 is one. These findings demonstrate the appropriate methodology and objective function design utilized in obtaining the parameters of the SD PV model. However, the GCAOA_{EmNR} requires more processing time than CHCLPSO_{NR}, which slower by two times. This is owing to the complicated procedure obtained to address this issue. Keeping in mind that the SD PV model's equation is nonlinear, multivariable, and contains nine parameters that must be optimally determined. The GCAOA_{AdLM} model ranked second and displays same experimental findings as the GCAOA_{EmNR} except for the convergence rate, where the GCAOA_{EmNR} significantly outperforms GCAOA_{AdLM} model owing to powerful OFD based on a modified third order NR method, as seen in Fig. 10. The preference can be given to GCAOA_{EmNR} to be more affective and efficient for practical PV model applications.

The HAOA_{ENR} model is ranked third, followed by GCAOA_{mNR}, GCAOA_{INR}, ELSHADE_{INR}, DEAM_{NR}, AEO_{NR}, ELPSO_{NR}, MPA_{LW}, MRFO_{NR}, CHCLPSO_{NR}, FFA_{NR}, ALO_{LW}, and ImSMA_{LW}. The average RMSE values for these methods are 4.97e-35, 5.23E-05, 0.0058, 0.0058, 0.0596,

0.0596, 0.0597, 0.0597, 0.0599, 0.0599, 0.0600, 0.0602, 0.0602, 0.0604, and 0.0608, respectively. The HAOA_{ENR} presents zero values under only two environmental conditions S_4 and S_7 . The worst accuracy and stability registered model is MPSO_{NR}, demonstrating low methodology performance in spite of employing the same objective function method. Similarly, the MBE, MBE, d_i , and TS statistical criteria exhibit the same pattern with trivial variations between them. To summarize, both methodology and objective function design are important in improving the accuracy, stability, reliability, and CPU-execution time when optimizing the SD PV model's problem. It is worth to mention that the type of complexity of methodology and the objective function used have a considerable impact on the time required to process the optimization problem as shown in Table 5.

Another crucial statistical parameter is AE, which depicts the individual error between each data point of the predicated currents and the observed experimental current in Fig. 8. The GCAOA_{EmNR} dominate other methods by deteriorating the errors to zero values for all experimental data points at all weather circumstances. The GCAOA_{AdLM} model has the same AE values as the GCAOA_{EmNR} model, but the difference is in the resulting OFD, demonstrating superiority in terms of rapid convergence and a highly exact set of initial solutions values. According to the Fig. 8, the best individual AE values are colored with dark blue, whereas the worst individual AE values are dramatically change through green, yellow, and dusky red colors. The largest AE values are clearly occurred at MPP, where the majority of the models with typical OFD have difficulty replicating the experimental data points. Also, when sun irradiation and ambient temperature rise, the mistakes ratio tends to increase. MPSO_{NR} records the worst individual AE and worst average AE values, as shown in Fig. 8 and summarized in Table 6.

The primary objective of this research study is to offer a model capable of simulating genuine experimental data in every weather condition. As a consequence, the key principle of this study is to reduce the error up to zero and enhance precision, resulting high level of dependability and lowering the overall cost of the PV system. Fig. 9, illustrates the RMSE values for the proposed GCAOA_{EmNR} model and other peers under different climatic conditions. This figure indicates that the methodology and OFD of the proposed GCAOA_{EmNR} model are well-suited for not only in avoiding stagnation in local minima and discovering new promising solutions throughout the problem's search space, but also for solving the PV model's equation in advance by always providing precise optimum solutions during the optimization process, courtesy of the modified third order NR method and adaptive damping parameter of the LM method. As seen in Fig. 9, the overwhelming of models optimize the SD PV problem to a specified degree of accuracy for

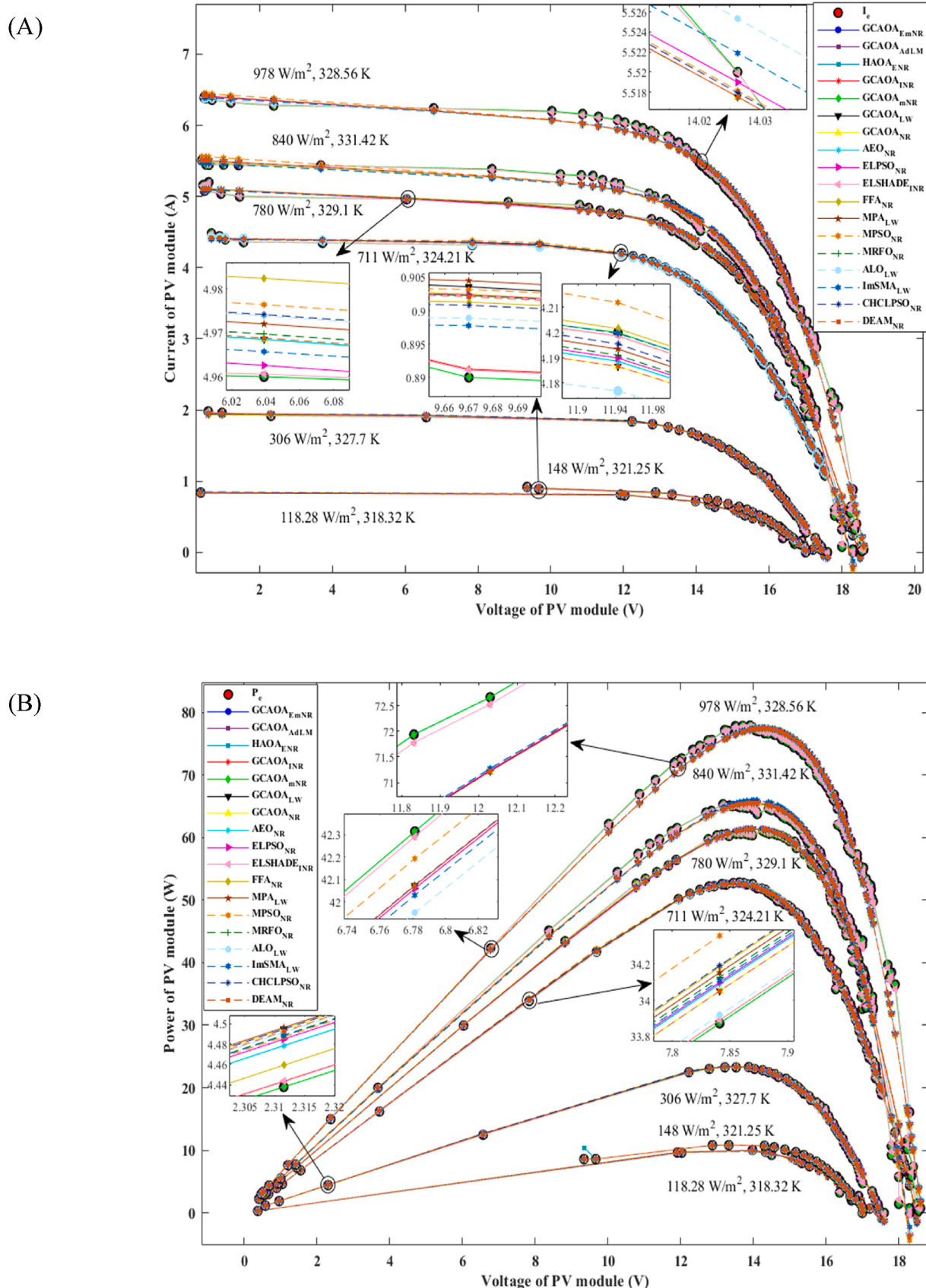


Fig. 7. Plotting the I-V and P-V data curves for the SD PV model using the GCAOA_{E_mNR} and other models. (A) I-V curve (B) P-V curve.

Table 5

Statistical criteria for alternative SD PV models.

Parameter	Method	S ₁	S ₂	S ₃	S ₄	S ₅	S ₆	S ₇	Average
RMSE	GCAOA _{EmNR}	0.0000	0.0000	0.0000	0.0000	0.0000	0.0000	0.0000	0.0000
	GCAOA _{AdLM}	0.0000	0.0000	0.0000	0.0000	0.0000	0.0000	0.0000	0.0000
	HAOA _{ENR}	6.84E-35	2.17E-35	2.25E-35	0.0000	2.07E-34	2.83E-35	0.0000	4.97E-35
	GCAOA _{INR}	0.0033	0.0012	0.0024	0.0027	0.0087	0.0099	0.0121	0.0058
	GCAOA _{mNR}	1.43E-09	3.48E-13	5.00E-09	3.57E-08	4.97E-05	1.71E-04	1.46E-04	5.23E-05
	GCAOA _{NR}	0.0329	0.0123	0.0253	0.0280	0.0907	0.1024	0.1256	0.0596
	GCAOA _{LW}	0.0329	0.0123	0.0253	0.0280	0.0907	0.1024	0.1256	0.0596
	AE _{NR}	0.0330	0.0127	0.0256	0.0281	0.0907	0.1024	0.1256	0.0597
	ELPSO _{NR}	0.0330	0.0130	0.0264	0.0280	0.0908	0.1025	0.1256	0.0599
	ELSHADE _{INR}	0.0033	0.0012	0.0024	0.0027	0.0087	0.0099	0.0121	0.0058
	FFA _{NR}	0.0336	0.0132	0.0270	0.0285	0.0911	0.1026	0.1256	0.0602
	MPA _{LW}	0.0329	0.0130	0.0264	0.0282	0.0908	0.1024	0.1256	0.0599
	MPSO _{NR}	0.0340	0.0134	0.0274	0.0298	0.0918	0.1041	0.1261	0.0610
	MRFO _{NR}	0.0332	0.0129	0.0268	0.0282	0.0907	0.1024	0.1256	0.0600
	ALO _{LW}	0.0344	0.0134	0.0260	0.0284	0.0908	0.1031	0.1268	0.0604
	ImSMA _{LW}	0.0330	0.0133	0.0253	0.0285	0.0909	0.1088	0.1257	0.0608
	CHCLPSO _{NR}	0.0340	0.0131	0.0270	0.0284	0.0908	0.1024	0.1256	0.0602
	DEAM _{NR}	0.0329	0.0126	0.0253	0.0280	0.0907	0.1024	0.1256	0.0597
MBE	GCAOA _{EmNR}	0.0000	0.0000	0.0000	0.0000	0.0000	0.0000	0.0000	0.0000
	GCAOA _{AdLM}	0.0000	0.0000	0.0000	0.0000	0.0000	0.0000	0.0000	0.0000
	HAOA _{ENR}	4.68E-69	4.70E-70	5.04E-70	0.0000	4.28E-68	8.03E-70	0.0000	7.03E-69
	GCAOA _{INR}	1.08E-05	1.45E-06	5.90E-06	7.44E-06	7.61E-05	9.71E-05	1.46E-04	4.93E-05
	GCAOA _{mNR}	2.05E-18	1.21E-25	2.50E-17	1.28E-15	2.47E-09	2.92E-08	2.12E-08	7.56E-09
	GCAOA _{NR}	1.08E-03	1.51E-04	6.38E-04	7.84E-04	8.23E-03	1.05E-02	1.58E-02	5.31E-03
	GCAOA _{LW}	1.08E-03	1.51E-04	6.38E-04	7.84E-04	8.23E-03	1.05E-02	1.58E-02	5.31E-03
	AE _{NR}	1.09E-03	1.61E-04	6.56E-04	7.87E-04	8.23E-03	1.05E-02	1.58E-02	5.31E-03
	ELPSO _{NR}	1.09E-03	1.69E-04	6.96E-04	7.87E-04	8.24E-03	1.05E-02	1.58E-02	5.32E-03
	ELSHADE _{INR}	1.08E-05	1.56E-06	6.00E-06	7.44E-06	7.61E-05	9.71E-05	1.46E-04	4.93E-05
	FFA _{NR}	1.13E-03	1.74E-04	7.31E-04	8.12E-04	8.30E-03	1.05E-02	1.58E-02	5.35E-03
	MPA _{LW}	1.08E-03	1.70E-04	6.98E-04	7.96E-04	8.24E-03	1.05E-02	1.58E-02	5.32E-03
	MPSO _{NR}	1.16E-03	1.80E-04	7.52E-04	8.87E-04	8.43E-03	1.08E-02	1.59E-02	5.45E-03
	MRFO _{NR}	1.10E-03	1.66E-04	7.18E-04	7.97E-04	8.23E-03	1.05E-02	1.58E-02	5.33E-03
	ALO _{LW}	1.18E-03	1.81E-04	6.77E-04	8.09E-04	8.24E-03	1.06E-02	1.61E-02	5.40E-03
	ImSMA _{LW}	1.09E-03	1.77E-04	6.39E-04	8.10E-04	8.26E-03	1.18E-02	1.58E-02	5.52E-03
	CHCLPSO _{NR}	1.16E-03	1.72E-04	7.30E-04	8.07E-04	8.24E-03	1.05E-02	1.58E-02	5.34E-03
	DEAM _{NR}	1.08E-03	1.59E-04	6.38E-04	7.84E-04	8.23E-03	1.05E-02	1.58E-02	5.31E-03
R ²	GCAOA _{EmNR}	1.0000	1.0000	1.0000	1.0000	1.0000	1.0000	1.0000	1.0000
	GCAOA _{AdLM}	1.0000	1.0000	1.0000	1.0000	1.0000	1.0000	1.0000	1.0000
	HAOA _{ENR}	1.0000	1.0000	1.0000	1.0000	1.0000	1.0000	1.0000	1.0000
	GCAOA _{INR}	0.9998	1.0000	1.0000	1.0000	1.0000	0.9999	0.9999	0.9999
	GCAOA _{mNR}	1.0000	1.0000	1.0000	1.0000	1.0000	1.0000	1.0000	1.0000
	GCAOA _{NR}	0.9836	0.9980	0.9981	0.9994	0.9949	0.9944	0.9932	0.9945
	GCAOA _{LW}	0.9836	0.9980	0.9981	0.9994	0.9949	0.9944	0.9932	0.9945
	AE _{NR}	0.9836	0.9979	0.9981	0.9994	0.9949	0.9944	0.9932	0.9945
	ELPSO _{NR}	0.9835	0.9978	0.9980	0.9994	0.9949	0.9944	0.9932	0.9945
	ELSHADE _{INR}	0.9998	1.0000	1.0000	1.0000	1.0000	0.9999	0.9999	0.9999
	FFA _{NR}	0.9829	0.9977	0.9979	0.9993	0.9949	0.9943	0.9932	0.9943
	MPA _{LW}	0.9836	0.9978	0.9980	0.9993	0.9949	0.9944	0.9932	0.9945
	MPSO _{NR}	0.9825	0.9977	0.9978	0.9993	0.9948	0.9942	0.9932	0.9942
	MRFO _{NR}	0.9834	0.9978	0.9979	0.9993	0.9949	0.9944	0.9932	0.9944
	ALO _{LW}	0.9821	0.9977	0.9980	0.9993	0.9949	0.9943	0.9931	0.9942
	ImSMA _{LW}	0.9835	0.9977	0.9981	0.9993	0.9949	0.9936	0.9932	0.9944
	CHCLPSO _{NR}	0.9825	0.9978	0.9979	0.9993	0.9949	0.9944	0.9932	0.9943
	DEAM _{NR}	0.9836	0.9979	0.9981	0.9994	0.9949	0.9944	0.9932	0.9945
d _i	GCAOA _{EmNR}	0.0000	0.0000	0.0000	0.0000	0.0000	0.0000	0.0000	0.0000
	GCAOA _{AdLM}	0.0000	0.0000	0.0000	0.0000	0.0000	0.0000	0.0000	0.0000
	HAOA _{ENR}	1.88E-35	-2.80E-35	-2.72E-35	-4.97E-35	1.57E-34	-2.13E-35	-4.97E-35	5.32E-69
	GCAOA _{INR}	-0.0025	-0.0046	-0.0033	-0.0030	0.0030	0.0041	0.0063	1.88E-05
	GCAOA _{mNR}	-5.23E-05	-5.23E-05	-5.23E-05	-5.23E-05	-2.64E-06	1.19E-04	9.33E-05	5.62E-09
	GCAOA _{NR}	-0.0267	-0.0473	-0.0344	-0.0316	0.0311	0.0428	0.0660	0.0020
	GCAOA _{LW}	-0.0267	-0.0473	-0.0344	-0.0316	0.0311	0.0428	0.0660	0.0020
	AE _{NR}	-0.0268	-0.0470	-0.0341	-0.0317	0.0310	0.0427	0.0659	0.0020
	ELPSO _{NR}	-0.0269	-0.0469	-0.0335	-0.0318	0.0309	0.0426	0.0657	0.0020
	ELSHADE _{INR}	-0.0025	-0.0045	-0.0033	-0.0030	0.0030	0.0041	0.0063	1.87E-05
	FFA _{NR}	-0.0266	-0.0471	-0.0332	-0.0317	0.0309	0.0424	0.0654	0.0020
	MPA _{LW}	-0.0270	-0.0469	-0.0335	-0.0317	0.0309	0.0425	0.0657	0.0020
	MPSO _{NR}	-0.0269	-0.0475	-0.0335	-0.0312	0.0309	0.0432	0.0652	0.0020
	MRFO _{NR}	-0.0268	-0.0471	-0.0332	-0.0317	0.0308	0.0425	0.0656	0.0020
	ALO _{LW}	-0.0260	-0.0470	-0.0344	-0.0320	0.0304	0.0427	0.0664	0.0020
	ImSMA _{LW}	-0.0278	-0.0475	-0.0355	-0.0323	0.0301	0.0481	0.0649	0.0021
	CHCLPSO _{NR}	-0.0262	-0.0471	-0.0332	-0.0318	0.0306	0.0422	0.0654	0.0020
	DEAM _{NR}	-0.0267	-0.0471	-0.0344	-0.0316	0.0311	0.0428	0.0659	0.0020
TS	GCAOA _{EmNR}	0.0000	0.0000	0.0000	0.0000	0.0000	0.0000	0.0000	0.0000
	GCAOA _{AdLM}	0.0000	0.0000	0.0000	0.0000	0.0000	0.0000	0.0000	0.0000

(continued on next page)

Table 5 (continued)

Parameter	Method	S_1	S_2	S_3	S_4	S_5	S_6	S_7	Average
CPU	HAOA _{ENR}	3.14E-34	1.04E-34	1.57E-34	0.0000	1.97E-33	2.83E-34	0.0000	4.04E-34
	GCAOA _{INR}	0.0151	0.0058	0.0170	0.0259	0.0839	0.0995	0.1231	0.0529
	GCAOA _{mNR}	6.56E-09	1.67E-12	3.50E-08	3.39E-07	4.74E-04	1.71E-03	1.46E-03	5.21E-04
	GCAOA _{NR}	0.1561	0.0597	0.1814	0.2733	0.9518	1.1414	1.4435	0.6010
	GCAOA _{LW}	0.1561	0.0598	0.1814	0.2733	0.9518	1.1414	1.4435	0.6010
	AE _{NR}	0.1562	0.0617	0.1839	0.2739	0.9518	1.1414	1.4435	0.6018
	ELPSO _{NR}	0.1563	0.0631	0.1897	0.2738	0.9521	1.1415	1.4437	0.6029
	ELSHADE _{INR}	0.0151	0.0060	0.0172	0.0259	0.0839	0.0995	0.1231	0.0530
	FFA _{NR}	0.1594	0.0640	0.1945	0.2783	0.9564	1.1436	1.4435	0.6057
	MPA _{LW}	0.1561	0.0633	0.1900	0.2755	0.9524	1.1414	1.4435	0.6032
	MPSO _{NR}	0.1614	0.0653	0.1974	0.2911	0.9645	1.1624	1.4506	0.6132
	MRFO _{NR}	0.1571	0.0626	0.1927	0.2756	0.9519	1.1414	1.4435	0.6036
	ALO _{LW}	0.1633	0.0654	0.1869	0.2777	0.9527	1.1496	1.4594	0.6079
	ImSMA _{LW}	0.1564	0.0646	0.1815	0.2780	0.9539	1.2213	1.4452	0.6144
	CHCLPSO _{NR}	0.1614	0.0638	0.1943	0.2774	0.9525	1.1414	1.4435	0.6049
	DEAM _{NR}	0.1510	0.0604	0.1769	0.2658	0.8690	1.0299	1.2723	0.5465
	GCAOA _{EmNR}	18.73	17.92	21.37	19.77	20.28	20.64	20.00	19.82
	GCAOA _{AdLM}	20.05	18.80	19.47	20.94	20.42	20.69	20.83	20.17
	HAOA _{ENR}	19.41	20.30	22.53	19.03	22.89	20.86	22.38	21.06
	GCAOA _{INR}	20.41	19.66	20.58	22.02	22.11	23.50	23.08	21.62
	GCAOA _{mNR}	17.58	17.92	19.38	19.20	19.39	19.64	20.55	19.09
	GCAOA _{NR}	19.02	19.98	20.67	26.06	22.50	23.08	22.83	22.02
	GCAOA _{LW}	280.56	1771.03	4087.94	4548.53	5062.27	5622.55	6209.84	3940.39
	AE _{NR}	16.03	16.05	16.63	18.30	17.39	17.45	17.52	17.05
	ELPSO _{NR}	14.52	11.39	11.28	14.42	12.97	14.86	11.89	13.05
	ELSHADE _{INR}	7.58	8.14	8.39	8.80	8.41	12.73	8.94	9.00
	FFA _{NR}	21.42	17.28	18.53	19.22	19.67	19.08	19.52	19.25
	MPA _{LW}	484.56	1766.77	3009.11	9283.61	12254.98	15959.61	334.84	6156.21
	MPSO _{NR}	9.06	9.16	9.52	10.02	11.53	12.58	11.03	10.41
	MRFO _{NR}	15.70	17.89	24.98	17.75	24.31	17.44	19.83	19.70
	ALO _{LW}	237.38	445.52	1977.28	2401.88	954.20	1850.80	2054.98	1417.43
	ImSMA _{LW}	2213.84	2610.55	3382.05	4368.72	5061.72	6633.94	7959.20	4604.29
	CHCLPSO _{NR}	7.92	8.47	7.83	8.78	8.14	7.91	8.13	8.17
	DEAM _{NR}	14.11	15.63	14.88	16.58	15.36	16.77	15.70	15.57

the S_{1-4} weather conditions, as indicated with gleaming blue hue. However, the level of accuracy is slightly decreased at S_5 with green color and continues to deteriorate their accuracy with yellow color, particularly at high sun irradiance and ambient temperature ranges.

The proceeding discussions and analyses can be clearly justified in Fig. 10 between the proposed GCAOA_{EmNR}, GCAOA_{AdLM}, and HAOA_{ENR} models, which are all ranked in the top three in the literature. The proposed GCAOA_{EmNR} is novel because of the powerful and efficient hybridization of OFD, as evidenced by the following: To begin, third order convergence of the NR method. Secondly, combining adaptive damping LM's parameters. Finally, the convergence of the quadratic and fourth terms Eq. (17) [135]. This hybridization of the OFD enables the generation of a desired set of initial solutions at each iteration while neglecting the oscillations and noise effects, resulting in global convergence with a very small RMSE value at the start of the optimization process, as illustrated in zoomed figures.

4.2. Results on double diode PV model

In comparison with SD PV model, two additional parameter are included allowing to generate a higher accuracy and specificity in extreme environmental circumstances. Table 7 contains the estimated seven parameters of the GCAOA_{EmNR} model and other models under a variety of arbitrary conditions for the DD PV models. The extracted seven parameters of the DD PV model based on GCAOA_{EmNR} approach are inside the optimization problem's designed lower and upper variables. According to Ohm's law, decreasing resistance results an increase in current, as conducted by the proposed GCAOA_{EmNR} approach. This can be seen for I_{ph} , which has somewhat higher values than others

within the range of (0.7489–6.7525), and R_s and R_p are often smaller. Extraction parameters by the HAOA_{ENR} model and a few of other models are scanty. This is because of developing only the algorithm itself is insufficient for to provide a higher level of stability. Despite the fact that the HAOA_{ENR} employs LM's damping parameter, but its OFD has second order convergence, resulting in certain undesired initial solutions. As an outcome, the GCAOA_{EmNR} approach is superior for real-world PV applications. Moreover, this model is capable of determining any sort of PV technology under any environmental conditions. A high degree of agreement between the actual and projected currents is seen utilizing the GCAOA_{EmNR} model by drawing the I-V and P-V characteristics curves as represented in Fig. 11. Even at hard edges, the GCAOA_{EmNR} can confidently capture all experimental data points.

The predetermined parameters for the DD PV model using GCAOA_{EmNR} approaches and other methods indicate the degree of precision, stability, dependability, and CPU computing time, as described in Table 8. The RMSE, MBE, d_i , and TS statistical criterion for the proposed GCAOA_{EmNR} are zero, and R^2 is one under all weather conditions. The GCAOA_{EmNR} has an acceptable computing time 21.08 s on average. This is related the algorithm's and OFD's complexity. There is, however, no substantial difference between the GCAOA_{EmNR} and the faster model, while the CHCLPSO_{NR} model is two times quicker. CPU processing time is given less weight in optimizing PV problems, and majority of priority may be given to the most accurate model that is relevant to real-world PV systems. The GCAOA_{AdLM} is rated second, with comparable to the GCAOA_{EmNR} model except for the period of convergence.

The HAOA_{ENR} is ranked third, followed by GCAOA_{mNR}, GCAOA_{INR}, ELSHAD_{INR}, GCAOA_{LW}, MPA_{LW}, GCAOA_{NR}, DEAM_{NR}, AE_{NR}, MRFO_{NR}, ALO_{LW}, CHCLPSO_{NR}, ELPSO_{NR}, ImSMA_{LW}, and FFA_{NR}. Their

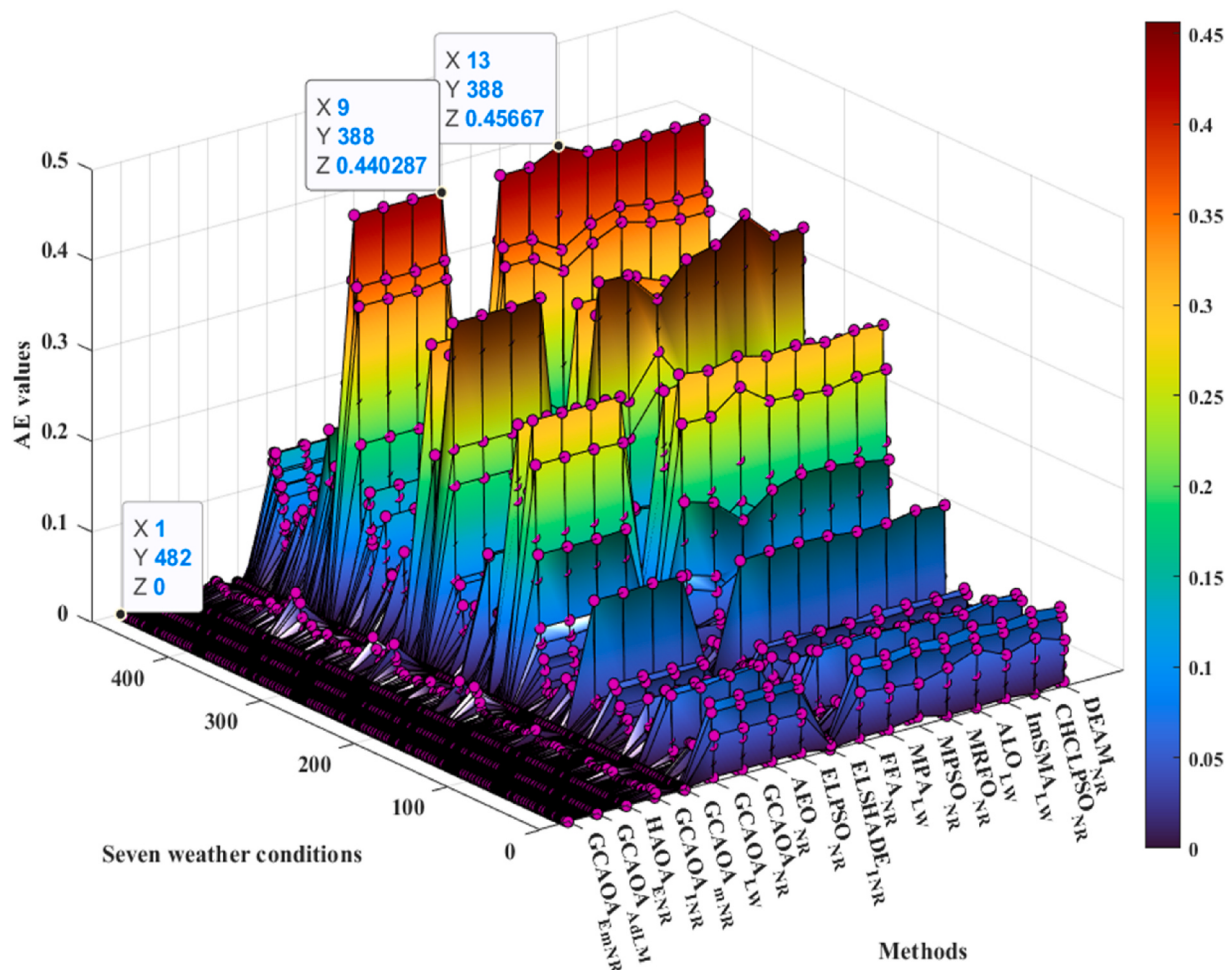


Fig. 8. Comparison of individual AE of GCAOA_{EmNR} and other models for the SD PV model.

Table 6
Average AE values for the SD PV model using different approaches.

Method	S ₁	S ₂	S ₃	S ₄	S ₅	S ₆	S ₇	Average
GCAOA _{EmNR}	0.000000	0.000000	0.000000	0.000000	0.000000	0.000000	0.000000	0.000000
GCAOA _{AdLM}	0.000000	0.000000	0.000000	0.000000	0.000000	0.000000	0.000000	0.000000
HAOA _{ENR}	1.46E-35	4.42E-36	3.18E-36	0.000000	2.16E-35	2.82E-36	0.000000	6.65E-36
GCAOA _{INR}	0.003136	0.002106	0.002043	0.003713	0.007346	0.007106	0.009223	0.004953
GCAOA _{mNR}	0.000909	0.001333	0.000400	0.001758	0.001539	0.000052	0.000046	0.000863
GCAOA _{NR}	0.023528	0.009212	0.017400	0.021860	0.062376	0.073587	0.095685	0.043378
GCAOA _{LW}	0.023528	0.009199	0.017400	0.021860	0.062376	0.073587	0.095685	0.043377
AEO _{NR}	0.023794	0.009580	0.017638	0.021851	0.062377	0.073587	0.095685	0.043502
ELPSO _{NR}	0.023947	0.010030	0.018507	0.021779	0.062699	0.073566	0.095954	0.043783
ELSHADE _{INR}	0.003141	0.002146	0.002057	0.003712	0.007346	0.007106	0.009223	0.004962
FFA _{NR}	0.024748	0.010382	0.019416	0.021676	0.061820	0.073747	0.095684	0.043925
MPA _{LW}	0.023528	0.010099	0.018631	0.021850	0.062075	0.073587	0.095685	0.043636
MPSO _{NR}	0.025229	0.010675	0.019962	0.022711	0.061314	0.075757	0.096845	0.044642
MRFON _{NR}	0.023872	0.009890	0.019505	0.021873	0.062171	0.073587	0.095685	0.043798
ALO _{LW}	0.024890	0.010548	0.018031	0.022424	0.062030	0.074453	0.095625	0.044000
ImSMA _{LW}	0.022829	0.009184	0.017211	0.020170	0.062243	0.080736	0.094856	0.043890
CHCLPSO _{NR}	0.024953	0.010234	0.019374	0.021936	0.061962	0.073602	0.095691	0.043965
DEAM _{NR}	0.023528	0.009457	0.017358	0.021860	0.062325	0.073587	0.095685	0.043400

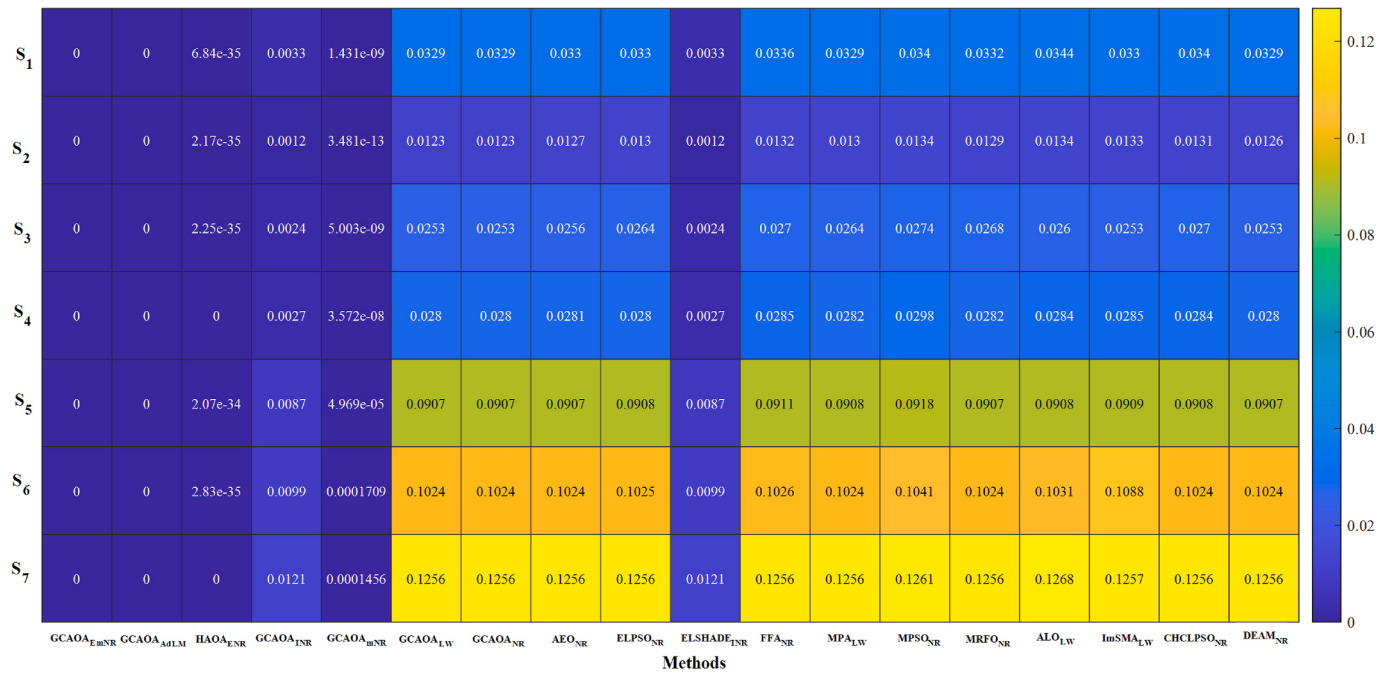


Fig. 9. Comparison of RMSE of GCAOA_{EmNR} and other peer algorithms for the SD PV model.

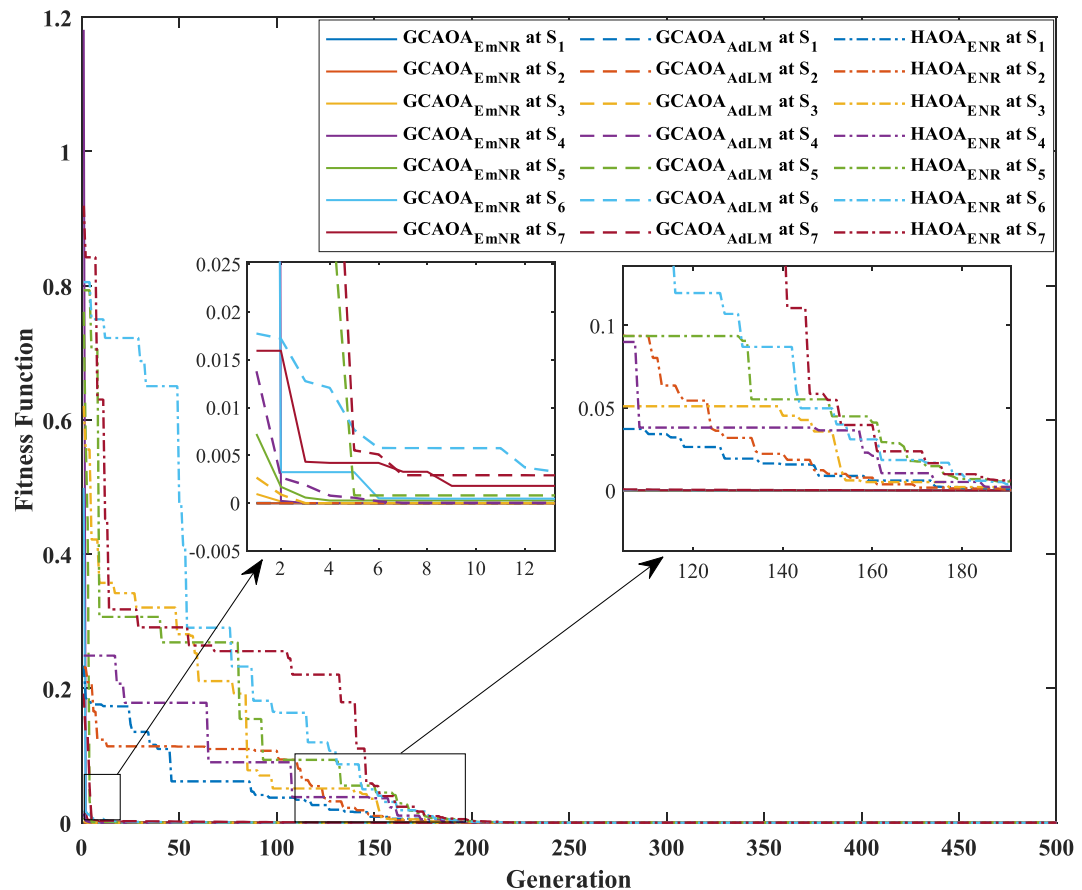


Fig. 10. Development of the fitness function using GCAOA_{EmNR}, GCAOA_{AdLM}, and HAOA_{ENR} for the SD PV model.

Table 7

Parameters extracted from the DD PV model using various approaches.

Parameter	Method	S_1	S_2	S_3	S_4	S_5	S_6	S_7
d_1	GCAOA _{EmNR}	1.7141	1.5417	1.2847	1.9052	1.4115	1.0007	1.9997
	GCAOA _{AdLM}	1.0180	1.4256	1.0000	1.2214	1.3418	1.4129	1.4464
	HAOA _{ENR}	1.0000	2.0000	2.0000	1.4161	2.0000	1.0000	2.0000
	GCAOA _{InR}	1.0000	1.1538	1.9999	1.9987	1.0000	1.4231	1.4515
	GCAOA _{mNR}	1.6621	1.5815	1.5068	1.4964	1.4705	1.4342	1.4314
	GCAOA _{NR}	1.0000	1.0000	1.0000	1.1558	1.4767	1.4231	1.4516
	GCAOA _{LW}	1.0000	1.0082	2.0000	1.0472	1.0699	1.0000	1.4285
	AEO _{NR}	1.3169	1.2157	1.0834	1.1801	1.1628	1.4232	1.4521
	ELPSO _{NR}	1.0000	1.5329	1.2075	2.0000	1.2519	1.3661	1.4633
	ELSHADE _{INR}	1.0000	1.0053	1.9948	1.1871	1.6160	1.4230	1.4515
	FFA _{NR}	1.2641	1.4076	1.9481	1.3241	1.3640	1.3458	1.6214
	MPA _{LW}	2.0000	1.9820	2.0000	2.0000	1.1700	1.4699	1.4676
	MPSO _{NR}	1.9488	1.4141	1.2284	1.0000	1.3837	1.0000	2.0000
	MRFO _{NR}	1.0000	1.6170	1.1553	1.2204	1.3842	1.4132	1.4517
	ALO _{LW}	1.2792	1.2135	1.3641	1.2894	1.3357	1.4277	1.4298
	ImSMA _{LW}	1.0015	1.5818	1.2565	1.0000	1.1229	1.2693	1.5526
	CHCLPSO _{NR}	1.6897	1.2646	1.9264	1.2846	1.2846	1.4272	1.4220
	DEAM _{NR}	1.9992	1.5161	1.0153	1.3716	1.0016	1.4231	1.4516
d_2	GCAOA _{EmNR}	1.6608	1.4558	1.4130	1.3827	1.3529	1.3804	1.2660
	GCAOA _{AdLM}	1.2171	1.0112	1.9268	1.3854	1.0003	1.4513	1.4447
	HAOA _{ENR}	1.0000	1.5194	1.4174	2.0000	1.0000	2.0000	1.1517
	GCAOA _{InR}	1.0000	1.0002	1.0000	1.1759	1.4918	1.4230	1.4515
	GCAOA _{mNR}	1.6619	1.5036	1.5013	1.4964	1.4705	1.4342	1.0074
	GCAOA _{NR}	1.0000	2.0000	1.9995	1.5750	1.0000	1.4231	1.4516
	GCAOA _{LW}	1.9992	1.3256	1.0000	1.8820	1.4816	1.4170	1.0000
	AEO _{NR}	1.0000	1.9903	1.9415	1.4184	1.4511	1.4230	1.4511
	ELPSO _{NR}	2.0000	1.3108	1.9558	1.3054	1.8927	1.5411	1.4026
	ELSHADE _{INR}	1.0000	1.3191	1.0000	1.9992	1.1523	1.4230	1.4515
	FFA _{NR}	1.7624	1.5921	1.2637	1.7140	1.9301	1.6195	1.3840
	MPA _{LW}	1.0000	1.2785	1.0392	1.2357	1.5195	1.4725	1.5769
	MPSO _{NR}	1.0000	2.0000	1.0919	1.4056	2.0000	1.3494	1.3788
	MRFO _{NR}	1.7079	1.0777	1.4396	1.6082	1.0001	1.4339	1.4513
	ALO _{LW}	1.7406	1.4203	1.0746	1.9634	1.3806	1.4441	1.2847
	ImSMA _{LW}	1.0000	1.0422	1.1279	1.4095	1.3329	1.4441	1.4938
	CHCLPSO _{NR}	1.2458	1.7296	1.2544	1.5084	1.5492	1.4114	1.4593
	DEAM _{NR}	1.0000	1.2067	1.2371	1.1783	1.3169	1.4231	1.4516
I_{ph}	GCAOA _{EmNR}	0.7489	0.9211	1.9781	4.5291	5.0654	5.7813	6.7525
	GCAOA _{AdLM}	0.8428	0.9402	2.0430	4.4410	5.1486	5.5241	6.4508
	HAOA _{ENR}	0.5000	0.7531	1.8622	4.4030	4.7337	5.3642	7.0237
	GCAOA _{InR}	0.8406	1.0565	1.9714	4.4472	5.1665	5.5349	6.4539
	GCAOA _{mNR}	0.9194	1.0050	2.0283	4.5131	5.4095	5.8501	6.7714
	GCAOA _{NR}	0.8403	1.0557	1.9713	4.4502	5.1639	5.5358	6.4559
	GCAOA _{LW}	0.8403	1.0529	1.9713	4.4553	5.1924	5.5481	6.4558
	AEO _{NR}	0.8329	0.9953	1.9657	4.4523	5.1604	5.5343	6.4556
	ELPSO _{NR}	0.8376	0.9647	1.9512	4.4191	5.1557	5.5430	6.4590
	ELSHADE _{INR}	0.8406	1.0490	1.9714	4.4456	5.1666	5.5348	6.4539
	FFA _{NR}	0.8494	0.9214	1.9466	4.4087	5.1102	5.4594	6.4387
	MPA _{LW}	0.8400	0.9834	1.9671	4.4221	5.1795	5.5412	6.4648
	MPSO _{NR}	0.8462	0.9100	1.9419	4.3951	5.1298	5.4829	6.5042
	MRFO _{NR}	0.8395	0.8641	1.9600	4.4376	5.1533	5.5358	6.4560
	ALO _{LW}	0.8406	0.9180	1.9376	4.3844	5.1649	5.5415	6.4618
	ImSMA _{LW}	0.8409	0.9129	1.9404	4.3945	5.1262	5.3871	6.3926
	CHCLPSO _{NR}	0.8463	0.9578	1.9509	4.4264	5.1510	5.5300	6.4467
	DEAM _{NR}	0.8403	0.9872	1.9697	4.4452	5.1622	5.5357	6.4559
I_{o1}	GCAOA _{EmNR}	9.62E-06	8.89E-06	2.81E-12	5.42E-06	1.00E-05	3.70E-11	3.43E-12
	GCAOA _{AdLM}	2.01E-08	5.29E-06	5.82E-08	1.22E-06	6.43E-06	1.00E-05	9.99E-06
	HAOA _{ENR}	1.00E-08	1.04E-12	1.00E-05	1.00E-05	1.16E-12	9.98E-08	1.00E-05
	GCAOA _{InR}	4.47E-09	1.20E-09	1.00E-12	1.00E-12	4.04E-08	1.00E-05	1.00E-05
	GCAOA _{mNR}	1.00E-05	5.19E-06	1.00E-05	1.00E-05	1.00E-05	1.00E-05	1.00E-05
	GCAOA _{NR}	1.00E-12	2.96E-08	6.15E-08	5.11E-07	1.00E-05	1.00E-05	1.00E-05
	GCAOA _{LW}	1.95E-08	3.40E-08	1.00E-12	5.88E-08	3.22E-08	7.76E-09	1.00E-05
	AEO _{NR}	2.26E-11	6.49E-07	2.33E-07	6.47E-07	6.12E-07	1.00E-05	1.00E-05
	ELPSO _{NR}	1.95E-08	1.05E-06	1.23E-06	6.40E-06	2.45E-06	1.00E-05	7.49E-06
	ELSHADE _{INR}	1.97E-08	3.25E-08	1.87E-12	7.85E-07	1.00E-05	1.00E-05	1.00E-05
	FFA _{NR}	7.35E-07	4.00E-06	1.95E-07	4.02E-06	8.22E-06	8.72E-06	8.21E-06
	MPA _{LW}	4.38E-09	2.41E-12	1.00E-05	3.07E-06	1.98E-07	1.00E-05	1.00E-05
	MPSO _{NR}	1.00E-05	4.74E-06	1.61E-06	1.00E-12	9.99E-06	1.00E-12	1.00E-05
	MRFO _{NR}	1.94E-08	1.68E-07	6.42E-07	1.21E-06	6.24E-06	9.98E-06	1.00E-05
	ALO _{LW}	9.38E-07	2.78E-07	8.79E-07	2.41E-06	1.29E-06	7.69E-06	8.67E-06
	ImSMA _{LW}	1.00E-12	9.88E-06	2.18E-06	1.00E-12	1.00E-12	6.10E-07	9.81E-06
	CHCLPSO _{NR}	1.12E-09	1.05E-06	4.56E-09	2.57E-06	3.31E-06	9.90E-06	8.26E-06
	DEAM _{NR}	1.00E-12	1.11E-06	7.99E-08	1.15E-07	1.66E-08	1.00E-05	1.00E-05
I_{o2}	GCAOA _{EmNR}	9.91E-06	2.86E-06	8.63E-06	6.99E-06	2.79E-07	9.93E-06	3.02E-06
	GCAOA _{AdLM}	1.36E-12	1.63E-09	4.83E-09	1.87E-12	1.32E-10	1.00E-05	9.99E-06

(continued on next page)

Table 7 (continued)

Parameter	Method	S_1	S_2	S_3	S_4	S_5	S_6	S_7
R_s	HAOA _{ENR}	2.12E-12	1.00E-05	8.94E-06	2.80E-11	6.22E-08	2.82E-11	7.55E-07
	GCAOA _{INR}	1.52E-08	2.96E-08	6.16E-08	6.76E-07	1.00E-05	1.00E-05	1.00E-05
	GCAOA _{mNR}	1.00E-05	6.81E-06	1.00E-05	1.00E-05	1.00E-05	1.00E-05	2.86E-08
	GCAOA _{NR}	1.95E-08	1.00E-12	1.00E-12	8.95E-08	3.70E-08	1.00E-05	1.00E-05
	GCAOA _{LW}	1.00E-12	1.37E-09	6.15E-08	7.89E-06	4.95E-06	1.00E-05	3.36E-09
	AEO _{NR}	1.95E-08	1.37E-08	2.13E-06	1.00E-06	4.82E-06	1.00E-05	1.00E-05
	ELPSO _{NR}	1.00E-12	1.69E-06	1.51E-06	3.24E-06	9.76E-06	7.98E-06	8.51E-06
	ELSHADE _{INR}	1.21E-12	3.72E-09	6.16E-08	2.18E-09	6.11E-07	1.00E-05	1.00E-05
	FFA _{NR}	2.84E-06	2.93E-06	2.35E-06	1.00E-12	9.48E-06	9.90E-06	9.58E-06
	MPA _{LW}	1.95E-08	1.31E-06	1.04E-07	1.38E-06	6.20E-06	8.36E-06	1.00E-05
	MPSO _{NR}	1.75E-08	1.00E-05	1.00E-12	9.14E-06	1.00E-05	1.00E-05	1.00E-05
	MRFO _{NR}	1.00E-12	1.08E-07	4.79E-10	2.73E-09	2.52E-08	9.99E-06	1.00E-05
	ALO _{LW}	4.33E-09	1.74E-06	5.22E-08	5.54E-06	2.11E-06	5.27E-06	3.67E-07
	ImSMA _{LW}	1.94E-08	1.65E-08	1.00E-12	9.48E-06	6.13E-06	9.94E-06	1.00E-05
	CHCLPSO _{NR}	6.45E-07	3.89E-06	2.11E-06	2.58E-07	3.96E-06	9.41E-06	9.90E-06
	DEAM _{NR}	1.95E-08	5.27E-07	1.08E-09	6.85E-07	3.89E-06	1.00E-05	1.00E-05
	GCAOA _{EmNR}	0.8405	0.1003	0.6614	0.4866	0.1662	0.1354	0.1000
	GCAOA _{AdLM}	1.8689	0.1967	0.7779	0.5485	0.2663	0.3093	0.1488
	HAOA _{ENR}	2.0000	0.1000	0.7212	0.5130	0.4985	2.0000	0.3347
	GCAOA _{INR}	1.9091	0.6912	0.7763	0.5642	0.3176	0.1642	0.1685
	GCAOA _{mNR}	0.8826	0.1000	0.4836	0.4562	0.1600	0.1000	0.1000
	GCAOA _{NR}	1.9324	0.6927	0.7779	0.5712	0.3118	0.1638	0.1674
	GCAOA _{LW}	1.9324	0.6842	0.7779	0.7270	0.5690	0.3569	0.3184
	AEO _{NR}	1.9524	0.4270	0.7139	0.5531	0.2955	0.1640	0.1676
	ELPSO _{NR}	1.9542	0.3118	0.6359	0.5183	0.2851	0.1725	0.1745
	ELSHADE _{INR}	1.9091	0.6912	0.7763	0.5606	0.3016	0.1642	0.1685
	FFA _{NR}	1.4683	0.2226	0.6117	0.5193	0.2611	0.1866	0.1835
	MPA _{LW}	1.9327	0.3577	0.8002	0.5635	0.5255	0.3002	0.2856
	MPSO _{NR}	2.0000	0.2484	0.6486	0.4912	0.2498	0.1987	0.1814
	MRFO _{NR}	1.9376	0.6766	0.6752	0.5486	0.3005	0.1636	0.1678
	ALO _{LW}	1.3496	0.8343	1.2782	0.5749	0.5137	0.3214	0.3160
	ImSMA _{LW}	1.9327	0.7143	0.6312	0.4879	0.2681	0.3729	0.3138
	CHCLPSO _{NR}	1.5236	0.3656	0.6161	0.5255	0.2729	0.1663	0.1719
	DEAM _{NR}	1.9324	0.4003	0.7683	0.5626	0.2953	0.1639	0.1675
R_p	GCAOA _{EmNR}	699.9745	7986.8325	102.8899	58.8309	16.4763	10.0075	12.6552
	GCAOA _{AdLM}	156.0298	231.7269	143.4172	120.8876	43.4811	40.8985	41.0732
	HAOA _{ENR}	7999.9991	7993.6518	7999.9998	7999.9016	143.4927	7999.9995	14.8024
	GCAOA _{INR}	1034.7237	67.5675	141.5192	102.4436	39.0806	39.8828	33.4999
	GCAOA _{mNR}	111.9637	115.4899	115.7415	77.5817	15.9705	13.7644	12.6796
	GCAOA _{NR}	1115.5458	67.7305	141.9168	96.2665	39.8385	39.5924	33.0424
	GCAOA _{LW}	1115.5934	68.9675	141.9170	96.2273	41.9044	44.1258	39.5856
	AEO _{NR}	3761.1858	111.5478	178.5018	105.8322	39.4647	39.8462	33.1146
	ELPSO _{NR}	2044.6190	171.8760	398.3747	225.7805	40.8266	37.7270	32.4338
	ELSHADE _{INR}	1034.7218	70.5775	141.5184	106.9036	38.6152	39.8893	33.4999
	FFA _{NR}	7080.6061	667.7284	826.3789	357.8495	56.7532	53.3396	34.7171
	MPA _{LW}	1144.8265	130.9440	181.9664	173.8522	43.9924	44.0008	36.7450
	MPSO _{NR}	7999.9877	3578.3598	6793.3801	7881.9006	50.9979	47.7095	28.0940
	MRFO _{NR}	1210.4975	4225.6088	259.2819	124.1326	41.6465	39.4010	33.1923
	ALO _{LW}	3658.5506	574.9605	978.9990	2449.0474	47.4974	43.6716	36.8790
	ImSMA _{LW}	1021.5552	1666.6884	6443.1590	3296.4123	48.0886	122.2280	49.6232
	CHCLPSO _{NR}	7988.0370	190.3726	577.5710	174.2369	42.8804	40.4675	34.0129
	DEAM _{NR}	1115.6239	121.1387	149.8121	105.9790	39.4120	39.6057	33.0435

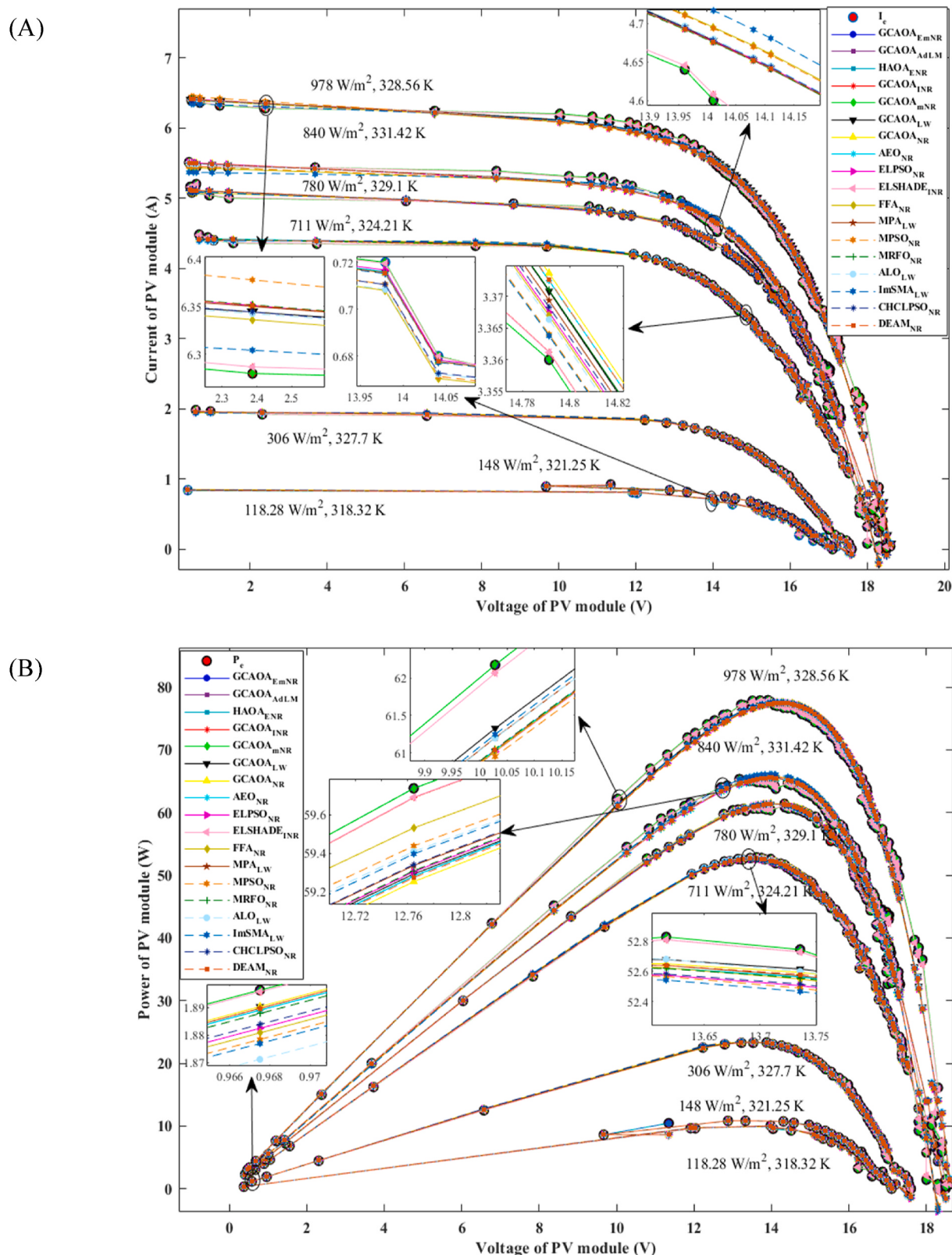


Fig. 11. Plotting the I-V and P-V data curves for the DD PV model using the GCAOA_{EmNR} and other models. (A) I-V curve (B) P-V curve.

Table 8

Statistical criteria for alternative DD PV models.

Parameter	Method	S ₁	S ₂	S ₃	S ₄	S ₅	S ₆	S ₇	Average
RMSE	GCAOA _{EmNR}	0.0000	0.0000	0.0000	0.0000	0.0000	0.0000	0.0000	0.0000
	GCAOA _{AdLM}	0.0000	0.0000	0.0000	0.0000	0.0000	0.0000	0.0000	0.0000
	HAOA _{ENR}	2.26E-37	1.23E-35	6.64E-36	0.0000	4.07E-35	6.18E-36	0.0000	9.43E-36
	GCAOA _{INR}	0.0033	0.0012	0.0024	0.0027	0.0087	0.0097	0.0118	0.0057
	GCAOA _{mNR}	1.19E-09	3.37E-13	4.23E-09	3.03E-08	4.20E-05	1.35E-04	1.38E-04	4.51E-05
	GCAOA _{NR}	0.0329	0.0123	0.0253	0.0280	0.0905	0.1007	0.1222	0.0588
	GCAOA _{LW}	0.0329	0.0123	0.0253	0.0278	0.0905	0.0994	0.1152	0.0576
	AE _{NR}	0.0330	0.0127	0.0260	0.0281	0.0907	0.1007	0.1222	0.0591
	ELPSO _{NR}	0.0329	0.0130	0.0272	0.0288	0.0907	0.1014	0.1234	0.0596
	ELSHADE _{INR}	0.0033	0.0012	0.0024	0.0027	0.0087	0.0097	0.0118	0.0057
	FFA _{NR}	0.0340	0.0133	0.0278	0.0290	0.0916	0.1035	0.1242	0.0605
	MPA _{LW}	0.0329	0.0129	0.0260	0.0283	0.0908	0.0997	0.1190	0.0585
	MPSO _{NR}	0.0335	0.0134	0.0284	0.0300	0.0914	0.1040	0.1253	0.0608
	MRFO _{NR}	0.0329	0.0124	0.0266	0.0281	0.0906	0.1007	0.1222	0.0591
	ALO _{LW}	0.0343	0.0134	0.0274	0.0298	0.0911	0.1004	0.1196	0.0594
	ImSMA _{LW}	0.0329	0.0133	0.0279	0.0300	0.0911	0.1069	0.1201	0.0603
	CHCLPSO _{NR}	0.0338	0.0130	0.0276	0.0285	0.0908	0.1008	0.1227	0.0596
	DEAM _{NR}	0.0329	0.0128	0.0254	0.0280	0.0907	0.1007	0.1222	0.0590
MBE	GCAOA _{EmNR}	0.0000	0.0000	0.0000	0.0000	0.0000	0.0000	0.0000	0.0000
	GCAOA _{AdLM}	0.0000	0.0000	0.0000	0.0000	0.0000	0.0000	0.0000	0.0000
	HAOA _{ENR}	5.10E-74	1.51E-70	4.41E-71	0.0000	1.66E-69	3.81E-71	0.0000	2.70E-70
	GCAOA _{INR}	1.08E-05	1.45E-06	5.90E-06	7.44E-06	7.55E-05	9.40E-05	1.39E-04	4.77E-05
	GCAOA _{mNR}	1.41E-18	1.13E-25	1.79E-17	9.19E-16	1.77E-09	1.83E-08	1.90E-08	5.59E-09
	GCAOA _{NR}	1.08E-03	1.51E-04	6.38E-04	7.85E-04	8.19E-03	1.01E-02	1.49E-02	5.13E-03
	GCAOA _{LW}	1.08E-03	1.52E-04	6.38E-04	7.74E-04	8.19E-03	9.87E-03	1.33E-02	4.85E-03
	AE _{NR}	1.09E-03	1.63E-04	6.75E-04	7.91E-04	8.22E-03	1.01E-02	1.49E-02	5.14E-03
	ELPSO _{NR}	1.09E-03	1.70E-04	7.41E-04	8.27E-04	8.23E-03	1.03E-02	1.52E-02	5.22E-03
	ELSHADE _{INR}	1.08E-05	1.45E-06	5.90E-06	7.44E-06	7.58E-05	9.40E-05	1.39E-04	4.78E-05
	FFA _{NR}	1.16E-03	1.78E-04	7.71E-04	8.41E-04	8.39E-03	1.07E-02	1.54E-02	5.35E-03
	MPA _{LW}	1.08E-03	1.67E-04	6.77E-04	8.02E-04	8.25E-03	9.94E-03	1.41E-02	5.01E-03
	MPSO _{NR}	1.12E-03	1.80E-04	8.05E-04	8.97E-04	8.34E-03	1.08E-02	1.57E-02	5.41E-03
	MRFO _{NR}	1.08E-03	1.54E-04	7.08E-04	7.89E-04	8.21E-03	1.01E-02	1.49E-02	5.15E-03
	ALO _{LW}	1.18E-03	1.80E-04	7.51E-04	8.87E-04	8.31E-03	1.01E-02	1.43E-02	5.10E-03
	ImSMA _{LW}	1.08E-03	1.76E-04	7.77E-04	9.00E-04	8.30E-03	1.14E-02	1.44E-02	5.30E-03
	CHCLPSO _{NR}	1.14E-03	1.69E-04	7.64E-04	8.12E-04	8.25E-03	1.02E-02	1.51E-02	5.20E-03
	DEAM _{NR}	1.08E-03	1.64E-04	6.43E-04	7.84E-04	8.22E-03	1.01E-02	1.49E-02	5.14E-03
R ²	GCAOA _{EmNR}	1.0000	1.0000	1.0000	1.0000	1.0000	1.0000	1.0000	1.0000
	GCAOA _{AdLM}	1.0000	1.0000	1.0000	1.0000	1.0000	1.0000	1.0000	1.0000
	HAOA _{ENR}	1.0000	1.0000	1.0000	1.0000	1.0000	1.0000	1.0000	1.0000
	GCAOA _{INR}	0.9998	1.0000	1.0000	1.0000	1.0000	0.9999	0.9999	0.9999
	GCAOA _{mNR}	1.0000	1.0000	1.0000	1.0000	1.0000	1.0000	1.0000	1.0000
	GCAOA _{NR}	0.9836	0.9980	0.9981	0.9994	0.9950	0.9945	0.9936	0.9946
	GCAOA _{LW}	0.9836	0.9980	0.9981	0.9994	0.9950	0.9947	0.9943	0.9947
	AE _{NR}	0.9836	0.9979	0.9980	0.9994	0.9949	0.9945	0.9936	0.9946
	ELPSO _{NR}	0.9836	0.9978	0.9978	0.9993	0.9949	0.9945	0.9935	0.9945
	ELSHADE _{INR}	0.9998	1.0000	1.0000	1.0000	1.0000	0.9999	0.9999	0.9999
	FFA _{NR}	0.9825	0.9977	0.9977	0.9993	0.9948	0.9943	0.9942	0.9942
	MPA _{LW}	0.9836	0.9978	0.9980	0.9993	0.9949	0.9947	0.9939	0.9946
	MPSO _{NR}	0.9830	0.9977	0.9976	0.9993	0.9949	0.9942	0.9933	0.9943
	MRFO _{NR}	0.9836	0.9976	0.9979	0.9994	0.9949	0.9945	0.9936	0.9945
	ALO _{LW}	0.9822	0.9977	0.9978	0.9993	0.9949	0.9946	0.9939	0.9943
	ImSMA _{LW}	0.9836	0.9977	0.9977	0.9993	0.9949	0.9939	0.9938	0.9944
	CHCLPSO _{NR}	0.9827	0.9978	0.9978	0.9993	0.9949	0.9945	0.9935	0.9944
	DEAM _{NR}	0.9836	0.9979	0.9981	0.9994	0.9949	0.9945	0.9936	0.9946
d _i	GCAOA _{EmNR}	0.0000	0.0000	0.0000	0.0000	0.0000	0.0000	0.0000	0.0000
	GCAOA _{AdLM}	0.0000	0.0000	0.0000	0.0000	0.0000	0.0000	0.0000	0.0000
	HAOA _{ENR}	-9.21E-36	2.84E-36	-2.80E-36	-9.43E-36	3.13E-35	-3.26E-36	-9.43E-36	2.11E-70
	GCAOA _{INR}	-0.0024	-0.0045	-0.0033	-0.0030	0.0030	0.0040	0.0061	1.79E-05
	GCAOA _{mNR}	-4.50E-05	-4.51E-05	-4.50E-05	-4.50E-05	-3.01E-06	9.02E-05	9.30E-05	4.15E-09
	GCAOA _{NR}	-0.0259	-0.0465	-0.0336	-0.0308	0.0316	0.0419	0.0633	0.0019
	GCAOA _{LW}	-0.0247	-0.0453	-0.0324	-0.0298	0.0329	0.0417	0.0575	0.0018
	AE _{NR}	-0.0261	-0.0463	-0.0331	-0.0309	0.0316	0.0417	0.0631	0.0019
	ELPSO _{NR}	-0.0267	-0.0466	-0.0324	-0.0309	0.0311	0.0417	0.0638	0.0019
	ELSHADE _{INR}	-0.0024	-0.0045	-0.0033	-0.0030	0.0030	0.0040	0.0061	1.79E-05
	FFA _{NR}	-0.0265	-0.0471	-0.0327	-0.0315	0.0311	0.0430	0.0637	0.0020
	MPA _{LW}	-0.0256	-0.0456	-0.0325	-0.0302	0.0323	0.0412	0.0604	0.0018
	MPSO _{NR}	-0.0273	-0.0474	-0.0325	-0.0309	0.0305	0.0431	0.0645	0.0020
	MRFO _{NR}	-0.0261	-0.0467	-0.0325	-0.0310	0.0315	0.0417	0.0631	0.0019
	ALO _{LW}	-0.0251	-0.0460	-0.0320	-0.0297	0.0317	0.0410	0.0602	0.0018
	ImSMA _{LW}	-0.0274	-0.0471	-0.0325	-0.0303	0.0308	0.0466	0.0598	0.0019
	CHCLPSO _{NR}	-0.0258	-0.0466	-0.0320	-0.0311	0.0312	0.0412	0.0631	0.0019
	DEAM _{NR}	-0.0260	-0.0461	-0.0336	-0.0309	0.0317	0.0418	0.0632	0.0019
TS	GCAOA _{EmNR}	0.0000	0.0000	0.0000	0.0000	0.0000	0.0000	0.0000	0.0000
	GCAOA _{AdLM}	0.0000	0.0000	0.0000	0.0000	0.0000	0.0000	0.0000	0.0000

(continued on next page)

Table 8 (continued)

Parameter	Method	S_1	S_2	S_3	S_4	S_5	S_6	S_7	Average
CPU	HAOA _{ENR}	1.04E-36	5.88E-35	4.65E-35	0.0000	3.88E-34	6.18E-35	0.0000	7.95E-35
	GCAOA _{INR}	0.0151	0.0058	0.0170	0.0259	0.0836	0.0979	0.1198	0.0522
	GCAOA _{mNR}	5.45E-09	1.61E-12	2.96E-08	2.88E-07	4.01E-04	1.35E-03	1.39E-03	4.49E-04
	GCAOA _{NR}	0.1561	0.0597	0.1814	0.2735	0.9490	1.1200	1.3986	0.5912
	GCAOA _{LW}	0.1561	0.0598	0.1814	0.2715	0.9493	1.1033	1.3081	0.5756
	AEO _{NR}	0.1562	0.0619	0.1868	0.2746	0.9511	1.1200	1.3986	0.5928
	ELPSO _{NR}	0.1561	0.0633	0.1958	0.2809	0.9519	1.1278	1.4154	0.5988
	ELSHADE _{INR}	0.0151	0.0058	0.0170	0.0259	0.0838	0.0979	0.1198	0.0522
	FFA _{NR}	0.1612	0.0648	0.1999	0.2834	0.9618	1.1539	1.4252	0.6072
	MPA _{LW}	0.1561	0.0627	0.1869	0.2765	0.9530	1.1074	1.3568	0.5856
	MPSO _{NR}	0.1589	0.0653	0.2044	0.2929	0.9590	1.1604	1.4399	0.6116
	MRFO _{NR}	0.1561	0.0602	0.1913	0.2742	0.9504	1.1202	1.3987	0.5930
	ALO _{LW}	0.1628	0.0651	0.1972	0.2912	0.9567	1.1163	1.3654	0.5935
	ImSMA _{LW}	0.1561	0.0645	0.2007	0.2934	0.9561	1.1975	1.3722	0.6058
	CHCLPSO _{NR}	0.1602	0.0631	0.1990	0.2783	0.9531	1.1213	1.4061	0.5973
	DEAM _{NR}	0.1561	0.0622	0.1822	0.2734	0.9510	1.1200	1.3986	0.5919
	GCAOA _{EmNR}	21.50	19.28	19.44	19.77	21.06	25.61	20.88	21.08
	GCAOA _{AdLM}	20.75	20.58	20.30	20.66	20.81	21.27	23.33	21.10
	HAOA _{ENR}	19.72	19.75	23.80	24.73	24.95	24.28	24.33	23.08
	GCAOA _{INR}	19.61	19.69	21.36	23.70	22.97	24.78	23.20	22.19
	GCAOA _{mNR}	19.14	19.84	21.91	20.16	20.25	23.50	19.95	20.68
	GCAOA _{NR}	19.9375	19.5625	21.7188	26.2031	22.7656	23.8906	24.1094	22.5982
	GCAOA _{LW}	172.27	611.95	1201.28	2954.05	3146.45	4549.16	5821.95	2636.73
	AEO _{NR}	16.45	16.39	17.13	18.28	18.55	18.13	19.00	17.70
	ELPSO _{NR}	12.66	11.67	12.31	13.56	14.44	14.19	13.44	13.18
	ELSHADE _{INR}	8.14	8.28	10.17	12.61	12.13	9.39	8.67	9.91
	FFA _{NR}	21.59	15.27	16.48	20.73	17.28	14.95	17.72	17.72
	MPA _{LW}	1238.50	319.98	1650.80	11980.80	5408.17	6896.75	5453.92	4706.99
	MPSO _{NR}	10.41	11.33	10.44	15.89	11.16	11.61	11.58	11.77
	MRFO _{NR}	16.11	18.20	16.92	18.05	18.19	18.19	18.14	17.69
	ALO _{LW}	672.98	1533.92	2277.08	655.28	1972.66	2622.52	1967.41	1671.69
	ImSMA _{LW}	2643.72	3666.25	4356.14	5779.84	6939.30	777.48	1611.38	3682.02
	CHCLPSO _{NR}	8.11	8.27	8.63	8.95	8.80	9.13	9.05	8.70
	DEAM _{NR}	10.08	12.70	10.23	12.08	13.30	11.53	11.03	11.56

average RMSE values are 9.43E-36, 4.51E-05, 0.0057, 0.0057, 0.0576, 0.0585, 0.0588, 0.0590, 0.0591, 0.0591, 0.0594, 0.0596, 0.0603, and 0.0605, respectively. The worst RMSE value is registered by MPSO_{NR} within an average RMSE of 0.0608. To summarize the analysis of the other statistical criteria, the LW is more accurate than the NR method, but takes inordinate amount of time. Furthermore, the variations between the approaches that use classic NR and LW methods are modest owing to weak convergence of the OFD. Therefore, it is essential to provide an accurate and trustworthy the algorithm itself in terms of exploration and exploitation, as well as OFD for precisely supplying initial solutions in order to predict the true output current of the PV cell.

Individual AE values must be visualized to convey the degree of stability of each model during the optimization process, and to indicate which experimental data points are difficult to mimic. Keeping in mind that increasing the number of the data points tends to increase in AE values. In this context, Fig. 12. Illustrates the individual AE values for the proposed GCAOA_{EmNR} model and other peers at seven climatic conditions. There is no doubt that the GCAOA_{EmNR} model is able of precisely simulating all the data points for all environmental condition, as indicated in dark blue in the Fig. 12. Similarly, the GCAOA_{AdLM} model displays zero value for all experimental data points, while GCAOA_{ENR} model is able to minimize the error values to zero for just two weather circumstances, S₄ and S₇, as presented in Table 9. The other models contain a large number of erroneous values, which increases dramatically at high levels of weather conditions, as indicated by yellow and red colors.

The depiction of OFD for the proposed GCAOA_{EmNR} model and other peers using RMSE statistical criteria under a range of weather conditions is shown in Fig. 13. According to Fig. 13, the best RMSE value is referred

by a blue intensity color, whilst the worst RMSE value is indicated by a dark red color. The intensity blue color indicates that the GCAOA_{EmNR}, GCAOA_{AdLM}, HAOA_{ENR}, GCAOA_{mNR}, and some of weather conditions of GCAOA_{INR} and ELSHAD_{INR} models have zero or very tiny RMSE values. The lighted-blue hue is distinguished by other models exhibits low accuracy until reaching to the S₅, at which point the color changes from orange to dark red, resulting in very poor accuracy, especially at S₇.

Fig. 14 exhibits the evolution of the fitness function for the first three models: GCAOA_{EmNR}, GCAOA_{AdLM}, and HAOA_{ENR} across a variety of climatic conditions. Zoomed-in Fig. 14 shows GCAOA_{EmNR} model's rapid convergence when compared to two alternative models. This is due to algorithm's sufficient exploration and exploitation tactics, in which the IGOL and DE/best/2/bin play a critical role in remaining stuck in locality and searching around best solution found so far to enhance the efficacy. Additionally, the impactful and effective transformation of clothing solutions by methodical use. This strategy returns near-optimum solutions rather than predetermined lower and upper variables, considerably boosting the convergence. Finally, the augmented four arithmetic operators with their associated control parameters enable the decision-maker to explore the whole feature space's boundary during the optimization process. The second contributions refers to newly designed objective function that is capable of simulating the change in the meteorological circumstances and the seven variables of the PV model's equation. This is achieved in the following manner: the adaptive λ control parameter begins with a large step size and lowers linearly with iterations to effectively eliminate the oscillations' effective and provide precisely initial solutions. Furthermore, contemplate the advantage of the NR's third-order convergence by covering each distance between I-V and P-V curves' data points. Finally, the quadratic

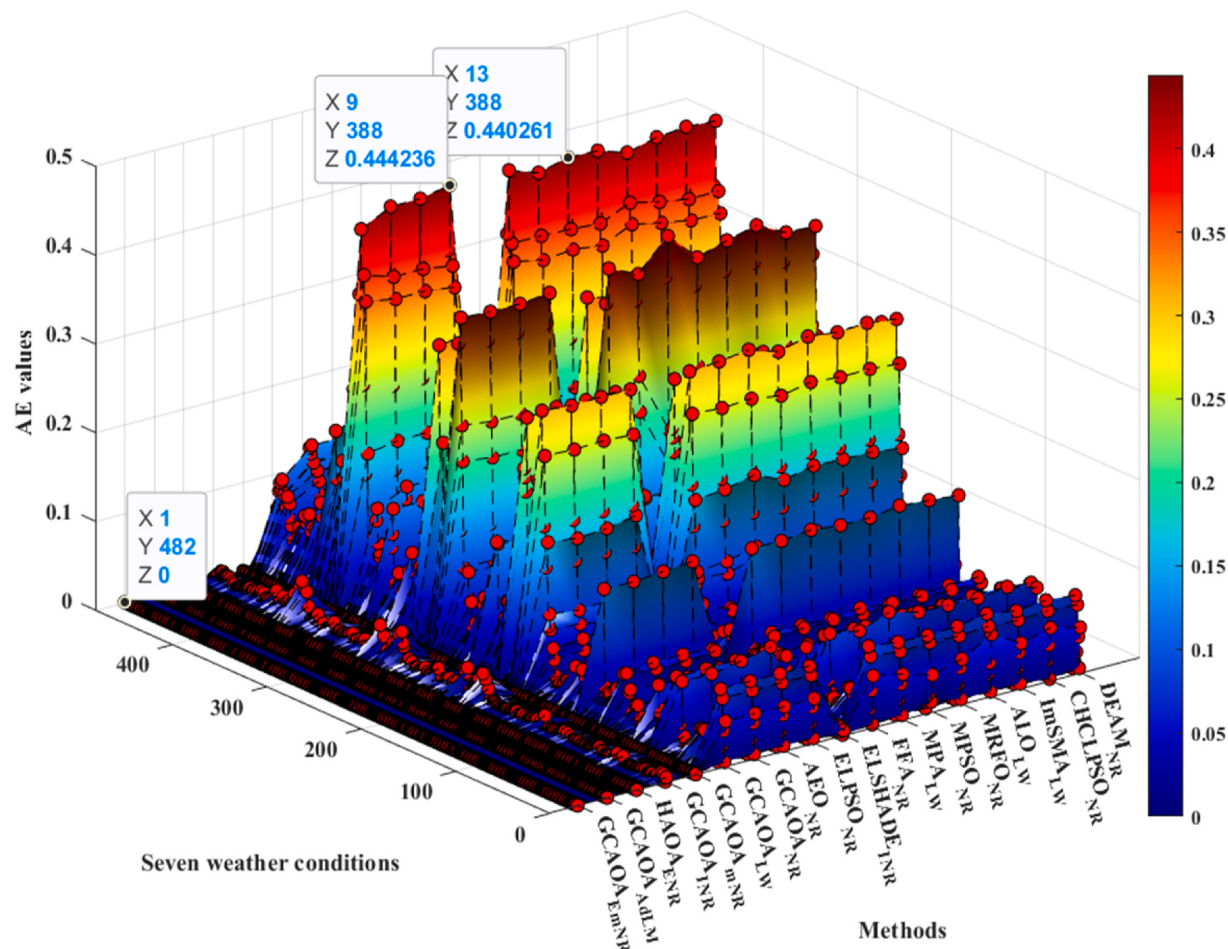


Fig. 12. Comparison of individual AE of GCAOA_{EmNR} and other models for the DD PV model.

Table 9

Average AE values for the DD PV model using different approaches.

Method	S ₁	S ₂	S ₃	S ₄	S ₅	S ₆	S ₇	Average
GCAOA _{EmNR}	0.000000	0.000000	0.000000	0.000000	0.000000	0.000000	0.000000	0.000000
GCAOA _{AdLM}	0.000000	0.000000	0.000000	0.000000	0.000000	0.000000	0.000000	0.000000
HAOA _{ENR}	4.816E-38	2.505E-36	9.386E-37	0.000000	4.245E-36	6.145E-37	0.000000	1.193E-36
GCAOA _{INR}	0.002227	0.000780	0.001643	0.001956	0.006018	0.006866	0.008865	0.004051
GCAOA _{mNR}	9.091E-04	1.333E-03	4.000E-04	1.758E-03	1.536E-03	4.053E-05	4.673E-05	8.605E-04
GCAOA _{NR}	0.022619	0.007961	0.017000	0.020208	0.062102	0.071054	0.091902	0.041835
GCAOA _{LW}	0.022619	0.007964	0.017000	0.019720	0.061368	0.068608	0.082776	0.040008
AOE _{NR}	0.023862	0.008366	0.017533	0.020242	0.062080	0.071084	0.091880	0.042150
ELPSO _{NR}	0.022838	0.008789	0.019153	0.020277	0.061782	0.071930	0.093396	0.042595
ELSHADE _{INR}	0.002227	0.000789	0.001643	0.001954	0.006004	0.006866	0.008865	0.004050
FFA _{NR}	0.024158	0.009277	0.019911	0.020397	0.061797	0.075217	0.092941	0.043385
MPA _{LW}	0.022628	0.008611	0.017561	0.019826	0.061246	0.069393	0.087833	0.041014
MPSO _{NR}	0.024564	0.009510	0.021106	0.021090	0.061349	0.074410	0.096325	0.044051
MRFO _{NR}	0.022669	0.008482	0.018459	0.020077	0.061867	0.071002	0.091867	0.042060
ALO _{LW}	0.023467	0.009433	0.019484	0.020930	0.061167	0.070412	0.087573	0.041781
ImSMA _{LW}	0.022592	0.009167	0.020051	0.021162	0.061421	0.080216	0.088286	0.043271
CHCLPSO _{NR}	0.023794	0.008819	0.019752	0.020219	0.061341	0.071269	0.092233	0.042490
DEAM _{NR}	0.022619	0.008365	0.017074	0.020086	0.061905	0.071053	0.091901	0.041858

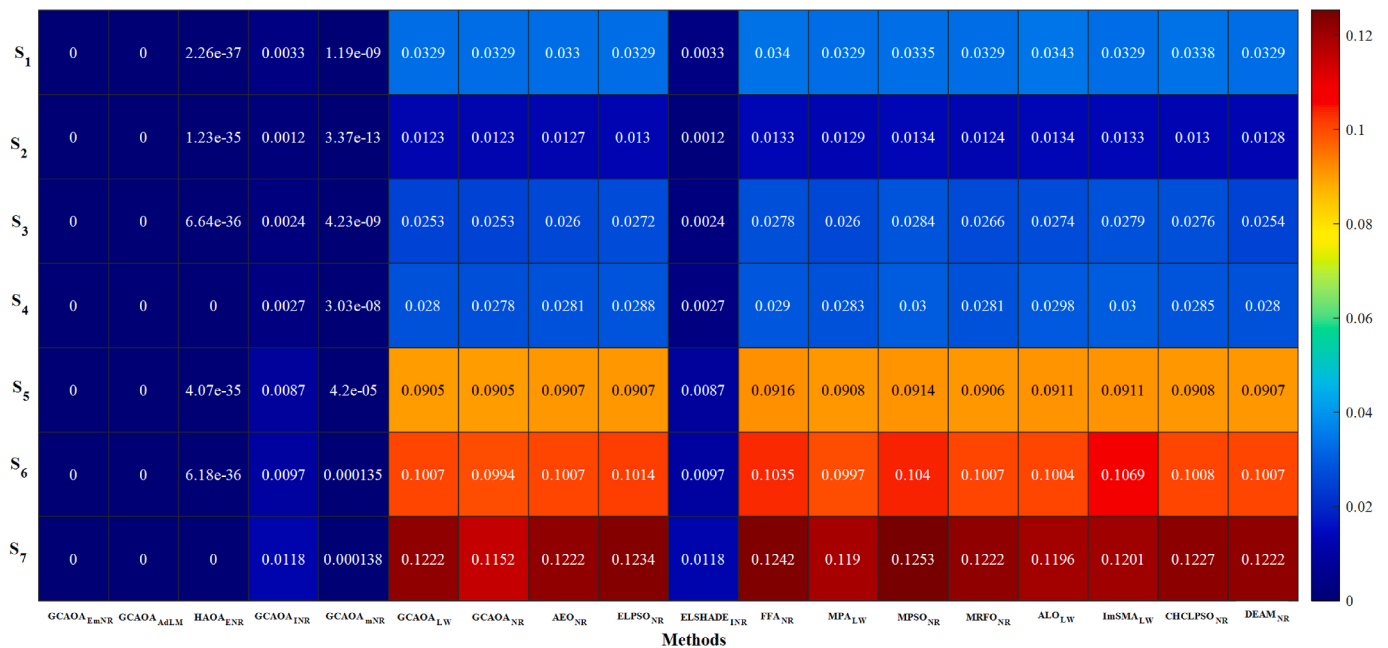


Fig. 13. Comparison of RMSE of GCAOA_{EmNR} and other peer algorithms for the DD PV model.

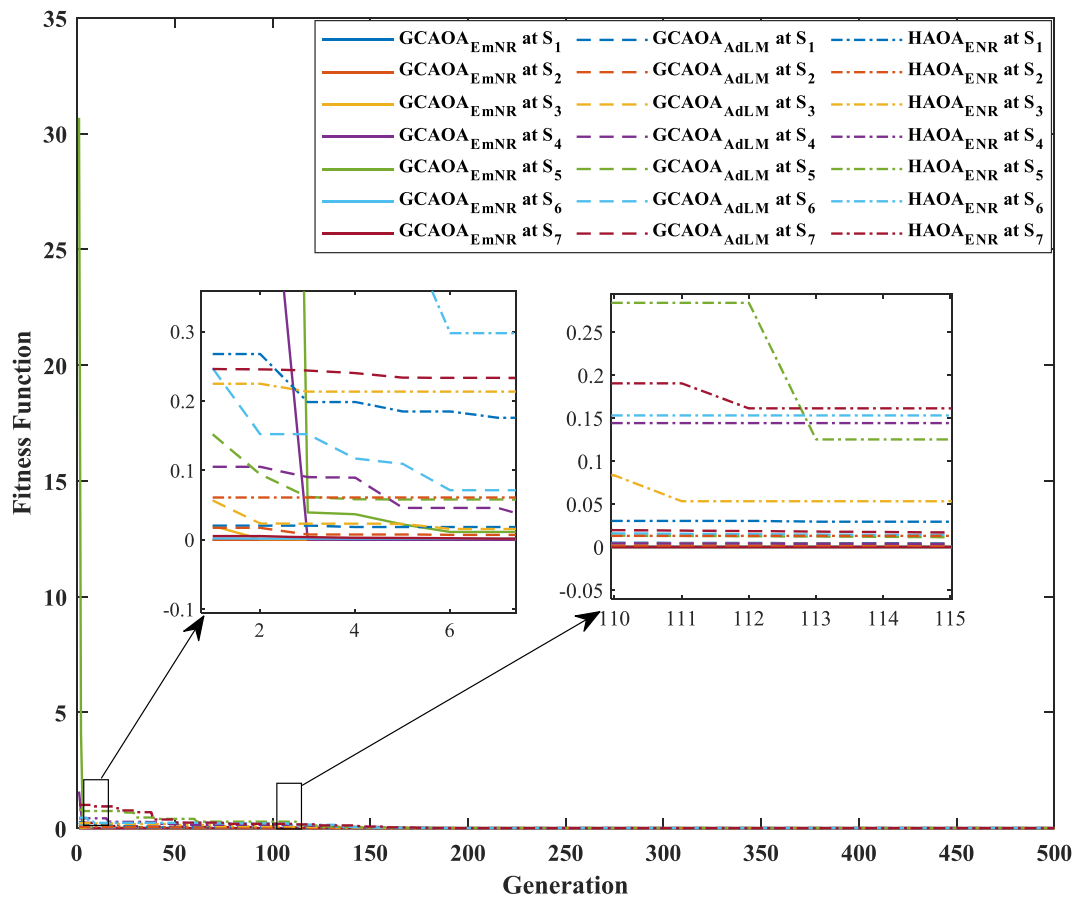


Fig. 14. Development of the fitness function using GCAOA_{EmNR}, GCAOA_{AdLM}, and HAOA_{ENR} for the DD PV model.

Table 10

Parameters extracted from the TD PV model using various approaches.

Parameter	Method	S ₁	S ₂	S ₃	S ₄	S ₅	S ₆	S ₇
<i>d</i> ₁	GCAOA _{EmNR}	1.6673	1.5656	1.0760	1.4293	1.4696	1.4373	1.1703
	GCAOA _{AdLM}	2.0000	1.3623	1.1597	1.3906	1.2119	1.5391	1.9989
	HAOA _{ENR}	2.0000	2.0000	2.0000	1.3998	2.0000	1.0000	2.0000
	GCAOA _{INR}	1.0000	1.9535	1.0000	1.1759	1.6250	1.4702	1.4989
	GCAOA _{mNR}	1.7418	1.5218	1.5074	1.7681	1.4915	1.4343	1.4759
	GCAOA _{NR}	1.0000	1.4869	1.0000	1.1772	1.5574	1.4700	1.4990
	GCAOA _{LW}	2.0000	1.0000	1.4965	1.1189	1.4943	1.6244	1.0000
	AEO _{NR}	1.4814	1.7393	1.2794	1.9524	1.3065	1.5193	1.6667
	ELPSO _{NR}	1.0000	1.3262	1.1787	1.8169	1.8126	1.4452	1.4371
	ELSHADE _{INR}	1.1911	1.4063	1.0000	1.2305	1.5681	1.4713	1.5008
	FFA _{NR}	1.4479	1.8433	1.2040	1.3471	1.3793	1.4021	1.5674
	MPA _{LW}	1.9751	1.3113	1.8659	1.5888	1.8416	1.5819	1.4864
	MPSO _{NR}	1.0000	1.8059	1.9497	2.0000	1.6418	1.4015	1.9930
	MRFO _{NR}	1.0000	1.3556	1.6783	1.2311	1.2384	1.4479	1.4608
	ALO _{LW}	1.4317	1.3966	1.8058	1.2877	1.9115	1.2242	1.7314
	ImSMA _{LW}	1.2964	1.0000	1.0278	1.3431	1.3322	1.4898	1.0000
	CHCLPSO _{NR}	1.3470	1.6431	1.1488	1.7010	1.2643	1.4897	1.4295
	DEAM _{NR}	1.0000	1.6000	1.2765	1.2065	1.2292	1.4813	1.4808
<i>d</i> ₂	GCAOA _{EmNR}	1.6893	1.3029	1.3486	1.2318	1.4286	1.6610	1.5238
	GCAOA _{AdLM}	1.2844	1.4443	1.0009	2.0000	1.6668	1.4228	1.3783
	HAOA _{ENR}	2.0000	1.0000	1.0672	1.0000	1.3342	2.0000	1.0268
	GCAOA _{INR}	1.0000	1.3741	1.0000	1.4238	1.5555	1.4702	1.4989
	GCAOA _{mNR}	1.7178	1.7739	1.5350	1.4301	1.4463	1.5624	1.1910
	GCAOA _{NR}	1.0000	1.0000	2.0000	2.0000	1.3879	1.4704	1.4990
	GCAOA _{LW}	1.0000	1.1760	1.0000	1.7633	1.0000	1.0027	1.4674
	AEO _{NR}	1.9121	1.4832	1.5169	1.2677	1.3851	1.1118	1.3586
	ELPSO _{NR}	2.0000	1.8908	1.7616	1.2708	1.2530	1.4749	1.4560
	ELSHADE _{INR}	1.1604	1.0418	1.9861	1.1748	1.6745	1.4662	1.4961
	FFA _{NR}	1.2313	1.4067	1.7456	1.8048	1.8241	1.4567	1.4067
	MPA _{LW}	1.0000	1.5588	1.0615	1.0424	1.2719	1.5878	1.6432
	MPSO _{NR}	1.9553	1.0273	2.0000	1.3404	1.9582	1.8856	1.6607
	MRFO _{NR}	1.0000	1.7695	1.0238	1.9001	1.8729	1.4551	1.5006
	ALO _{LW}	1.7481	1.9419	1.0948	1.4967	1.3251	1.4523	1.5028
	ImSMA _{LW}	1.0000	1.1080	1.2515	1.0000	1.3354	1.4874	1.3738
	CHCLPSO _{NR}	1.3374	1.3934	1.5941	1.2816	1.6712	1.5078	1.5247
	DEAM _{NR}	1.3386	1.2830	1.0000	1.2626	1.7393	1.4480	1.5152
<i>d</i> ₃	GCAOA _{EmNR}	4.8846	1.5979	1.2988	1.3393	1.1010	1.4783	2.8038
	GCAOA _{AdLM}	1.0000	3.6800	1.0275	1.0686	1.2785	1.3961	3.1953
	HAOA _{ENR}	1.0000	1.4701	5.0000	4.9977	5.0000	5.0000	5.0000
	GCAOA _{INR}	3.8876	1.0000	4.9869	4.9996	1.0000	1.4701	1.4989
	GCAOA _{mNR}	1.7182	1.6137	1.5884	1.7817	4.8949	1.4468	1.6158
	GCAOA _{NR}	4.9151	1.9481	4.9999	1.1037	1.0000	1.4703	1.4990
	GCAOA _{LW}	4.9898	4.7166	4.9967	1.7911	4.0049	1.5104	1.0000
	AEO _{NR}	3.9046	1.4451	3.8436	4.1820	2.7305	4.4589	2.8591
	ELPSO _{NR}	5.0000	1.9723	1.0000	1.0000	4.9911	1.4589	2.5116
	ELSHADE _{INR}	1.0038	3.8006	1.0000	2.0432	1.0162	1.4730	1.5000
	FFA _{NR}	3.1187	2.0518	4.2454	4.5188	4.0958	1.8479	1.6486
	MPA _{LW}	5.0000	4.1940	4.4438	4.4012	1.2334	1.5446	1.6154
	MPSO _{NR}	1.0000	1.0026	1.0000	5.0000	1.0000	1.4314	1.3830
	MRFO _{NR}	4.4739	3.4585	4.3919	5.0000	1.9431	1.4710	1.5588
	ALO _{LW}	4.4292	2.3308	2.1603	2.4057	3.8910	2.8442	1.6931
	ImSMA _{LW}	1.0000	1.0232	4.9733	1.0012	4.6970	1.0000	1.7089
	CHCLPSO _{NR}	1.9909	1.6556	1.6603	1.6556	1.5509	1.4214	1.5251
	DEAM _{NR}	4.3885	3.9779	2.1735	3.0259	2.0768	1.4853	1.5039
<i>I_{ph}</i>	GCAOA _{EmNR}	0.8496	0.8668	1.9085	4.5691	5.5304	5.8344	6.7599
	GCAOA _{AdLM}	0.5992	0.9602	2.0042	4.4086	5.1626	5.4516	6.4665
	HAOA _{ENR}	0.5000	1.0964	2.3141	4.4177	8.0000	1.8301	5.5195
	GCAOA _{INR}	0.8406	1.0560	1.9714	4.4472	5.1602	5.5268	6.4461
	GCAOA _{mNR}	0.9178	0.9637	1.9998	4.5477	5.4128	5.8303	6.7679
	GCAOA _{NR}	0.8402	1.0557	1.9713	4.4471	5.1620	5.5278	6.4480
	GCAOA _{LW}	0.8403	1.0558	1.9713	4.4507	5.2035	5.5453	6.4374
	AEO _{NR}	0.6046	1.0760	2.1704	4.0972	5.2606	5.1130	6.6604
	ELPSO _{NR}	0.8348	0.9713	1.9605	4.4230	5.1616	5.5136	6.4417
	ELSHADE _{INR}	0.8461	1.0035	1.9714	4.4471	5.1639	5.5252	6.4459
	FFA _{NR}	0.8492	0.9337	1.9497	4.4198	5.1101	5.4529	6.3759
	MPA _{LW}	0.8402	0.9735	1.9609	4.4442	5.1719	5.5220	6.4817
	MPSO _{NR}	0.8402	0.9675	1.9580	4.3918	5.2399	5.3335	6.4831
	MRFO _{NR}	0.8402	0.9426	1.9637	4.4369	5.1601	5.5267	6.4256
	ALO _{LW}	0.8639	0.9140	1.9294	4.3918	5.1474	5.5380	6.2238
	ImSMA _{LW}	0.8393	1.3521	1.9447	4.4109	5.1618	5.5357	6.3569
	CHCLPSO _{NR}	0.8516	0.9298	1.9514	4.4194	5.1514	5.5284	6.4476
	DEAM _{NR}	0.8402	0.9656	1.9692	4.4415	5.1581	5.5274	6.4470
<i>I_{o1}</i>	GCAOA _{EmNR}	9.96E-06	2.37E-06	1.91E-11	1.46E-06	9.73E-06	9.99E-06	6.66E-07
	GCAOA _{AdLM}	1.67E-10	3.16E-06	3.27E-12	5.10E-06	1.49E-06	9.13E-06	1.14E-08

(continued on next page)

Table 10 (continued)

Parameter	Method	S_1	S_2	S_3	S_4	S_5	S_6	S_7
I_{o2}	HAOA _{ENR}	1.05E-12	1.00E-12	8.84E-12	6.43E-06	1.00E-05	1.73E-12	1.00E-05
	GCAOA _{INR}	1.97E-08	1.00E-12	6.16E-08	6.76E-07	1.00E-05	1.00E-05	1.00E-05
	GCAOA _{mNR}	1.00E-05	9.14E-06	1.00E-05	6.37E-06	1.00E-05	8.09E-06	1.85E-06
	GCAOA _{NR}	7.19E-09	1.00E-12	6.15E-08	6.83E-07	1.00E-05	1.00E-05	1.00E-05
	GCAOA _{LW}	1.00E-12	2.96E-08	1.00E-12	2.52E-07	5.31E-06	9.99E-06	1.24E-09
	AEO _{NR}	3.64E-06	9.31E-06	2.91E-06	4.88E-06	4.91E-06	1.45E-07	8.83E-06
	ELPSO _{NR}	1.94E-08	2.01E-06	8.43E-07	1.00E-05	7.28E-06	1.00E-05	9.16E-06
	ELSHADE _{INR}	1.61E-07	1.39E-06	1.00E-12	4.08E-08	9.97E-06	1.00E-05	1.00E-05
	FFA _{NR}	1.00E-12	1.00E-12	1.18E-06	5.11E-06	9.39E-06	1.00E-05	9.78E-06
	MPA _{LW}	2.41E-11	1.85E-06	1.65E-07	2.85E-06	2.31E-06	9.70E-06	9.77E-06
	MPSO _{NR}	1.07E-09	9.69E-06	1.00E-05	7.25E-06	8.65E-06	1.00E-05	9.53E-06
	MRFO _{NR}	1.95E-08	2.55E-06	5.74E-06	1.38E-06	2.08E-06	7.61E-06	1.00E-05
	ALO _{LW}	2.50E-06	4.26E-06	3.73E-06	3.38E-07	2.47E-06	5.67E-07	9.84E-06
	ImSMA _{LW}	1.02E-12	1.25E-08	1.00E-12	4.89E-06	1.88E-09	8.90E-06	7.79E-10
	CHCLPSO _{NR}	1.01E-06	3.66E-06	5.57E-07	4.20E-06	2.56E-06	9.96E-06	7.62E-06
	DEAM _{NR}	1.95E-08	1.35E-07	1.23E-07	9.67E-07	1.79E-06	1.00E-05	1.00E-05
	GCAOA _{EmNR}	8.88E-06	1.50E-06	2.49E-06	1.16E-06	5.68E-06	9.99E-06	1.00E-05
	GCAOA _{AdLM}	1.10E-10	3.23E-08	8.11E-12	2.59E-12	5.55E-12	8.84E-06	1.00E-05
	HAOA _{ENR}	1.78E-12	1.00E-12	2.06E-07	1.15E-08	1.00E-05	1.00E-12	9.87E-08
	GCAOA _{INR}	2.31E-11	1.00E-12	1.00E-12	1.00E-12	9.95E-06	1.00E-05	1.00E-05
	GCAOA _{mNR}	9.93E-06	9.87E-06	6.75E-06	9.89E-06	9.41E-06	1.00E-05	9.52E-07
	GCAOA _{NR}	1.23E-08	2.96E-08	1.00E-12	2.96E-12	2.35E-06	1.00E-05	1.00E-05
	GCAOA _{LW}	1.95E-08	1.02E-12	6.15E-08	1.55E-06	8.82E-09	3.62E-09	1.00E-05
	AEO _{NR}	3.50E-07	3.22E-06	6.46E-06	2.21E-06	5.55E-07	5.66E-07	5.60E-06
	ELPSO _{NR}	1.00E-12	6.52E-06	2.81E-06	2.10E-06	2.47E-06	6.92E-06	1.00E-05
	ELSHADE _{INR}	7.97E-08	4.19E-08	2.97E-11	6.46E-07	1.00E-05	1.00E-05	1.00E-05
	FFA _{NR}	5.46E-07	4.63E-06	8.98E-10	3.32E-09	8.71E-06	9.95E-06	9.49E-06
	MPA _{LW}	1.95E-08	1.00E-12	1.68E-07	1.20E-08	9.10E-11	9.69E-06	8.00E-06
	MPSO _{NR}	1.00E-12	5.29E-09	1.00E-05	4.68E-06	9.09E-07	5.96E-08	9.75E-06
	MRFO _{NR}	1.00E-12	6.94E-06	8.55E-08	3.13E-07	8.51E-06	9.54E-06	1.00E-05
	ALO _{LW}	3.88E-06	4.20E-07	2.40E-07	1.77E-06	5.51E-06	6.79E-06	8.95E-06
	ImSMA _{LW}	1.50E-12	1.00E-12	2.05E-06	1.00E-12	6.25E-06	9.69E-06	6.09E-06
	CHCLPSO _{NR}	7.77E-07	3.28E-06	1.07E-06	2.27E-06	1.71E-06	9.86E-06	9.99E-06
	DEAM _{NR}	1.45E-12	1.38E-06	5.88E-08	9.07E-08	9.19E-06	9.98E-06	1.00E-05
I_{o3}	GCAOA _{EmNR}	1.10E-12	2.03E-10	1.25E-06	3.74E-08	1.36E-11	9.99E-06	1.10E-12
	GCAOA _{AdLM}	9.81E-09	1.45E-06	8.92E-08	4.97E-08	2.47E-08	5.02E-06	2.57E-11
	HAOA _{ENR}	1.00E-08	1.00E-05	1.00E-05	5.21E-12	1.00E-05	1.02E-12	1.00E-12
	GCAOA _{INR}	1.00E-12	2.96E-08	1.00E-12	1.02E-12	4.16E-08	1.00E-05	1.00E-05
	GCAOA _{mNR}	1.00E-05	6.66E-07	1.00E-05	1.00E-05	3.21E-06	9.49E-06	1.00E-05
	GCAOA _{NR}	1.00E-12	1.14E-12	1.00E-12	1.49E-09	3.59E-08	1.00E-05	1.00E-05
	GCAOA _{LW}	1.28E-12	5.01E-06	1.00E-12	2.00E-07	2.44E-09	1.00E-05	1.24E-09
	AEO _{NR}	6.97E-06	4.16E-06	2.98E-06	5.52E-06	9.85E-07	2.51E-06	5.18E-07
	ELPSO _{NR}	1.00E-12	1.00E-12	1.00E-12	1.00E-12	7.31E-06	1.00E-05	7.52E-06
	ELSHADE _{INR}	3.88E-09	9.91E-06	6.16E-08	2.60E-12	6.03E-08	1.00E-05	1.00E-05
	FFA _{NR}	8.33E-06	2.63E-07	1.00E-12	2.87E-07	3.74E-06	9.44E-06	9.88E-06
	MPA _{LW}	4.11E-06	9.96E-06	9.31E-06	6.39E-06	1.94E-06	1.00E-05	5.21E-06
	MPSO _{NR}	1.84E-08	2.45E-08	5.85E-08	2.39E-06	5.95E-08	8.90E-06	9.70E-06
	MRFO _{NR}	1.00E-12	5.31E-06	1.00E-12	1.00E-05	2.86E-06	1.00E-05	9.86E-06
	ALO _{LW}	2.72E-06	4.13E-08	2.80E-06	1.98E-06	1.54E-06	6.62E-06	9.63E-06
R_s	ImSMA _{LW}	1.95E-08	1.76E-08	6.71E-08	1.03E-12	1.00E-12	6.70E-10	9.95E-06
	CHCLPSO _{NR}	3.31E-06	1.49E-07	1.18E-07	6.67E-07	1.00E-05	8.04E-09	2.79E-09
	DEAM _{NR}	1.37E-09	7.83E-07	4.08E-08	1.20E-06	7.52E-06	1.00E-05	9.99E-06
	GCAOA _{EmNR}	0.9811	0.3910	0.6454	0.5275	0.1961	0.1000	0.1000
	GCAOA _{AdLM}	1.9732	0.2315	1.1766	0.5394	0.2957	0.3642	0.1842
	HAOA _{ENR}	2.0000	2.0000	1.0605	0.5374	2.0000	2.0000	0.5009
	GCAOA _{INR}	1.9091	0.6910	0.7763	0.5642	0.3122	0.1525	0.1568
	GCAOA _{mNR}	0.8205	0.1001	0.4943	0.4628	0.1610	0.1000	0.1000
	GCAOA _{NR}	0.1558	0.1558	0.1558	0.1558	0.1558	0.1558	0.1558
	GCAOA _{LW}	1.9324	0.6920	0.7779	0.6341	0.5888	0.4638	0.4268
	AEO _{NR}	0.8456	1.0260	0.5875	0.4145	0.3945	0.2353	0.5052
	ELPSO _{NR}	2.0000	0.2131	0.6541	0.5243	0.2849	0.1618	0.1654
	ELSHADE _{INR}	1.6970	0.5289	0.7763	0.5640	0.3170	0.1525	0.1569
	FFA _{NR}	1.5779	0.2500	0.6496	0.5062	0.2555	0.1759	0.1716
	MPA _{LW}	1.9328	0.3157	0.7430	1.0100	0.3009	0.3796	0.3252
R_p	MPSO _{NR}	1.9330	0.6771	0.7659	0.5184	0.3046	0.1763	0.1664
	MRFO _{NR}	1.9324	0.2374	0.7464	0.5450	0.2876	0.1497	0.1724
	ALO _{LW}	1.8680	0.3216	0.8169	0.9940	0.2730	0.3944	0.4065
	ImSMA _{LW}	1.9325	0.1222	0.6246	0.5130	0.2669	0.3451	0.2816
	CHCLPSO _{NR}	1.4059	0.1864	0.6731	0.5171	0.2759	0.1561	0.1603
	DEAM _{NR}	1.9324	0.3562	0.7712	0.5524	0.2868	0.1525	0.1561
	GCAOA _{EmNR}	147.2080	1547.8412	87.9648	41.9767	12.3659	14.0101	12.8442
R_s	GCAOA _{AdLM}	156.5448	191.5745	116.1642	312.5831	38.7548	50.2627	18.7435
	HAOA _{ENR}	7999.9999	8000.0000	632.7138	3851.6104	7999.9987	10.0000	59.7739
	GCAOA _{INR}	1034.7240	67.6063	141.5189	102.4431	41.5068	43.1133	35.5520
	GCAOA _{mNR}	121.4652	203.2116	247.9576	60.9330	15.8578	14.6178	12.7687
	GCAOA _{NR}	1117.5708	67.7309	141.9089	102.5583	40.4338	42.7599	35.0667

(continued on next page)

Table 10 (continued)

Parameter	Method	S_1	S_2	S_3	S_4	S_5	S_6	S_7
GCAOA _{LW}	1115.5888	67.6935	141.9169	99.4113	39.7430	52.5941	53.2187	
AEO _{NR}	3652.6932	2548.1111	911.0005	5034.1197	7189.2020	2714.6552	4789.2326	
ELPSO _{NR}	8000.0000	151.4610	286.0486	206.0624	40.5267	46.2559	33.4116	
ELSHADE _{INR}	7766.1863	103.1649	141.5322	102.6770	40.2506	43.3365	35.5943	
FFA _{NR}	7019.9851	376.5615	431.4561	259.9667	57.4838	60.1014	44.8760	
MPA _{LW}	1134.3639	149.6391	193.9980	144.5733	37.6721	56.4396	37.1423	
MPSO _{NR}	1125.3095	151.0395	225.6881	3497.5515	25.0290	118.7042	31.1296	
MRFO _{NR}	1116.1669	284.8224	210.5264	133.0692	39.9120	40.7598	41.6757	
ALO _{LW}	7160.1862	1176.4633	2048.5113	5473.9045	44.3564	42.4538	1669.6632	
ImSMA _{LW}	1216.6290	24.7706	927.3409	347.0360	42.6282	49.0213	50.2242	
CHCLPSO _{NR}	7793.3786	431.1974	370.2184	241.9895	42.5985	42.8013	34.5177	
DEAM _{NR}	1117.0743	161.2917	150.7313	116.8526	40.7707	42.8161	35.1542	

and fourth convergences are utilized to further improve the objective function, yielding highly promising results and guaranteed global convergence at each execution of the problem optimization.

4.3. Results on three diode PV model

This model includes two additional parameters, d_3 and I_{03} , which results in very high accuracy for under all environmental conditions and therefore is more suitable for industrial PV system applications. The extracted nine parameters of the TD PV model for the proposed GCAOA_{EmNR} and other peers under seven climatic conditions are presented in Table 10. The GCAOA_{EmNR} model extracts affectively the nine parameters of the TD PV model despite of its complexity within domain search space. The range of d_3 is (1.1010–4.8846), while I_{03} values are typically minimal within the range of (9.99E-06-1.10E-12). Close extraction parameter of the TD PV model can be observed for the GCAOA_{AdLM} model. However, it can be seen that the HAOA_{ENR} model extract the nine parameters of the TD PV model in a perturbation way. This due to only employing adaptive LM's control parameter to simulate the nature behavior of nonlinearity of the PV model equation, which is not sufficient. Hence, these physical parameters are strongly influenced by the natural fluctuations like solar irradiance, ambient temperature, formulation of the objective function, and type of the PV technology. The extracted nine parameters by the proposed GCAOA_{EmNR} and other models are then obtained to plot the I-V and P-V data characteristics curves using real experimental data at different sunlight days are depicted in Fig. 15. In general, there are acceptable variance between the experimental currents and the proposed models. However, the zoomed-in view displays considerable variations between these methods. The proposed GCAOA_{EmNR} definitely overlaps all experimental data points. This validates the competency of the proposed methods, which may swiftly converge to the RMSE minimum values.

Various statistical criteria are obtained to reflect the accuracy, stability, efficiency, CPU execution time of the proposed GCAOA_{EmNR} model and other peers as presented in Table 11 it is evident that the proposed GCAOA_{EmNR} model dominates all others approaches in terms RMSE, MBE, R^2 , d_i , and TS statistical criteria except for the CPU processing time. Similar performance can be accomplished by the GCAOA_{AdLM} model which is ranked second.

The HAOA_{ENR} is ranked third, followed by GCAOA_{mNR}, GCAOA_{INR}, ELSHADE_{INR}, GCAOA_{LW}, MPA_{LW}, GCAOA_{NR}, DEAM_{NR}, AEO_{NR}, MRFO_{NR}, CHCLPSO_{NR}, ELPSO_{NR}, FFA_{NR}, ALO_{LW}, and ImSMA_{LW}. The average RMSE values for these methods are 7.06e-36, 4.46e-5, 0.0056, 0.0057, 0.0564, 0.0579, 0.0584, 0.0586, 0.0587, 0.0589, 0.0593, 0.0593, 0.0600, 0.0610, and 0.0612, respectively. The HAOA_{ENR} presents zero values under only two environmental conditions S_4 and S_7 . The preference can be given to GCAOA_{EmNR} to be more affective and efficient for practical PV model applications. Similarly, the MBE, MBE,

d_i , and TS statistical criteria exhibit the same pattern. The CHCLPSO_{NR} and ELPSO_{NR} have the same averages RMSE and d_i values, but CHCLPSO_{NR} has superior averages MBE, TS than ELPSO_{NR}, with excepting of average R^2 , which favors ELPSO_{NR}, as shown in Table 11. The ALO_{LW} and ImSMA_{LW} take 16th and 17th ranks for RMSE, MBE, and d_i , respectively. The worst accuracy and stability registered model is MPSO_{NR}, demonstrating low methodology performance in spite of employing the same objective function method. The superiority in terms of CPU execution time is taken by ELSHADE_{INR} with an average 8.85 s due to powerful employed linear size population reduction strategy. To summarize, both methodology and objective function design are important in improving the accuracy, stability, reliability, and CPU-execution time when optimizing the TD PV model's problem.

Fig. 5 depicts the individual error between each data point of the predicated currents and the observed experimental current using the proposed GCAOA_{EmNR} and other models. The GCAOA_{EmNR} dominate other methods by deteriorating the errors to zero values for all experimental data points at all weather circumstances. Following GCAOA_{AdLM}, HAOA_{ENR}, GCAOA_{mNR}, ELSHADE_{INR}, GCAOA_{INR}, GCAOA_{LW}, MPA_{LW}, GCAOA_{NR}, DEAM_{NR}, MRFO_{NR}, AEO_{NR}, CHCLPSO_{NR}, ELPSO_{NR}, FFA_{NR}, ALO_{LW}, and ALO_{LW}. Their average AE values are as follows: 1.07E-36, 1.33E-5, 0.003992, 0.00752, 0.03835, 0.04036, 0.04125, 0.04132, 0.04137, 0.04145, 0.04206, 0.04217, 0.04280, 0.04345, and, 0.04381, respectively. The MPSO_{NR}, on the other hand, has lowest average AE value, where its average AE value is 0.04606. Therefore, optimizing the PV model in general should be considered for both methodology and objective function design.

The major obstacle of the LW method is that it takes prolong execution time than NR method. However, it outperforms NR method in terms of convergence, particularly in the high-level voltage domains. This issue is handled by the modified NR method by calculating its third order derivative, which can visibly boost the convergence to forecast more accurate solutions with a few more steps and iterations. Moreover, as shown in Fig. 17, the adaptive LM parameter can obviously assist to reduce the nonlinearity and oscillations when combined with the PV model's equation. The visualization of the RMSE values in seven climatic conditions are demonstrated in this figure for various methods, with the intensity blue color cueing the best RMSE values occurred so far. The proposed GCAOA_{EmNR} clearly reveals that the RMSE values for all environmental conditions are zero. Similarly, the GCAOA_{AdLM} model acts well in reducing the RMSE values due to its well-organized algorithm and OFD, followed by HAOA_{ENR}, GCAOA_{mNR}, and some of the environmental conditions for the GCAOA_{INR} and ELSHADE_{INR} models. Whilst, the worst RMSE values are dark red in color at S_5 - S_7 levels of weather conditions and may be readily identified by the most models. The range of the RMSE values, from best to the worst, is shown by color bar on the right side of the Fig. 17. Another point to note is that, all methods have acceptable degree of accuracy at S_2 , whereas the color of

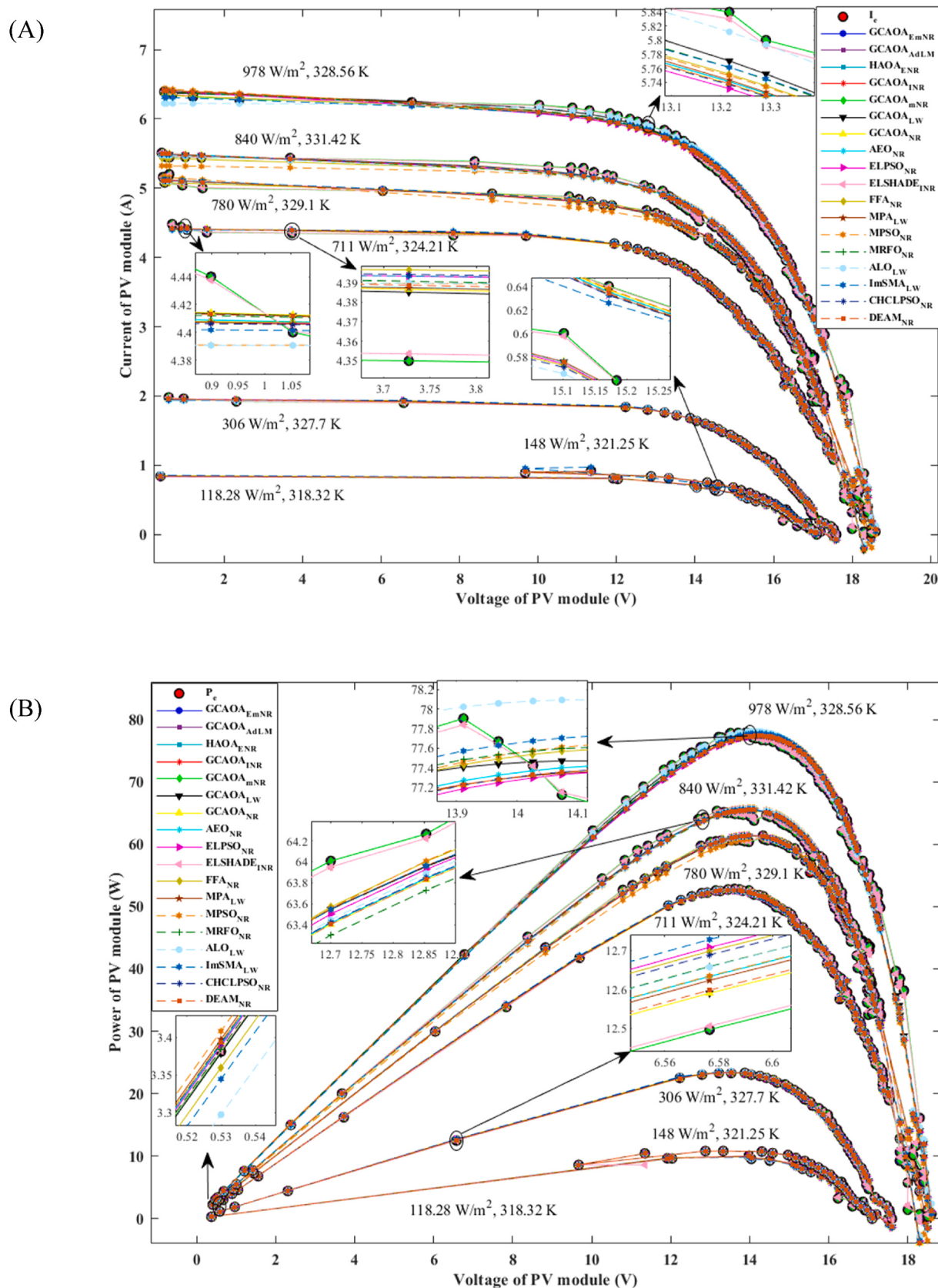


Fig. 15. Plotting the I-V and P-V data curves for the TD PV model using the GCAOA_{EmNR} and other models. (A) I-V curve (B) P-V curve.

Table 11

Statistical criteria for alternative TD PV models.

Parameter	Method	S ₁	S ₂	S ₃	S ₄	S ₅	S ₆	S ₇	Average
RMSE	GCAOA _{EmNR}	0.0000	0.0000	0.0000	0.0000	0.0000	0.0000	0.0000	0.0000
	GCAOA _{AdLM}	0.0000	0.0000	0.0000	0.0000	0.0000	0.0000	0.0000	0.0000
	HAOA _{ENR}	1.82E-36	9.05E-36	3.47E-35	0.0000	2.12E-38	3.84E-36	0.0000	7.07E-36
	GCAOA _{INR}	0.0033	0.0012	0.0024	0.0027	0.0087	0.0096	0.0116	0.0056
	GCAOA _{mNR}	1.06E-09	3.28E-13	4.01E-09	3.34E-08	4.25E-05	1.27E-04	1.43E-04	4.46E-05
	GCAOA _{NR}	0.0329	0.0123	0.0252	0.0280	0.0905	0.0998	0.1201	0.0584
	GCAOA _{LW}	0.0329	0.0123	0.0253	0.0278	0.0904	0.0980	0.1080	0.0564
	AE _{NR}	0.0330	0.0127	0.0259	0.0281	0.0907	0.1000	0.1203	0.0587
	ELPSO _{NR}	0.0330	0.0133	0.0270	0.0287	0.0907	0.1003	0.1224	0.0593
	ELSHADE _{INR}	0.0033	0.0012	0.0024	0.0027	0.0087	0.0096	0.0116	0.0057
	FFA _{NR}	0.0337	0.0133	0.0271	0.0291	0.0916	0.1023	0.1228	0.0600
	MPA _{LW}	0.0329	0.0130	0.0258	0.0281	0.0908	0.0983	0.1161	0.0579
	MPSO _{NR}	0.0329	0.0128	0.0257	0.0297	0.0996	0.1095	0.1255	0.0623
	MRFO _{NR}	0.0329	0.0132	0.0259	0.0282	0.0907	0.1003	0.1214	0.0589
	ALO _{LW}	0.0354	0.0135	0.0277	0.0298	0.0910	0.1030	0.1264	0.0610
	ImSMA _{LW}	0.0329	0.0271	0.0277	0.0291	0.0910	0.0997	0.1211	0.0612
	CHCLPSO _{NR}	0.0342	0.0133	0.0268	0.0289	0.0908	0.1000	0.1209	0.0593
	DEAM _{NR}	0.0329	0.0129	0.0253	0.0281	0.0907	0.0998	0.1202	0.0586
MBE	GCAOA _{EmNR}	0.0000	0.0000	0.0000	0.0000	0.0000	0.0000	0.0000	0.0000
	GCAOA _{AdLM}	0.0000	0.0000	0.0000	0.0000	0.0000	0.0000	0.0000	0.0000
	HAOA _{ENR}	3.30E-72	8.18E-71	1.21E-69	0.0000	4.49E-76	1.48E-71	0.0000	1.87E-70
	GCAOA _{INR}	1.08E-05	1.45E-06	5.90E-06	7.44E-06	7.54E-05	9.24E-05	1.35E-04	4.68E-05
	GCAOA _{mNR}	1.13E-18	1.08E-25	1.60E-17	1.12E-15	1.81E-09	1.62E-08	2.03E-08	5.48E-09
	GCAOA _{NR}	1.08E-03	1.51E-04	6.38E-04	7.84E-04	8.18E-03	9.96E-03	1.44E-02	5.03E-03
	GCAOA _{LW}	1.08E-03	1.51E-04	6.38E-04	7.75E-04	8.17E-03	9.61E-03	1.17E-02	4.58E-03
	AE _{NR}	1.09E-03	1.62E-04	6.72E-04	7.92E-04	8.22E-03	1.00E-02	1.45E-02	5.06E-03
	ELPSO _{NR}	1.09E-03	1.76E-04	7.29E-04	8.22E-04	8.23E-03	1.01E-02	1.50E-02	5.16E-03
	ELSHADE _{INR}	1.11E-05	1.51E-06	5.90E-06	7.44E-06	7.54E-05	9.24E-05	1.35E-04	4.69E-05
	FFA _{NR}	1.14E-03	1.76E-04	7.35E-04	8.46E-04	8.40E-03	1.05E-02	1.51E-02	5.26E-03
	MPA _{LW}	1.08E-03	1.69E-04	6.64E-04	7.91E-04	8.25E-03	9.66E-03	1.35E-02	4.87E-03
	MPSO _{NR}	1.08E-03	1.65E-04	6.60E-04	8.85E-04	9.92E-03	1.20E-02	1.58E-02	5.78E-03
	MRFO _{NR}	1.08E-03	1.74E-04	6.70E-04	7.93E-04	8.23E-03	1.01E-02	1.47E-02	5.11E-03
	ALO _{LW}	1.25E-03	1.82E-04	7.68E-04	8.88E-04	8.28E-03	1.06E-02	1.60E-02	5.42E-03
	ImSMA _{LW}	1.08E-03	7.32E-04	7.65E-04	8.48E-04	8.29E-03	9.93E-03	1.47E-02	5.19E-03
	CHCLPSO _{NR}	1.17E-03	1.77E-04	7.20E-04	8.34E-04	8.24E-03	9.99E-03	1.46E-02	5.11E-03
	DEAM _{NR}	1.08E-03	1.67E-04	6.42E-04	7.87E-04	8.22E-03	9.97E-03	1.44E-02	5.05E-03
R ²	GCAOA _{EmNR}	1.0000	1.0000	1.0000	1.0000	1.0000	1.0000	1.0000	1.0000
	GCAOA _{AdLM}	1.0000	1.0000	1.0000	1.0000	1.0000	1.0000	1.0000	1.0000
	HAOA _{ENR}	1.0000	1.0000	1.0000	1.0000	1.0000	1.0000	1.0000	1.0000
	GCAOA _{INR}	0.9998	1.0000	1.0000	1.0000	1.0000	1.0000	0.9999	0.9999
	GCAOA _{mNR}	1.0000	1.0000	1.0000	1.0000	1.0000	1.0000	1.0000	1.0000
	GCAOA _{NR}	0.9836	0.9980	0.9981	0.9994	0.9950	0.9947	0.9938	0.9947
	GCAOA _{LW}	0.9836	0.9980	0.9981	0.9994	0.9950	0.9948	0.9950	0.9948
	AE _{NR}	0.9835	0.9979	0.9980	0.9994	0.9949	0.9946	0.9938	0.9946
	ELPSO _{NR}	0.9835	0.9977	0.9979	0.9993	0.9949	0.9946	0.9936	0.9945
	ELSHADE _{INR}	0.9998	1.0000	1.0000	1.0000	1.0000	1.0000	0.9999	0.9999
	FFA _{NR}	0.9828	0.9977	0.9978	0.9993	0.9948	0.9944	0.9935	0.9943
	MPA _{LW}	0.9836	0.9978	0.9981	0.9994	0.9949	0.9948	0.9942	0.9947
	MPSO _{NR}	0.9836	0.9979	0.9981	0.9993	0.9939	0.9936	0.9933	0.9942
	MRFO _{NR}	0.9836	0.9977	0.9980	0.9994	0.9949	0.9946	0.9937	0.9946
	ALO _{LW}	0.9810	0.9976	0.9978	0.9993	0.9949	0.9943	0.9932	0.9940
	ImSMA _{LW}	0.9836	0.9905	0.9978	0.9993	0.9949	0.9947	0.9937	0.9935
	CHCLPSO _{NR}	0.9823	0.9977	0.9979	0.9993	0.9949	0.9946	0.9937	0.9944
	DEAM _{NR}	0.9836	0.9978	0.9981	0.9994	0.9949	0.9946	0.9938	0.9946
d _i	GCAOA _{EmNR}	0.0000	0.0000	0.0000	0.0000	0.0000	0.0000	0.0000	0.0000
	GCAOA _{AdLM}	0.0000	0.0000	0.0000	0.0000	0.0000	0.0000	0.0000	0.0000
	HAOA _{ENR}	-5.25E-36	1.98E-36	2.77E-35	-7.07E-36	-7.05E-36	-3.22E-36	-7.07E-36	1.60E-70
	GCAOA _{INR}	-0.0024	-0.0044	-0.0032	-0.0029	0.0030	0.0040	0.0059	0.0000
	GCAOA _{mNR}	-4.46E-05	-4.46E-05	-4.46E-05	-4.46E-05	-2.11E-06	8.28E-05	9.79E-05	4.07E-09
	GCAOA _{NR}	-0.0255	-0.0461	-0.0332	-0.0304	0.0320	0.0414	0.0617	0.0019
	GCAOA _{LW}	-0.0235	-0.0441	-0.0311	-0.0285	0.0340	0.0416	0.0516	0.0016
	AE _{NR}	-0.0257	-0.0460	-0.0328	-0.0305	0.0320	0.0413	0.0616	0.0019
	ELPSO _{NR}	-0.0263	-0.0461	-0.0323	-0.0307	0.0314	0.0409	0.0631	0.0019
	ELSHADE _{INR}	-0.0023	-0.0044	-0.0032	-0.0029	0.0030	0.0040	0.0059	0.0000
	FFA _{NR}	-0.0262	-0.0467	-0.0329	-0.0309	0.0316	0.0423	0.0628	0.0019
	MPA _{LW}	-0.0249	-0.0449	-0.0321	-0.0297	0.0330	0.0404	0.0582	0.0018
	MPSO _{NR}	-0.0293	-0.0494	-0.0366	-0.0325	0.0373	0.0473	0.0633	0.0022
	MRFO _{NR}	-0.0260	-0.0457	-0.0331	-0.0308	0.0318	0.0413	0.0625	0.0019
	ALO _{LW}	-0.0256	-0.0475	-0.0333	-0.0312	0.0300	0.0420	0.0654	0.0020
	ImSMA _{LW}	-0.0283	-0.0342	-0.0336	-0.0321	0.0298	0.0384	0.0599	0.0017
	CHCLPSO _{NR}	-0.0251	-0.0459	-0.0324	-0.0304	0.0315	0.0407	0.0616	0.0019
	DEAM _{NR}	-0.0256	-0.0456	-0.0332	-0.0305	0.0321	0.0413	0.0616	0.0019
TS	GCAOA _{EmNR}	0.0000	0.0000	0.0000	0.0000	0.0000	0.0000	0.0000	0.0000
	GCAOA _{AdLM}	0.0000	0.0000	0.0000	0.0000	0.0000	0.0000	0.0000	0.0000

(continued on next page)

Table 11 (continued)

Parameter	Method	S_1	S_2	S_3	S_4	S_5	S_6	S_7	Average
CPU	HAOA _{ENR}	8.33E-36	4.34E-35	2.43E-34	0.0000	2.02E-37	3.84E-35	0.0000	4.77E-35
	GCAOA _{INR}	0.0151	0.0058	0.0170	0.0259	0.0835	0.0971	0.1179	0.0518
	GCAOA _{mNR}	4.87E-09	1.57E-12	2.80E-08	3.17E-07	4.06E-04	1.27E-03	1.43E-03	4.45E-04
	GCAOA _{NR}	0.1560	0.0597	0.1813	0.2733	0.9487	1.1085	1.3723	0.5857
	GCAOA _{LW}	0.1561	0.0597	0.1814	0.2717	0.9478	1.0866	1.2163	0.5599
	AE _{NR}	0.1564	0.0618	0.1862	0.2746	0.9511	1.1109	1.3746	0.5879
	ELPSO _{NR}	0.1564	0.0645	0.1943	0.28	0.952	1.1142	1.4023	0.5948
	ELSHADE _{INR}	0.0153	0.0059	0.017	0.0259	0.0836	0.0971	0.1179	0.0518
	FFA _{NR}	0.1600	0.0645	0.1951	0.2843	0.9623	1.1391	1.4071	0.6018
	MPA _{LW}	0.151	0.0623	0.1804	0.2669	0.87	0.9877	1.1746	0.5276
	MPSO _{NR}	0.151	0.0616	0.1798	0.2823	0.9548	1.1019	1.2716	0.5719
	MRFO _{NR}	0.151	0.0633	0.1812	0.2673	0.8688	1.0076	1.2292	0.5199
	ALO _{LW}	0.1682	0.0656	0.1995	0.2914	0.9549	1.1485	1.4542	0.6118
	ImSMA _{LW}	0.1510	0.1298	0.1937	0.2764	0.8721	1.0016	1.2259	0.5501
	CHCLPSO _{NR}	0.1622	0.0647	0.193	0.2821	0.9527	1.1107	1.3821	0.5925
	DEAM _{NR}	0.1561	0.0629	0.182	0.2738	0.9514	1.109	1.3728	0.5869
	GCAOA _{EmNR}	20.39	19.17	20.44	21.06	21.00	21.42	22.11	20.80
	GCAOA _{AdLM}	18.63	18.48	20.58	20.63	20.09	19.64	19.58	19.66
	HAOA _{ENR}	18.48	18.72	19.63	23.52	22.20	22.44	24.06	21.29
	GCAOA _{INR}	19.00	18.53	19.92	22.97	22.09	22.58	22.80	21.13
	GCAOA _{mNR}	19.44	18.88	20.58	21.02	21.73	23.83	23.19	21.24
	GCAOA _{NR}	21.27	19.25	21.33	28.94	23.45	23.38	23.89	23.07
	GCAOA _{LW}	7166.58	6111.31	418.14	12370.03	1978.78	1652.36	8204.39	5414.51
	AE _{NR}	19.64	17.52	18.45	20.98	19.47	19.59	20.06	19.39
	ELPSO _{NR}	12.77	13.08	20.22	14.50	14.27	14.28	14.53	14.81
	ELSHADE _{INR}	8.56	8.59	8.55	9.16	8.89	8.88	9.36	8.85
	FFA _{NR}	19.27	22.19	19.02	20.20	20.05	20.84	21.95	20.50
	MPA _{LW}	250.48	1352.31	2846.45	5631.59	11101.31	1261.05	849.52	3327.53
	MPSO _{NR}	10.92	12.56	12.09	11.58	11.14	11.39	13.83	11.93
	MRFO _{NR}	18.14	19.31	17.92	19.42	19.86	23.05	19.44	19.59
	ALO _{LW}	1827.64	553.27	1383.69	1882.30	5615.73	345.59	3644.34	2178.94
	ImSMA _{LW}	1380.98	2828.44	5338.09	7827.30	256.86	3200.22	2090.84	3274.68
	CHCLPSO _{NR}	15.53	11.80	12.84	13.42	12.67	11.89	11.88	12.86
	DEAM _{NR}	11.19	11.41	11.20	13.08	13.66	12.30	12.22	12.15

Table 12

Average AE values for the TD PV model using different approaches.

Method	S_1	S_2	S_3	S_4	S_5	S_6	S_7	Average
GCAOA _{EmNR}	0.000000							
GCAOA _{AdLM}	0.000000							
HAOA _{ENR}	3.875E-37	1.846E-36	4.914E-36	0.000000	2.210E-39	3.824E-37	0.000000	1.076E-36
GCAOA _{INR}	0.002227	0.000779	0.001643	0.001956	0.005971	0.006722	0.008649	0.003992
GCAOA _{mNR}	6.024E-10	1.374E-13	1.251E-09	1.251E-08	1.430E-05	3.426E-05	4.516E-05	1.339E-05
GCAOA _{NR}	0.022617	0.007961	0.016998	0.020106	0.061955	0.069522	0.089629	0.041255
GCAOA _{LW}	0.022619	0.007951	0.017000	0.019743	0.061677	0.066040	0.073435	0.038352
AE _{NR}	0.022795	0.008282	0.017486	0.019994	0.061988	0.069959	0.089685	0.041456
ELPSO _{NR}	0.023226	0.008871	0.018842	0.020318	0.061810	0.070268	0.091920	0.042179
ELSHADE _{INR}	0.002331	0.000797	0.001643	0.001955	0.005999	0.031323	0.008648	0.007528
FFA _{NR}	0.024072	0.009239	0.019149	0.020521	0.061493	0.072857	0.092306	0.042805
MPA _{LW}	0.022624	0.008704	0.017505	0.019839	0.061996	0.066473	0.085445	0.040369
MPSO _{NR}	0.022623	0.008649	0.017484	0.020901	0.072837	0.082783	0.097187	0.046066
MRFO _{NR}	0.022619	0.009020	0.017740	0.020021	0.061854	0.070069	0.088264	0.041370
ALO _{LW}	0.026401	0.009700	0.019999	0.020929	0.061281	0.073658	0.092224	0.043456
ImSMA _{LW}	0.022647	0.022078	0.019816	0.020488	0.061062	0.068110	0.092507	0.043815
CHCLPSO _{NR}	0.024489	0.009100	0.018846	0.020412	0.061392	0.069771	0.090431	0.042063
DEAM _{NR}	0.022619	0.008654	0.017064	0.020070	0.061651	0.069564	0.089618	0.041320

these methods drastically changes to red color starting from level S_5 to S_7 of the weather conditions. This is due to the large number of the data points collected in each weather condition, and fluctuations in current and voltage throughout the sunlight day.

Last but not least, Fig. 18 depicts the convergence of the proposed GCAOA_{EmNR} model and the second and third competitive models for optimizing the TD PV model at arbitrary weather conditions. As seen in Fig. 18, the proposed GCAOA_{EmNR} model can minimize the RMSE value with a relatively short number of iterations. This is justified not only for a successful hybridization strategies, but also for adequate integration of the NR and LM methods. The GCAOA_{AdLM} model exhibits the second convergence, where its rapid convergence beginning after roughly 80 iterations. On the other hand, HAOA_{ENR} model enables to reduce the

RMSE values to good percentage of errors. However, it has very slow convergence rate to optimality. This is due to two major obstacles in terms of methodology which are: the obtained chaotic map strategy and traditional transformation of outfit variables, conducting several nonoptimal solutions.

There were numerous benefits and drawbacks have been observed between proposed GCAOA_{EmNR} model in a comparisons with others models for extracting the parameters of the TD PV model using real experimental data at seven climatic conditions, which can be demonstrated by the following table:

Based on the above findings analysis and discussions, we may emphasize the following contributions:

In term of methodology:

Table 13Advantage and disadvantage of the proposed GCAOA_{EmNR} model and other peers in terms of methodology and OFD.

Method	Advantage	Disadvantage
GCAOA _{EmNR}	<ul style="list-style-type: none"> Exhibits very high level of stability and accuracy, and convergence rate. It can reduce the error to zero at all weather conditions. Powerful at explorer-exploiter phases. EmNR is well-implemented to provide precise initial parameters with third order convergence. Control parameters are set to deal with complex and nonlinear optimization problem. Third order convergence. 	<ul style="list-style-type: none"> The new formulated EmNR method takes more computing time in a comparison with the traditional NR method. The D and M operators are harmful and mostly result very low solutions quality.
HAOA _{ENR} [19]	<ul style="list-style-type: none"> It can reduce the RMSE to zero in some level of weather conditions. Faster than GCAOA_{EmNR} model. Chaotic-mutant strategy assists to jump from locality to globally. Nonlinear adaptive LM's parameter can boost the converge to optimal solutions. 	<ul style="list-style-type: none"> Time consuming: due to complexity of the algorithm. Chaotic map technique produces many poor solutions during the optimization process. Slow convergence rate. Second order convergence. The level of accuracy of these models are limited.
GCAOA _{INR}	<ul style="list-style-type: none"> These models are powerful in terms of methodology. 	<ul style="list-style-type: none"> GCAOA_{INR} takes very prolong time due to the LW function. GCAOA_{NR} is less accurate than other variants of the GCAOA algorithms due to poor convergence to the basic NR method.
GCAOA _{NR}	<ul style="list-style-type: none"> Static LM's parameter of the GCAOA_{INR} model can provide better initial solutions than traditional NR and LM methods. 	
GCAOA _{LW}	<ul style="list-style-type: none"> GCAOA_{LW} is more accurate and stable than GCAOA_{NR}. GCAOA_{NR} faster than others proposed variants models. 	
AEO _{NR} [81]	<ul style="list-style-type: none"> Moderate performance during optimization process. Moderate convergence rate. 	<ul style="list-style-type: none"> Even though using NR method as objective function., but its level of accuracy is not promising. Has a difficulty in extracting the nine parameter of TD PV model. Time consuming: due to long procedure of methodology. Unbalancing between the exploration and exploitation phases. Acceptable computational time. Control parameters are required to fit the optimized problem. In some of execution optimization process, lack of exploitation tendency can be observed. Its level of accuracy is limited due to the static parameter of the LM method. Complicated structure.
ELPSO _{NR} [65]	<ul style="list-style-type: none"> Five successive mutation schemes can increase the diversity of solutions. Premature convergence of PSO algorithm is reduced. 	
ELSHADE _{INR} [20]	<ul style="list-style-type: none"> Population is divided into two phases: robust mutant at first and guided-strategy at second half. Fast convergence rate. Takes very slow time calculations due to using LSPR strategy. Uses an external archives and chaotic map strategies to enrich the diversity. Balancing between the exploration and exploitation is achieved. Divides the population into three portions to enhance its performance. The memory is used to save finest solutions. 	
FFA _{NR}	<ul style="list-style-type: none"> Performs well at exploration part due to employ LF and Brownian strategies. The population is separated into three phases to balance between the exploration and exploitation phases. Moderate convergence. Acceptable CPU processing time. Balancing between the explorative and exploitative ability is accomplished by suitably obtaining mutation probability. 	<ul style="list-style-type: none"> Poor solution quality. Needs large number of iterations to reach for optimality. Slow convergence. Takes very prolong execution time. Elite metric is updated based on best solution which can significantly limits the exploitation tendency Moderate performance at exploitation phase. The solutions are updated based on best optimal solution found, resulting poor solutions. Utilizing traditional NR method leads to insufficiently estimate the parameter of the TD PV model. Takes more computing time. Low exploitation especially at large set of data points. Has limited level of accuracy due to poor convergence of traditional NR method.
MPA _{LW} [23,29]		
MPSO _{NR} [94]		
MRFO _{NR} [111]	<ul style="list-style-type: none"> Its performance is excellent at short set data points. Alpha and beta control parameters can easily jump from locality to optima. Has a good exploration. 	
ALO _{LW} [87]	<ul style="list-style-type: none"> Moderate exploration. Simple, fast, and can be easily coded. Free control parameters. 	<ul style="list-style-type: none"> Poor stability and accuracy in optimization a complex problem. Time consuming due to using LW function. Premature convergence. Poor at exploitation phase. Complexity and time consuming. The exploitation ability is weak at TD PV model optimization problem causes premature convergence. It can easily fall in locality.
ImSMA _{LW}	<ul style="list-style-type: none"> The exploration is improved due to newly inserted control parameter and LF tactic. 	
CHCLPSO _{NR} [103]	<ul style="list-style-type: none"> Fast convergence rate. Low computational time. CL and PC control the exploration and exploitation of population. Chaotic map is obtained in enrich the diversity of solutions. Robust implemented exploration tactic. Fast convergence rate. Well-suited control parameters: mutant factor and crossover rate. High agreement and consistency between the exploration and exploitation phases. 	<ul style="list-style-type: none"> Moderate exploitation tendency. The employed NR method cannot simulate all experimental data points especially at MPP.
DEAM _{NR} [76]		

- The RL and e, along with nonlinear formula, can greatly enhance the diversification phase and the search for new attractive solutions.
- The F₁ and F₂ factors have a high ability in enhancing the intensification tendency when the best and worst solutions vectors are considered.
- A novel adaptive boundary strategy based on best solution and randomizing the lower and upper limits is obtained to transfer from locality to globally.
- Systematic explorer-exploiter tactic is acquired by an adaptive IGOL and mutation mechanisms, in which the IGOL serves a maximum of 166 iterations and the resilient mutation strategy performs the rest.

In term of objective function design:

- The modified third-order derivative NR method is applied to initially predict the parameters roots of the SD, DD, and TD PV models.
- The nonlinear adaptive LM parameter plays crucial role in minimizing the nonlinearity and oscillations in the PV model' equation and lowering the error between the pair current-voltage data points to zero.
- Quadratic and fourth convergences are addressed for widely discovering feature space.

The innovative GCAOA_{EmNR} is effective in extracting the parameters

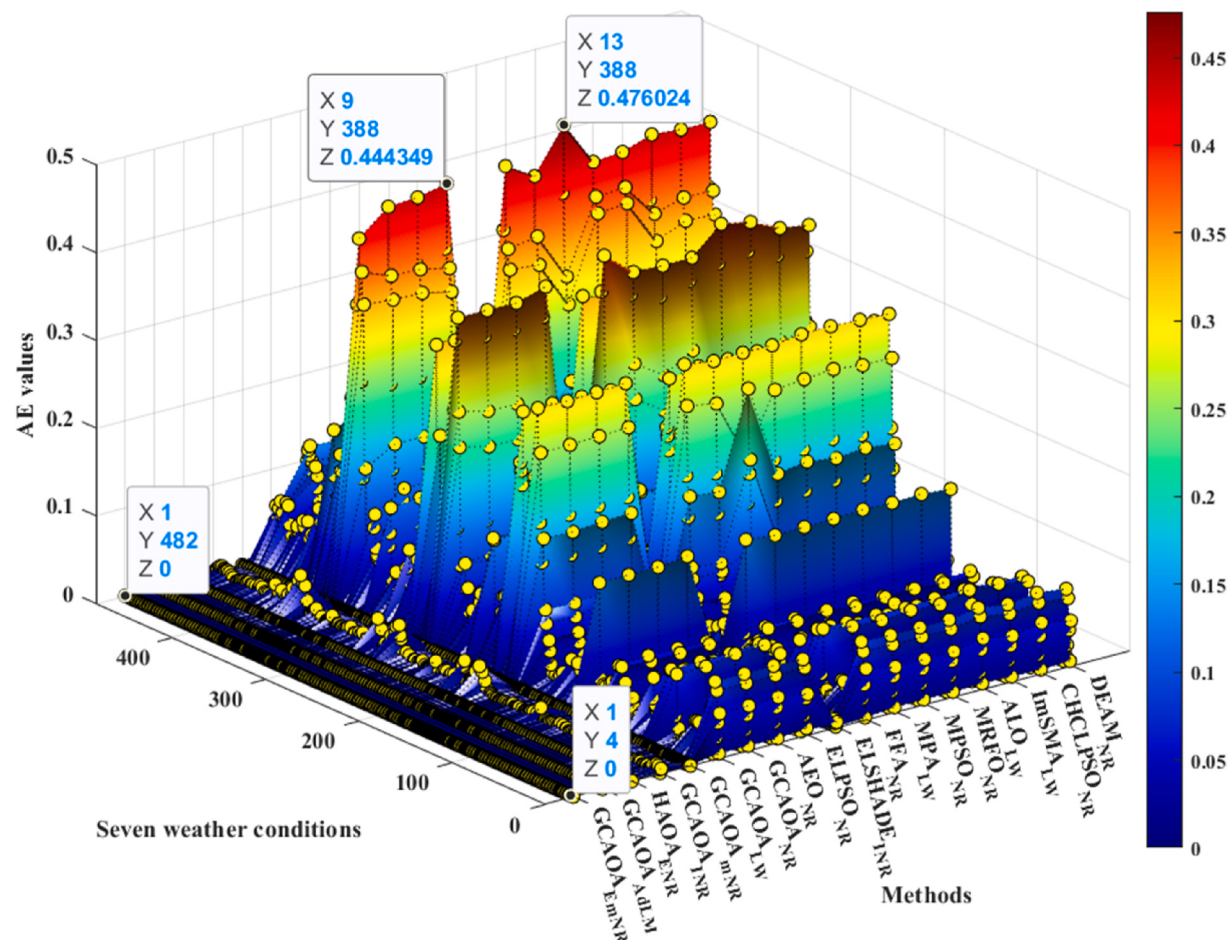


Fig. 16. Comparison of individual AE of GCAOA_{EmNR} and other models for the TD PV model.

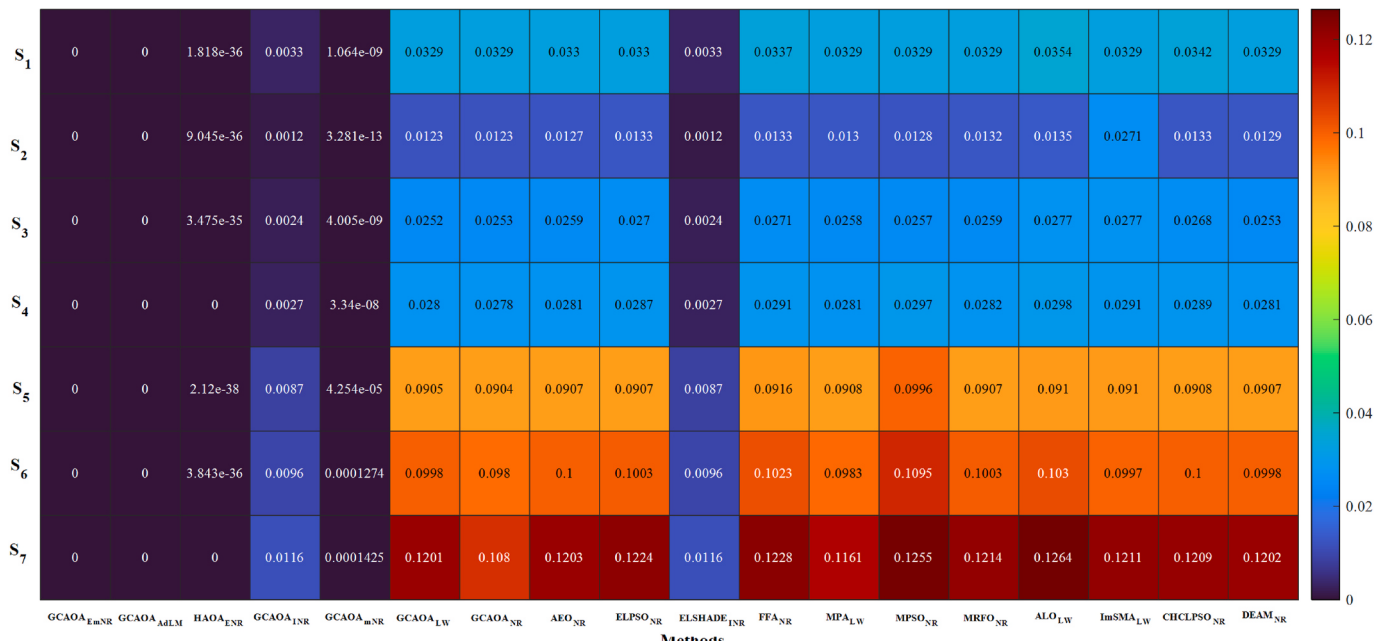


Fig. 17. Comparison of RMSE of GCAOA_{EmNR} and other peer algorithms for the TD PV model.

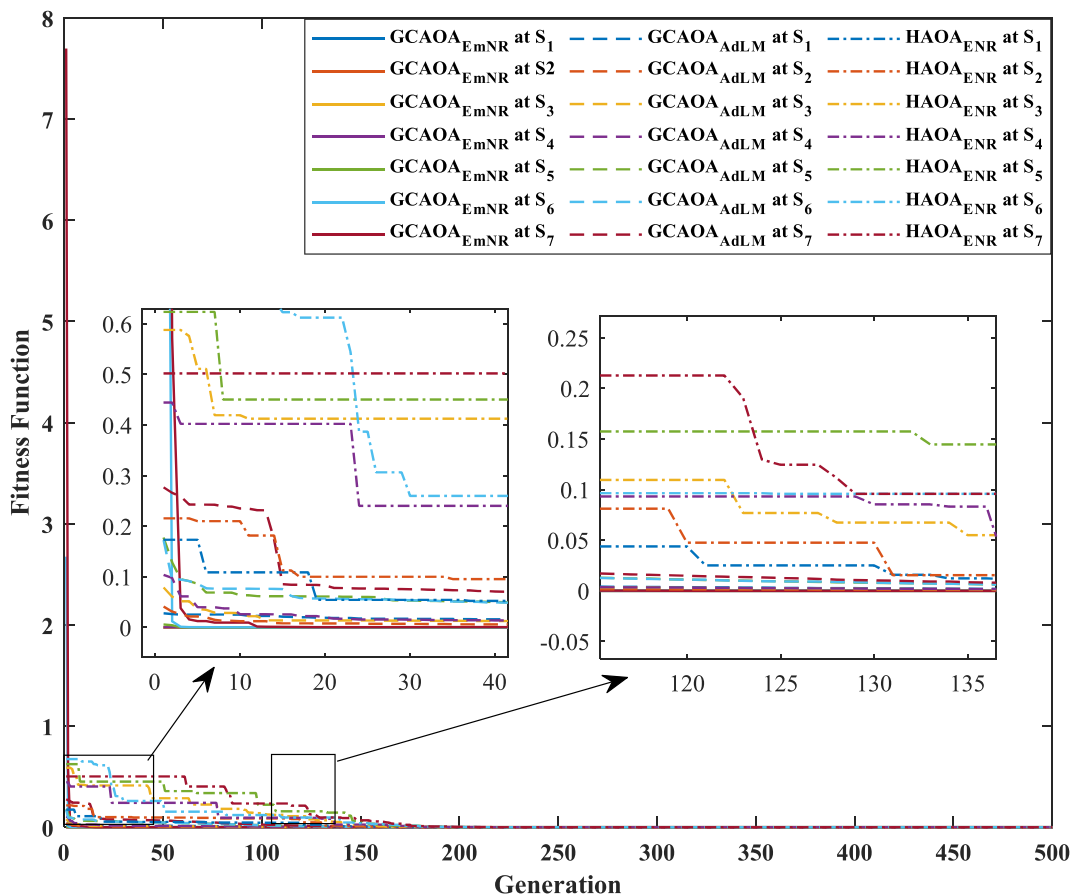


Fig. 18. Development of the fitness function using $\text{GCAOA}_{\text{EmNR}}$, $\text{GCAOA}_{\text{AdLM}}$, and HAOA_{ENR} for the TD PV model.

of the SD, DD, and TD PV models from real laboratory measured data at seven weather conditions. In addition, the $\text{GCAOA}_{\text{EmNR}}$ is compared to well-published approaches that deal with methodology and objective function formulation synchronously while considering multiple criterion analysis. The highlighted elements above provide guaranteed convergence for the AOA to globally extract the parameters of the SD, DD, and TD PV models by hybridizing different strategies with suitable CPU-execution durations.

Follows are some further observations:

- In the literature, most scholars deal with the PV model's equation linearly by directly obtaining the parameters in the equation, resulting poor performance of the PV model.
- Without any additional developments, the standard NR and LW methods are routinely applied to solve the nonlinear and multimodal PV model's equation. However, the accuracy of these methods is higher than that of solving it linearly.
- LW methods needs much more time and typically 2.8–4.1 times slower than linear and NR methods. It does, however, perform better in high-voltage ranges.
- Some of authors use 'fsolve' MATLAB built function to solve the PV model's equation, which is likewise time demanding.
- Without proper starting roots, the LW, NR, and LM methods are prone to falling into local minima. This is due to the fact that these methods need very precise initial solutions in order to predict the output current of the PV model equation.
- The parameters extracted at STC using the three key points methods display a good degree of agreement with I-V and P-V curves. However, these methods only consider the ideal solar irradiance and ambient temperature situations.

- Combining only adaptive parameter of LM method with NR, resulting a perturbation set of solutions for TD PV model. However, this combination performs excellently for the single and double diodes PV models.

Any further investigations for the LW, NR, LM, and other iterative methods can directly and accurately represent the actual performance of the PV model, particularly when combined with hybrid-metaheuristic methods.

5. Conclusion and future directions

This study includes a review and a research paper that address the methods used to solve the PV models' equations and to propose a novel integrated approach known as $\text{GCAOA}_{\text{EmNR}}$ to accurately estimate the parameters of the SD, DD, and TD PV models based on the real experimental data at various weather conditions. The $\text{GCAOA}_{\text{EmNR}}$ efficiently prevents the AOA's early convergence and the stagnation and initially anticipate the roots solutions of the SD, DD, and TD PV models' equations. The experimental findings and statistical analysis confirm the great agreement between the proposed and experimental currents in charting the I-V and P-V curves by reducing the RMSE, MBE, d_i , TS, and AE to zero. R^2 is one with acceptable computational time for all the weather conditions. Several well-published approaches in the literature are also utilized for verifications.

In this sense, the innovative $\text{GCAOA}_{\text{EmNR}}$ is capable to affectively and robustly determine any PV model's parameters at any weather conditions and promising to be applied for any type of PV technology with a highly degree of accuracy and consistency. Therefore, we believe that our model can be obtained for real-world PV system applications such as design, partial shading, and fault error detections.

Credit author statement

Hussein Mohammed Ridha; Conceptualization, Methodology, Resources, Writing – original draft, Writing – review & editing, Software, Formal analysis, Visualization, Investigation. **Seyedali Mirjalili:** Writing – review & editing, Methodology, Formal analysis, Visualization, Software, Data curation, Investigation, Supervision. **Hashim Hizam** Writing – review & editing, Methodology, Formal analysis, Visualization, Software, Data curation, Investigation, Supervision. **Mohammad Lutfi Othman** Formal analysis, Visualization, Investigation, Writing – review & editing. **Mohammad Effendy Ya'acob;** Formal analysis, Investigation, Visualization, Writing – review & editing. **Masoud Ahmadipour;** Formal analysis, Investigation, Visualization, Writing – review & editing.

Declaration of competing interest

The authors declare no conflict of interests for the publication of paper.

Appendix 1

The MATLAB code of the proposed EmNR method function [f] = fitness_function(Xnew,Tc,C_Iter);
 $a1 = Xnew(1)$; %Specified the diode ideality factor1 value from population
 $a2 = Xnew(2)$; %Specified the diode ideality factor2 value from population
 $a3 = Xnew(3)$; %Specified the diode ideality factor3 value from population.
 $Rs = Xnew(4)$; %Specified the PV series resistance value from population.
 $Rp = Xnew(5)$; %Specified the PV parallel resistance value from population.
 $Iph = Xnew(6)$; %Specified the photo current value from population.
 $Io1 = Xnew(7)$; %Specified the diode saturation current1 value from population.
 $Io2 = Xnew(8)$; %Specified the diode saturation current2 value from population.
 $Io3 = Xnew(9)$; %Specified the diode saturation current3 value from population.
 $Nsc = 36$; %Number of cells are connected in series per module
 $k = 1.3806503 \times 10^{-23}$; %Boltzmann constant (J/K)
 $q = 1.60217646 \times 10^{-19}$; %Electron charge in (Coulomb)
 $VT = (Nsc \cdot k \cdot Tc) / q$; %Diode thermal voltage (v)
%% Reading the experimental voltage and current data %%
%load ('var_fitness function AOA', 'Vp', 'Ie');
%% Computing the theoretical current %%
 $Ip = zeros(size(Vp))$;
 $N = length(Vp)$;
%% 1st order NR.
 $M = exp(-(5 \cdot C_Iter / 500)^2.5)$;
 $F = Iph - Io1 \cdot [exp((Vp + Ie \cdot Rs) / (a1 \cdot VT)) - 1] - Io2 \cdot [exp((Vp + Ie \cdot Rs) / (a2 \cdot VT)) - 1] - Io3 \cdot [exp((Vp + Ie \cdot Rs) / (a3 \cdot VT)) - 1] - ((Vp + Ie \cdot Rs) / Rp) \cdot Ie$;
 $fdd = -(Io1 \cdot (Rs / a1 \cdot VT) \cdot [exp((Vp + Ie \cdot Rs) / (a1 \cdot VT)) - 1]) - (Io2 \cdot (Rs / a2 \cdot VT) \cdot [exp((Vp + Ie \cdot Rs) / (a2 \cdot VT)) - 1]) - (Io3 \cdot (Rs / a3 \cdot VT) \cdot [exp((Vp + Ie \cdot Rs) / (a3 \cdot VT)) - 1]) - (Rs / Rp) \cdot Ie$;
 $Ip = Ie \cdot M \cdot (F / fdd)$;
%% 2nd order NR.
 $FF = Iph - Io1 \cdot [exp((Vp + Ie \cdot Rs) / (a1 \cdot VT)) - 1] - Io2 \cdot [exp((Vp + Ie \cdot Rs) / (a2 \cdot VT)) - 1] - Io3 \cdot [exp((Vp + Ie \cdot Rs) / (a3 \cdot VT)) - 1] - ((Vp + Ie \cdot Rs) / Rp) \cdot Ie$;
 $fdd = -(Io1 \cdot (Rs / a1 \cdot VT) \cdot [exp((Vp + Ie \cdot Rs) / (a1 \cdot VT)) - 1]) - (Io2 \cdot (Rs / a2 \cdot VT) \cdot [exp((Vp + Ie \cdot Rs) / (a2 \cdot VT)) - 1]) - (Io3 \cdot (Rs / a3 \cdot VT) \cdot [exp((Vp + Ie \cdot Rs) / (a3 \cdot VT)) - 1]) - (Rs / Rp) \cdot Ie$;

```

Ip = Ip-M.*(FF./fdd);
%% 3rd order NR.
FFF=Iph-Io1.*[exp((Vp+Ip.*Rs)./(a1*VT))-1]-Io2.*[exp((Vp+Ip.*Rs)./(a2*VT))-1]-Io3.*[exp((Vp+Ip.*Rs)./(a3*VT))-1]-((Vp+Ip.*Rs)./Rp)-Ip;
fddd = -(Io1.*((Rs/a1*VT).*([exp((Vp+Ip.*Rs)./(a1*VT))]-1)))-(Io2.*((Rs/a2*VT).*([exp((Vp+Ip.*Rs)./(a2*VT))]-1)))-(Io3.*((Rs/a3*VT).*([exp((Vp+Ip.*Rs)./(a3*VT))]-1)))-(Rs/Rp)-1; %% Modified 3rd order NR Eq. (17)
for i = 1:length(Vp)
Ip(i) = Ie(i)-M*[(2*F(i)^4)/(fddd(i)+fd(i))]^2;
end.
%% Computing the fitness function %%
f = sqrt((1/N)*sum((Ie-Ip).^2));

```

References

- [1] Nicola M, Alsafi Z, Sohrabi C, Kerwan A, Al-jabir A, Iosifidis C, et al. The socio-economic implications of the coronavirus pandemic (COVID-19): a review. *Int J Surg* 2020;78:185–93.
- [2] Gu W, Ma T, Ahmed S, Zhang Y, Peng J. A comprehensive review and outlook of bifacial photovoltaic (bPV) technology. *Energy Convers Manag* 2020;223. <https://doi.org/10.1016/j.enconman.2020.113283>.
- [3] Ridha HM, Gomes C, Hizam H, Mirjalili S. Multiple scenarios multi-objective salp swarm optimization for sizing of standalone photovoltaic system. *Renew Energy* 2020;153. <https://doi.org/10.1016/j.renene.2020.02.016>.
- [4] Zhou W, Wang P, Heidari AA, Zhao X, Turabieh H, Chen H. Random learning gradient based optimization for efficient design of photovoltaic models. *Energy Convers Manag* 2021;230. <https://doi.org/10.1016/j.enconman.2020.113751>.
- [5] Villalva MG, Gazoli JR, Filho ER. Comprehensive approach to modeling and simulation of photovoltaic arrays. *IEEE Trans Power Electron* 2009;24:1198–208. <https://doi.org/10.1109/TPEL.2009.2013862>.
- [6] Humada AM, Darweesh SY, Mohammed KG, Kamil M, Mohammed SF, Kasim NK, et al. Modeling of PV system and parameter extraction based on experimental data: review and investigation. *Sol Energy* 2020;199:742–60. <https://doi.org/10.1016/j.solener.2020.02.068>.
- [7] Li S, Gong W, Gu Q. A comprehensive survey on meta-heuristic algorithms for parameter extraction of photovoltaic models. *Renew Sustain Energy Rev* 2021; 141. <https://doi.org/10.1016/j.rser.2021.110828>.
- [8] Abbassi R, Abbassi A, Jemli M, Chebbi S. Identification of unknown parameters of solar cell models: a comprehensive overview of available approaches. *Renew Sustain Energy Rev* 2018;90:453–74. <https://doi.org/10.1016/j.rser.2018.03.011>.
- [9] Ma T, Yang H, Lu L. Development of a model to simulate the performance characteristics of crystalline silicon photovoltaic modules/strings/arrays. *Sol Energy* 2014;100:31–41. <https://doi.org/10.1016/j.solener.2013.12.003>.
- [10] Khan F, Al-ahmed A, Al-sulaiman FA. Critical analysis of the limitations and validity of the assumptions with the analytical methods commonly used to determine the photovoltaic cell parameters. *Renew Sustain Energy Rev* 2021;140: 110753. <https://doi.org/10.1016/j.rser.2021.110753>.
- [11] Muhsen DH, Ghazali AB, Khatib T, Abed IA. Parameters extraction of double diode photovoltaic module's model based on hybrid evolutionary algorithm. *Energy Convers Manag* 2015;105:552–61. <https://doi.org/10.1016/j.enconman.2015.08.023>.
- [12] Abbassi A, Gammoudi R, Ali Dami M, Hasnaoui O, Jemli M. An improved single-diode model parameters extraction at different operating conditions with a view to modeling a photovoltaic generator: a comparative study. *Sol Energy* 2017;155: 478–89. <https://doi.org/10.1016/j.solener.2017.06.057>.
- [13] Dkhichi F, Oukarfi B, Fakkari A, Belbounaguia N. Parameter identification of solar cell model using Levenberg-Marquardt algorithm combined with simulated annealing. *Sol Energy* 2014;110:781–8. <https://doi.org/10.1016/j.solener.2014.09.033>.
- [14] Tossa AK, Soro YM, Azoumah Y, Yamegueu D. A new approach to estimate the performance and energy productivity of photovoltaic modules in real operating conditions. *Sol Energy* 2014;110:543–60. <https://doi.org/10.1016/j.solener.2014.09.043>.
- [15] Louazni M, Al-Dahidi S. Approximation of photovoltaic characteristics curves using Bézier Curve. *Renew Energy* 2021;174:715–32. <https://doi.org/10.1016/j.renene.2021.04.103>.
- [16] Biswas PP, Suganthan PN, Wu G, Amaralunga GAJ. Parameter estimation of solar cells using datasheet information with the application of an adaptive differential evolution algorithm. *Renew Energy* 2019;132:425–38. <https://doi.org/10.1016/j.renene.2018.07.152>.
- [17] Lun SX, Du CJ, Guo TT, Wang S, Sang JS, Li JP. A new explicit i-v model of a solar cell based on taylor's series expansion. *Sol Energy* 2013;94:221–32. <https://doi.org/10.1016/j.solener.2013.04.013>.
- [18] Azab M. Identification of one-diode model parameters of PV devices from nameplate information using particle swarm and least square methods. 2015 1st Workshop on Smart Grid and Renewable Energy. 2015. <https://doi.org/10.1109/SGRE.2015.7208722>. SGRE 2015.

- [19] Ridha HM, Hizam H, Mirjalili S, Othman ML, Ya'acob ME, Abualigah L. A novel theoretical and practical methodology for extracting the parameters of the single and double diode photovoltaic models. *IEEE Access* 2022. <https://doi.org/10.1109/ACCESS.2022.3142779>. 1–1.
- [20] Ridha HM, Hizam H, Gomes C, Asghar A, Chen H, Ahmadipour M, et al. Parameters extraction of three diode photovoltaic models using boosted LSHADE algorithm and Newton Raphson method. *Energy* 2021;224:120136. <https://doi.org/10.1016/j.energy.2021.120136>.
- [21] Pillai DS, Rajasekar N. Metaheuristic algorithms for PV parameter identification: a comprehensive review with an application to threshold setting for fault detection in PV systems. *Renew Sustain Energy Rev* 2018;82:3503–25. <https://doi.org/10.1016/j.rser.2017.10.107>.
- [22] Saha C, Agbu N, Jinks R. Review article of the solar PV parameters estimation using evolutionary algorithms. *MOJ Solar Photoen Syst* 2018;2:66–78. <https://doi.org/10.15406/mojsp.2018.00026>.
- [23] Yousri D, Abd Elaziz M, Oliva D, Abualigah L, Al-qaness MAA, Ewees AA. Reliable applied objective for identifying simple and detailed photovoltaic models using modern metaheuristics: comparative study. *Energy Convers Manag* 2020;223:113279. <https://doi.org/10.1016/j.enconman.2020.113279>.
- [24] Wolpert DH, Macready WG. No free lunch theorems for optimization. *IEEE Trans Evol Comput* 1997;1:67–82. <https://doi.org/10.1109/4235.585893>.
- [25] Venkateswari R, Rajasekar N. Review on parameter estimation techniques of solar photovoltaic systems. *Int Trans Electric Energy Syst* 2021;31:1–72. <https://doi.org/10.1002/2050-7038.13113>.
- [26] Oliva D, Elaziz MA, Elsheikh AH, Ewees AA. A review on meta-heuristics methods for estimating parameters of solar cells. *J Power Sources* 2019;435:126683. <https://doi.org/10.1016/j.jpowsour.2019.05.089>.
- [27] Yang B, Wang J, Zhang X, Yu T, Yao W, Shu H, et al. Comprehensive overview of meta-heuristic algorithm applications on PV cell parameter identification. *Energy Convers Manag* 2020;208:112595. <https://doi.org/10.1016/j.enconman.2020.112595>.
- [28] Yousri D, Thanikanti SB, Allam D, Ramachandaramurthy VK, Eteiba MB. Fractional chaotic ensemble particle swarm optimizer for identifying the single, double, and three diode photovoltaic models' parameters. *Energy* 2020;195:116979. <https://doi.org/10.1016/j.energy.2020.116979>.
- [29] Ridha HM. Parameters extraction of single and double diodes photovoltaic models using Marine Predators Algorithm and Lambert W function. *Sol Energy* 2020;209:674–93. <https://doi.org/10.1016/j.solener.2020.09.047>.
- [30] Sihwail R, Solaiman OS, Omar K, Akram K, Ariffin Z. A hybrid approach for solving systems of nonlinear equations using harris hawks optimization and Newton's method. *IEEE Access*; 2021. p. 1. <https://doi.org/10.1109/ACCESS.2021.3094471>.
- [31] Eswarakhanthan T, Bottin J, Bouhouc I, Boutrit C. Nonlinear minimization algorithm for determining the solar cell parameters with microcomputers. *Int J Sol Energy* 1986;4:1–12. <https://doi.org/10.1080/01425918608909835>.
- [32] Ndegwa R, Ayieta E, Simiyu J, Odero N. A simplified simulation procedure and analysis of a photovoltaic solar system using a single diode model. 2020. p. 65–93. <https://doi.org/10.4236/jpee.2020.89006>.
- [33] Chin VJ, Salam Z. Coyote optimization algorithm for the parameter extraction of photovoltaic cells. *Sol Energy* 2019;194:656–70. <https://doi.org/10.1016/j.solener.2019.10.093>.
- [34] Abdel-Basset M, Mohamed R, El-Fergany A, Askar SS, Abouhawwash M. Efficient ranking-based whale optimizer for parameter extraction of three-diode photovoltaic model: analysis and validations. *Energies* 2021;14:1–21. <https://doi.org/10.3390/en14133729>.
- [35] Gao X, Cui Y, Hu J, Xu G, Yu Y. Lambert W-function based exact representation for double diode model of solar cells: comparison on fitness and parameter extraction. *Energy Convers Manag* 2016;127:443–60. <https://doi.org/10.1016/j.enconman.2016.09.005>.
- [36] Chin VJ, Salam Z, Ishaque K. An accurate modelling of the two-diode model of PV module using a hybrid solution based on differential evolution. *Energy Convers Manag* 2016;124:42–50. <https://doi.org/10.1016/j.enconman.2016.06.076>.
- [37] Yousri D, Fathy A, Rezk H, Sudhakar T, Berber MR. A reliable approach for modeling the photovoltaic system under partial shading conditions using three diode model and hybrid marine predators-slime mould algorithm. *Energy Convers Manag* 2021;243:114269. <https://doi.org/10.1016/j.enconman.2021.114269>.
- [38] Gnetchejo PJ, Ndjakomo Essiane S, Dadje A, Ele P. A combination of Newton-Raphson method and heuristics algorithms for parameter estimation in photovoltaic modules. *Heliyon* 2021;7. <https://doi.org/10.1016/j.heliyon.2021.e06673>.
- [39] Kler D, Goswami Y, Rana KPS, Kumar V. A novel approach to parameter estimation of photovoltaic systems using hybridized optimizer. *Energy Convers Manag* 2019;187:486–511. <https://doi.org/10.1016/j.enconman.2019.01.102>.
- [40] Park JY, Choi SJ. A novel datasheet-based parameter extraction method for a single-diode photovoltaic array model. *Sol Energy* 2015;122:1235–44. <https://doi.org/10.1016/j.solener.2015.11.001>.
- [41] El-Fergany AA. Parameters identification of PV model using improved slime mould optimizer and Lambert W-function. *Energy Rep* 2021;7:875–87. <https://doi.org/10.1016/j.egyr.2021.01.093>.
- [42] Agwa AM, El-Fergany AA, Maksoud HA. Electrical characterization of photovoltaic modules using farmland fertility optimizer. *Energy Convers Manag* 2020;217:112990. <https://doi.org/10.1016/j.enconman.2020.112990>.
- [43] Ma X, Huang WH, Schnabel E, Kohl M, Brynjarsdottir J, Braid JL, et al. Data-driven I-V feature extraction for photovoltaic modules. *IEEE J Photovoltaics* 2019;9:1405–12. <https://doi.org/10.1109/JPHOTOV.2019.2928477>.
- [44] Zaimi M, el Achoubi H, Ibral A, Assaid EM. Determining combined effects of solar radiation and panel junction temperature on all model-parameters to forecast peak power and photovoltaic yield of solar panel under non-standard conditions. *Sol Energy* 2019;191:341–59. <https://doi.org/10.1016/j.solener.2019.09.007>.
- [45] Laudani A, Riganti Fulginei F, Salvini A. High performing extraction procedure for the one-diode model of a photovoltaic panel from experimental I-V curves by using reduced forms. *Sol Energy* 2014;103:316–26. <https://doi.org/10.1016/j.solener.2014.02.014>.
- [46] Louzazni M, Khouya A, Amechnoue K, Gandelli A, Mussetta M, Craciunescu A. Metaheuristic algorithm for photovoltaic parameters: comparative study and prediction with a Firefly algorithm. *Appl Sci* 2018;8. <https://doi.org/10.3390/app803039>.
- [47] Louzazni M, Khouya A, Amechnoue K, Mussetta M, Craciunescu A. Comparison and evaluation of statistical criteria in the solar cell and photovoltaic module parameters' extraction. *Int J Ambient Energy* 2018;1–20. <https://doi.org/10.1080/01430750.2018.1517678>.
- [48] Gnetchejo PJ, Ndjakomo Essiane S, Dadje A, Ele P, Mbadjoun Wapet DE, Perabi Ngoffe S, et al. A self-adaptive algorithm with Newton Raphson method for parameters identification of photovoltaic modules and array. *Trans Electric Electron Mater* 2021. <https://doi.org/10.1007/s42341-021-00312-5>.
- [49] Dizqah AM, Maher A, Busawon K. An accurate method for the PV model identification based on a genetic algorithm and the interior-point method. *Renew Energy* 2014;72:212–22. <https://doi.org/10.1016/j.renene.2014.07.014>.
- [50] Ibrahim IA, Hossain J, Duck BC, Fell CJ. An adaptive wind driven optimization algorithm for extracting the parameters of a single-diode PV cell model. *IEEE Trans Sustain Energy* 2019. <https://doi.org/10.1109/tse.2019.2917513>. 1–1.
- [51] Ibrahim IA, Hossain MJ, Duck BC, Nadarajah M. An improved wind driven optimization algorithm for parameters identification of a triple-diode photovoltaic cell model. *Energy Convers Manag* 2020;213:112872. <https://doi.org/10.1016/j.enconman.2020.112872>.
- [52] Chen Y, Sun Y, Meng Z. An improved explicit double-diode model of solar cells: fitness verification and parameter extraction. *Energy Convers Manag* 2018;169:345–58. <https://doi.org/10.1016/j.enconman.2018.05.035>.
- [53] Ishaque K, Salam Z. An improved modeling method to determine the model parameters of photovoltaic (PV) modules using differential evolution (DE). *Sol Energy* 2011;85:2349–59. <https://doi.org/10.1016/j.solener.2011.06.025>.
- [54] Rajasekar N, Kumar NK, Venugopalan R. ScienceDirect Bacterial Foraging Algorithm based solar PV parameter estimation. *Sol Energy* 2013;97:255–65. <https://doi.org/10.1016/j.solener.2013.08.019>.
- [55] Selem SI, El-Fergany AA, Hasanien HM. Artificial electric field algorithm to extract nine parameters of triple-diode photovoltaic model. *Int J Energy Res* 2021;45:590–604. <https://doi.org/10.1002/er.5756>.
- [56] Ismail MS, Moghavvemi M, Mahlia TMI. Characterization of PV panel and global optimization of its model parameters using genetic algorithm. *Energy Convers Manag* 2013;73:10–25. <https://doi.org/10.1016/j.enconman.2013.03.033>.
- [57] Nunes HGG, Pombo JAN, Bento PMR, Mariano SJPS, Calado MRA. Collaborative swarm intelligence to estimate PV parameters. *Energy Convers Manag* 2019;185:866–90. <https://doi.org/10.1016/j.enconman.2019.02.003>.
- [58] Rizk-Allah RM, El-Fergany AA. Conscious neighborhood scheme-based Laplacian barnacles mating algorithm for parameters optimization of photovoltaic single- and double-diode models. *Energy Convers Manag* 2020;226:113522. <https://doi.org/10.1016/j.enconman.2020.113522>.
- [59] Ridha HM, Gomes C, Hizam H. Estimation of photovoltaic module model's parameters using an improved electromagnetic-like algorithm. *Neural Comput Appl* 2020. <https://doi.org/10.1007/s00521-020-04714-z>.
- [60] Oliva D, Abd El Aziz M, Ella Hassanien A. Parameter estimation of photovoltaic cells using an improved chaotic whale optimization algorithm. *Appl Energy* 2017;200:141–54. <https://doi.org/10.1016/j.apenergy.2017.05.029>.
- [61] Abdulrazzaq AK, Bognár G, Plesz B. Evaluation of different methods for solar cells/modules parameters extraction. *Sol Energy* 2020;196:183–95. <https://doi.org/10.1016/j.solener.2019.12.010>.
- [62] Qais MH, Hasanien HM, Alghuwainem S. Identification of electrical parameters for three-diode photovoltaic model using analytical and sunflower optimization algorithm. *Appl Energy* 2019;250:109–17. <https://doi.org/10.1016/j.apenergy.2019.05.013>.
- [63] Kumar Patro S, Saini RP. Mathematical modeling framework of a PV model using novel differential evolution algorithm. *Sol Energy* 2020;211:210–26. <https://doi.org/10.1016/j.solener.2020.09.065>.
- [64] Kumar M, Kumar A. An efficient parameters extraction technique of photovoltaic models for performance assessment. *Sol Energy* 2017;158:192–206. <https://doi.org/10.1016/j.solener.2017.09.046>.
- [65] Rezaee Jordhei A. Enhanced leader particle swarm optimisation (ELPSO): an efficient algorithm for parameter estimation of photovoltaic (PV) cells and modules. *Sol Energy* 2018;159:78–87. <https://doi.org/10.1016/j.solener.2017.10.063>.
- [66] Ishaque K, Salam Z, Syafaruddin. A comprehensive MATLAB Simulink PV system simulator with partial shading capability based on two-diode model. *Sol Energy* 2011;85:2217–27. <https://doi.org/10.1016/j.solener.2011.06.008>.
- [67] Lim LHI, Ye Z, Ye J, Yang D, Du H. A linear identification of diode models from single I-V characteristics of PV panels. *IEEE Trans Ind Electron* 2015;62:4181–93. <https://doi.org/10.1109/TIE.2015.2390193>.
- [68] Dehghanzadeh A, Farahani G, Maboodi M. A novel approximate explicit double-diode model of solar cells for use in simulation studies. *Renew Energy* 2017;103:468–77. <https://doi.org/10.1016/j.renene.2016.11.051>.

- [69] Io Brano V, Ciulla G. An efficient analytical approach for obtaining a five parameters model of photovoltaic modules using only reference data. *Appl Energy* 2013;111:894–903. <https://doi.org/10.1016/j.apenergy.2013.06.046>.
- [70] Peng L, Sun Y, Meng Z. An improved model and parameters extraction for photovoltaic cells using only three state points at standard test condition. *J Power Sources* 2014;248:621–31. <https://doi.org/10.1016/j.jpowsour.2013.07.058>.
- [71] Chauhan A, Prakash S. A new emperor penguin optimisation-based approach for solar photovoltaic parameter estimation. *Int Trans Electric Energy Syst* 2021; 1–28. <https://doi.org/10.1002/2050-7038.12917>.
- [72] Bai J, Liu S, Hao Y, Zhang Z, Jiang M, Zhang Y. Development of a new compound method to extract the five parameters of PV modules. *Energy Convers Manag* 2014;79:294–303. <https://doi.org/10.1016/j.enconman.2013.12.041>.
- [73] Elbaset AA, Ali H, Abd-El Sattar M. Novel seven-parameter model for photovoltaic modules. *Sol Energy Mater Sol Cell* 2014;130:442–55. <https://doi.org/10.1016/j.solmat.2014.07.016>.
- [74] Ram JP, Babu TS, Dragicevic T, Rajasekar N. A new hybrid bee pollinator flower pollination algorithm for solar PV parameter estimation. *Energy Convers Manag* 2017;135:463–76. <https://doi.org/10.1016/j.enconman.2016.12.082>.
- [75] Derick M, Rani C, Rajesh M, Farrag ME, Wang Y, Busawon K. An improved optimization technique for estimation of solar photovoltaic parameters. *Sol Energy* 2017;157:116–24. <https://doi.org/10.1016/j.solener.2017.08.006>.
- [76] Muhsen DH, Ghazali AB, Khatib T, Abed IA. Extraction of photovoltaic module model's parameters using an improved hybrid differential evolution/electromagnetism-like algorithm. *Sol Energy* 2015;119:286–97. <https://doi.org/10.1016/j.solener.2015.07.008>.
- [77] Nunes HGG, Pombo JAN, Mariano SJPS, Calado MRA, Felippe de Souza JAM. A new high performance method for determining the parameters of PV cells and modules based on guaranteed convergence particle swarm optimization. *Appl Energy* 2018;211:774–91. <https://doi.org/10.1016/j.apenergy.2017.11.078>.
- [78] Alam DF, Yousri DA, Eteiba MB. Flower Pollination Algorithm based solar PV parameter estimation. *Energy Convers Manag* 2015;101:410–22. <https://doi.org/10.1016/j.enconman.2015.05.074>.
- [79] Appelbaum J, Peled A. Parameters extraction of solar cells - a comparative examination of three methods. *Sol Energy Mater Sol Cell* 2014;122:164–73. <https://doi.org/10.1016/j.solmat.2013.11.011>.
- [80] Ali EE, El-Hameed MA, El-Fergany AA, El-Arini MM. Parameter extraction of photovoltaic generating units using multi-verse optimizer. *Sustain Energy Technol Assessments* 2016;17:68–76. <https://doi.org/10.1016/j.seta.2016.08.004>.
- [81] Elkholmy MM. Artificial ecosystem-based optimiser to electrically characterise PV generating systems under various operating conditions reinforced by experimental validations Mohamed A. El-Hameed. *IET Renewable Power Generation* 2021;1–15. <https://doi.org/10.1049/rpg2.12059>.
- [82] Yousri D, Rezk H. Identifying the parameters of different configurations of photovoltaic models based on recent artificial ecosystem-based optimization approach. 2020. p. 1–21. <https://doi.org/10.1002/er.5747>.
- [83] Subudhi B, Pradhan R. Bacterial Foraging Optimization approach to parameter extraction of a photovoltaic module. *IEEE Trans Sustain Energy* 2018;9:381–9. <https://doi.org/10.1109/TSTE.2017.2736060>.
- [84] Ayang A, Wamkeue R, Ouhrouche M, Saad M, Andy Tamegne T, Deli K, et al. Least square estimator and IEC-60891 procedure for parameters estimation of single-diode model of photovoltaic generator at standard test conditions (STC). *Electr Eng* 2021;103:1253–64. <https://doi.org/10.1007/s00202-020-01131-2>.
- [85] Park JY, Choi SJ. A novel simulation model for PV panels based on datasheet parameter tuning. *Sol Energy* 2017;145:90–8. <https://doi.org/10.1016/j.solener.2016.12.003>.
- [86] Polo J, Martín-Chivelet N, Alonso-García MC, Zitouni H, Alonso-Abella M, Sanz-Saiz C, et al. Modeling I-V curves of photovoltaic modules at indoor and outdoor conditions by using the Lambert function. *Energy Convers Manag* 2019;195: 1004–11. <https://doi.org/10.1016/j.enconman.2019.05.085>.
- [87] Kanimozhhi G, Kumar Harish. Modeling of solar cell under different conditions by Ant Lion Optimizer with LambertW function. *Appl Soft Comput J* 2018;71: 141–51. <https://doi.org/10.1016/j.asoc.2018.06.025>.
- [88] Nunes HGG, Silva PNC, Pombo JAN, Mariano SJPS, Calado MRA. Multiswarm spiral leader particle swarm optimisation algorithm for PV parameter identification. *Energy Convers Manag* 2020;225:113388. <https://doi.org/10.1016/j.enconman.2020.113388>.
- [89] Achouby H el, Zaimi M, Ibral A, Assaid EM. New analytical approach for modelling effects of temperature and irradiance on physical parameters of photovoltaic solar module. *Energy Convers Manag* 2018;177:258–71. <https://doi.org/10.1016/j.enconman.2018.09.054>.
- [90] Fathy A, Rezk H. Parameter estimation of photovoltaic system using imperialist competitive algorithm. *Renew Energy* 2017;111:307–20. <https://doi.org/10.1016/j.renene.2017.04.014>.
- [91] Oulcaid M, El H, Ammeh L, Yahya A, Giri F. Parameter extraction of photovoltaic cell and module : analysis and discussion of various combinations and test cases. *Sustain Energy Technol Assessments* 2020;40:100736. <https://doi.org/10.1016/j.seta.2020.100736>.
- [92] Sudhakar Babu T, Prasanth Ram J, Sangeetha K, Laudani A, Rajasekar N. Parameter extraction of two diode solar PV model using Fireworks algorithm. *Sol Energy* 2016;140:265–76. <https://doi.org/10.1016/j.solener.2016.10.044>.
- [93] Qais MH, Hasanian HM, Alghuwainem S. Parameters extraction of three-diode photovoltaic model using computation and Harris Hawks optimization. *Energy* 2020;195. <https://doi.org/10.1016/j.energy.2020.117040>.
- [94] Merchaoui M, Sakly A, Mimouni MF. Particle swarm optimisation with adaptive mutation strategy for photovoltaic solar cell/module parameter extraction.
- [95] Energy Convers Manag 2018;175:151–63. <https://doi.org/10.1016/j.enconman.2018.08.081>.
- [96] Mughal MA, Ma Q, Xiao C. Photovoltaic cell parameter estimation using hybrid particle swarm optimization and simulated annealing. *Energies* 2017;10:1–14. <https://doi.org/10.3390/en10081213>.
- [97] Chen S, Gholami Farkoush S, Leto S. Photovoltaic cells parameters extraction using variables reduction and improved shark optimization technique. *Int J Hydrogen Energy* 2020;45:10059–69. <https://doi.org/10.1016/j.ijhydene.2020.01.236>.
- [98] Kharouch Y, Herbazzi R, Chahboun A. Parameter's extraction of solar photovoltaic models using an improved differential evolution algorithm. *Energy Convers Manag* 2022;251:114972. <https://doi.org/10.1016/j.enconman.2021.114972>.
- [99] Maouhoub N. Photovoltaic module parameter estimation using an analytical approach and least squares method. *J Comput Electron* 2018;17:784–90. <https://doi.org/10.1007/s10825-017-1121-5>.
- [100] Muhammad FF, Karim Sangawi AW, Hashim S, Ghoshal SK, Abdullah IK, Hameed SS. Simple and efficient estimation of photovoltaic cells and modules parameters using approximation and correction technique. *PLoS One* 2019;14: 1–19. <https://doi.org/10.1371/journal.pone.0216201>.
- [101] Pindado S, Roibas-Millan E, Cubas J, Alvarez JM, Alfonso-Corcuera D, Cubero-Estalrich JL, et al. Simplified Lambert W-function Math equations when applied to photovoltaic systems modeling. *IEEE Trans Ind Appl* 2021;57:1779–88. <https://doi.org/10.1109/TIA.2021.3052858>.
- [102] Bencherif M, Brahma N. Solar cell parameter identification using the three main points of the current-voltage characteristic. *Int J Ambient Energy* 2020;1–26. <https://doi.org/10.1080/01430750.2020.1789739>.
- [103] Yousri D, Allam D, Eteiba MB, Suganthan PN. Static and dynamic photovoltaic models' parameters identification using chaotic heterogeneous comprehensive learning particle swarm optimizer variants. *Energy Convers Manag* 2019;182: 546–63. <https://doi.org/10.1016/j.enconman.2018.12.022>.
- [104] Wang S, Yu Y, Hu W. Static and dynamic solar photovoltaic models' parameters estimation using hybrid Rao optimization algorithm. *J Clean Prod* 2021;315: 128080. <https://doi.org/10.1016/j.jclepro.2021.128080>.
- [105] Ghani F, Rosengarten G, Duke M. The characterisation of crystalline silicon photovoltaic devices using the manufacturer supplied data. *Sol Energy* 2016;132: 15–24. <https://doi.org/10.1016/j.solener.2016.03.008>.
- [106] Jordehi AR. Time varying acceleration coefficients particle swarm optimisation (TVACPSO): a new optimisation algorithm for estimating parameters of PV cells and modules. *Energy Convers Manag* 2016;129:262–74. <https://doi.org/10.1016/j.enconman.2016.09.085>.
- [107] Gao X, Cui Y, Hu J, Tahir N, Xu G. Performance comparison of exponential , Lambert W function and Special Trans function based single diode solar cell models. *Energy Convers Manag* 2018;171:1822–42. <https://doi.org/10.1016/j.enconman.2018.06.106>.
- [108] Ridha HM, Heidari AA, Wang M, Chen H. Boosted mutation-based Harris hawks optimizer for parameters identification of single-diode solar cell models. *Energy Convers Manag* 2020;209. <https://doi.org/10.1016/j.enconman.2020.112660>.
- [109] Mary CKDM. Parameter estimation of three - diode solar photovoltaic model using an Improved - african Vultures optimization algorithm with Newton – Raphson method. Springer US; 2021. <https://doi.org/10.1007/s10825-021-01812-6>.
- [110] Rezk H, Babu TS, Al-Dhaifallah M, Ziedan HA. A robust parameter estimation approach based on stochastic fractal search optimization algorithm applied to solar PV parameters. *Energy Rep* 2021;7:620–40. <https://doi.org/10.1016/j.egyr.2021.01.024>.
- [111] Houssine EH, Zaki GN, Diab AAZ, Younis EMG. An efficient Manta Ray Foraging Optimization algorithm for parameter extraction of three-diode photovoltaic model. *Comput Electr Eng* 2021;94:107304. <https://doi.org/10.1016/j.compeleceng.2021.107304>.
- [112] Abdel-Basset M, Mohamed R, El-Fergany A, Abouhawwash M, Askar SS. Parameters identification of pv triple-diode model using improved generalized normal distribution algorithm. *Mathematics* 2021;9:1–23. <https://doi.org/10.3390/math9090995>.
- [113] Ibrahim IA, Hossain MJ, Duck BC. A hybrid wind driven-based fruit fly optimization algorithm for identifying the parameters of a double-diode photovoltaic cell model considering degradation effects. *Sustain Energy Technol Assessments* 2022;50:101685. <https://doi.org/10.1016/j.seta.2021.101685>.
- [114] Tchakpedeou A-B, Lare Y, Napo K, Fousseni A. An improved levenberg–marquardt approach with a new reduced form for the identification of parameters of the one-diode photovoltaic model. *J Sol Energy Eng* 2022;144. <https://doi.org/10.1115/1.4053624>.
- [115] Ridha HM, Hizam H, Mirjalili S, Othman ML, Ya'acob ME, Ahmadipour M, et al. On the problem formulation for parameter extraction of the photovoltaic model: novel integration of hybrid evolutionary algorithm and Levenberg Marquardt based on adaptive damping parameter formula. *Energy Convers Manag* 2022;256: 115403. <https://doi.org/10.1016/j.enconman.2022.115403>.
- [116] Khanha V, Das BK, Bisha D, Vandana, Singh PK. A three diode model for industrial solar cells and estimation of solar cell parameters using PSO algorithm. *Renew Energy* 2015;78:105–13. <https://doi.org/10.1016/j.renene.2014.12.072>.
- [117] Čalasan M, Abdel Aleem SHE, Zobaa AF. On the root mean square error (RMSE) calculation for parameter estimation of photovoltaic models: a novel exact

- analytical solution based on Lambert W function. *Energy Convers Manag* 2020; 210:112716. <https://doi.org/10.1016/j.enconman.2020.112716>.
- [118] Ghani F, Rosengarten G, Duke M, Carson JK. The numerical calculation of single-diode solar-cell modelling parameters. *Renew Energy* 2014;72:105–12. <https://doi.org/10.1016/j.renene.2014.06.035>.
- [119] Easwarakhanthan T, Bottin J, Bouhouche I, Boutrit C. Nonlinear minimization algorithm for determining the solar cell parameters with microcomputers. *Int J Sol Energy* 1986;4:1–12. <https://doi.org/10.1080/01425918608909835>.
- [120] Weerakoon S, Fernando TGI. A variant of Newton's method with accelerated third-order convergence. *Appl Math Lett* 2000;13:87–93. [https://doi.org/10.1016/S0893-9659\(00\)00100-2](https://doi.org/10.1016/S0893-9659(00)00100-2).
- [121] Crisfield MA. Accelerating and damping the modified Newton-Raphson method. *Comput Struct* 1984;18:395–407. [https://doi.org/10.1016/0045-7949\(84\)90059-2](https://doi.org/10.1016/0045-7949(84)90059-2).
- [122] Amrein M, Wihler TP. An adaptive Newton-method based on a dynamical systems approach. *Commun Nonlinear Sci Numer Simulat* 2014;19:2958–73. <https://doi.org/10.1016/j.cnsns.2014.02.010>.
- [123] McDougall TJ, Wotherspoon SJ. A simple modification of Newton's method to achieve convergence of order $1 + \sqrt{2}$. *Appl Math Lett* 2014;29:20–5. <https://doi.org/10.1016/j.aml.2013.10.008>.
- [124] Abualigah L, Diabat A, Mirjalili S, Abd Elaziz M, Gandomi AH. The arithmetic optimization algorithm. *Comput Methods Appl Mech Eng* 2021;376:113609. <https://doi.org/10.1016/j.cma.2020.113609>.
- [129] Yang X-S. Engineering optimisation: an introduction with metaheuristic applications. John Wiley and Sons; 2010. <https://doi.org/10.1002/9781119483151.ch2>.
- [130] Chen X, Yu K, Du W, Zhao W, Liu G. Parameters identification of solar cell models using generalized oppositional teaching learning based optimization. *Energy* 2016;99:170–80. <https://doi.org/10.1016/j.energy.2016.01.052>.
- [131] Mahdavi S, Rahnamayan S, Deb K. Opposition based learning : a literature review. 2017. <https://doi.org/10.1016/j.swevo.2017.09.010>.
- [132] Xu S, Wang Y. Parameter estimation of photovoltaic modules using a hybrid flower pollination algorithm. *Energy Convers Manag* 2017;144:53–68. <https://doi.org/10.1016/j.enconman.2017.04.042>.
- [133] Das S, Mullick SS, Suganthan PN. Recent advances in differential evolution-An updated survey. *Swarm Evol Comput* 2016;27:1–30. <https://doi.org/10.1016/j.swevo.2016.01.004>.
- [134] Steingrube S, Breitenstein O, Ramspeck K, Glunz S, Schenk A, Altermatt PP. Explanation of commonly observed shunt currents in c-Si solar cells by means of recombination statistics beyond the Shockley-Read-Hall approximation. *J Appl Phys* 2011;110. <https://doi.org/10.1063/1.3607310>.
- [135] Mahapatra C, Mohanty AR. Explosive sound source localization in indoor and outdoor environments using modified Levenberg Marquardt algorithm. *Measurement* 2021;110362. <https://doi.org/10.1016/j.measurement.2021.110362>.